Influence of Hedgehog signaling and starvation on selected aspects of liver metabolism

Von der Fakultät für Lebenswissenschaften
der Universität Leipzig

genehmigte

DISSERTATION

zur Erlangung des akademischen Grades

Doctor rerum naturalium
Dr. rer. nat.

vorgelegt von

Master of Science Christiane Rennert
geboren am 13.03.1989 in Suhl

Dekan:	Prof. Dr. Tilo Pompe
Gutachter:	Prof. Dr. Torsten Schöneberg
	Prof. Dr. Claus Hellerbrand
Tag der Verteidigung:	21.06.2019

BIBLIOGRAPHISCHE DARSTELLUNG

Christiane Rennert

Influence of Hedgehog signaling and starvation on selected aspects of liver metabolism

Fakultät für Lebenswissenschaften

Universität Leipzig

Dissertation

64 Seiten, 161 Literaturangaben, 24 Abbildungen, 4 Tabellen

The liver is the central metabolic hub in organisms and a complex, intertwining regulatory network guarantees efficient liver processes. The morphogenic Hedgehog pathway was recently shown to play a role in regulating the underlying genetic program. Transgenic mouse models with hepatocyte-specific inactivation of Hedgehog signaling showed alterations in insulin-like growth factor homeostasis and in energy metabolism associated with increased lipid accumulation in the liver. In this thesis, it was possible to connect the observed infertility of female knockout mice with an unexpected activation of sex steroid synthesis in the liver. Associated with increased steroidogenic gene expression exclusively in hepatocytes, the plasma testosterone level was significantly elevated, which led to androgenization and an anovulatory phenotype. With these characteristics, the mouse model mimicked the human polycystic ovarian syndrome and suggested an influence of liver and hepatic Hedgehog signaling on reproduction under disease conditions.

Further, murine liver metabolism was challenged with starvation starting at different times of day. The transcriptomic results were analyzed with a self-organizing map approach, allowing an intuitive interpretation of data and a thus far unknown diurnally different response of hepatic regulatory mechanisms due to starvation was revealed. In contrast to the manifoldly published and observed switch from energy-consuming to energy-providing processes due to starvation started in the morning, evening starvation led to a novel hepatic expression signature with decreased gluconeogenic gene expression and increased levels of lipid and steroid metabolism-related genes. These differences can be explained by the equally diurnally regulated expression of the corresponding regulatory transcription factors and hormones. Additionally, lipidome analysis confirmed the diurnal differences after starvation. Thus, this study emphasized the immense impact of circadian regulation on liver metabolism and suggests high accuracy when starvation is the focus of research to avoid varying results.

LIST OF ABBREVIATIONS

CK1	casein kinase 1
CYP	cytochrome P450 enzyme
Cyp17a1	steroid 17α-hydroxylase
DHH	Desert Hedgehog
FASN	fatty acid synthase
FGF21	fibroblast growth factor 21
GLI	glioma-associated oncogene family zinc finger
GSK3	glycogen synthase kinase 3
HSD	hydroxysteroid dehydrogenase
IGF1	insulin-like growth factor 1
IGFBP1	insulin-like growth factor binding protein 1
IHH	Indian Hedgehog
KO	knockout
PCOS	polycystic ovarian syndrome
PKA	protein kinase A
PPAR	peroxisome proliferator activated receptor
PTCH	Patched
qPCR	quantitative real-time polymerase chain reaction
SAC	embryonic *Smo* knockout mice
SCN	suprachiasmatic nucleus
SHH	Sonic Hedgehog
SLC	conditional *Smo* knockout mice
SMO	Smoothened
SOM	self-organizing map
SREBP	sterol regulatory element binding protein
Star	steroidogenic acute regulatory protein
SUFU	suppressor of fused
WT	wild type

TABLE OF CONTENTS

SUMMARY

The liver is the central metabolic hub in organisms. Both the synthesis and the degradation of carbohydrates, lipids and proteins are carried out by the liver to ensure energy homeostasis. Many essential serum proteins, such as albumin and coagulation and complement factors, are synthesized and secreted by the liver. Furthermore, the liver synthesizes bile acids, which are used to eliminate metabolites and increase the solubility of lipophilic molecules in the intestine. All these functions can be simultaneously carried out by hepatocytes because of the special architecture of the tissue, which separates opposing reactions spatially.

A complex, intertwining regulatory network is the basis for efficient liver metabolism. In addition to hormones and growth factors, the morphogenic pathways Wnt/β-catenin and Hedgehog were recently identified to contribute to the regulation of the underlying genetic program. Additionally, metabolites act as signaling molecules, and the absence of food and prolonged starvation lead to regulatory mechanisms that dramatically alter liver metabolism to ensure a sufficient supply for the organism. Further, the role of the endogenous oscillation of physiological processes, called circadian rhythm, has gained much of importance in recent decades, and it was shown that the entire liver metabolism is synchronized with daytime and periods of activity. In the present thesis, the alterations in hepatocyte metabolism caused by i) changed signaling and ii) diurnally timed starvation were investigated in murine systems.

To study the role of morphogenic signaling in adult hepatocytes, mouse models with a hepatocyte-specific deletion of Smoothened (*Smo*) were established. Since the trans-membrane receptor SMO is essential to activate intracellular signaling and finally target gene expression, the Hedgehog pathway is down-regulated in these murine systems. Our previous work demonstrated a key role of hepatic Hedgehog signaling in the insulin-like growth factor axis and lipid metabolism associated with steatosis, which were new functions beside the long-known involvement in embryogenesis, regeneration and tumorigenesis. In the current work, female mice were examined, and it was possible to characterize the observed infertility and identify possible causes.

Two *Smo* knockout (KO) mouse models were used. The hepatocyte-specific *Smo* deletion was induced embryonically in the SAC mice, which were analyzed at 3 months of age. Alternatively, the KO was induced conditionally in the SLC mice after adolescence at 2 months of age to avoid the possible influence of the deleted *Smo* gene on prenatal liver development. The SLC mice were analyzed at 3 and 8 months of age. In addition to histo-

logical evaluations, the transcriptome was investigated by microarrays and quantitative real-time PCR (qPCR), and the steroid levels were determined by liquid chromatography-tandem mass spectrometry.

The embryonic KO of *Smo* in female SAC mice was associated with androgenization characterized by a 3.3-fold increase in plasma testosterone level at 3 months of age compared to that of the wild type (WT). These changes resulted from an unexpected induction of expression of genes related to sex steroid synthesis, such as the steroidogenic acute regulatory protein (*Star*) and the steroid 17α-hydroxylase (*Cyp17a1*), in hepatocytes of SAC-KO mice but not in the classic steroidogenic organs. Generally, steroidogenesis is located in the ovaries and adrenal glands, and thus far, it was assumed that steroidogenesis occurs in the liver only during embryogenesis and is down-regulated afterwards. Along with the elevated testosterone levels, infertility characterized by juvenile reproductive organs and acyclicity was observed in the female SAC-KO mice. Further, folliculogenesis was disturbed and associated with an anovulatory phenotype and lack of *corpora lutea* formation. Analysis of the SLC mice, the second *Smo* KO model, revealed that at 3 months of age, the fertility was not significantly altered, indicating that Hedgehog KO in the adult liver could not directly reverse the already initiated ovarian cycle. However, after an extended period of 8 months, the results of SAC-KO mice were confirmed in SLC-KO mice with a similar induction of steroidogenic gene expression in the liver and a reduced number of *corpora lutea* in the ovaries.

Infertility is a major medical issue, and human polycystic ovarian syndrome (PCOS) is the most common cause of this condition in women of childbearing age. PCOS is characterized by chronic anovulation, hyperandrogenism and/or polycystic ovaries and is associated with steatosis. The infertility caused by the deletion of hepatic Hedgehog signaling in the SAC-KO mice resembles the clinical symptoms of PCOS. These parallels suggest further investigation of the regulation of Hedgehog signaling and liver parameters in general in PCOS patients. Overall, down-regulation of hepatic Hedgehog signaling was shown to lead to an impaired hormonal balance by induction of steroidogenesis in the female liver and to result in androgenization and infertility. This finding indicates that the liver may influence reproduction crucially under disease conditions.

In the second part, feeding alterations were used to challenge the liver and investigate its regulatory and metabolic responses. Fasting has been studied for decades, and it is commonly accepted that upon prolonged starvation, liver metabolism switches from lipogenesis and glycogenesis to β-oxidation, gluconeogenesis and ketogenesis, which are regulated by hormones such as insulin and glucagon. It is also known that the oscillation of

processes adapts the physiology to external factors. In addition to the master regulator in the brain, the suprachiasmatic nucleus (SCN), each organ maintains its own circadian regulation coupled with that of the SCN. Beside the synchronization by the SCN, the liver clock is entrained and can be disturbed by sleeping and eating alterations, which can dramatically influence lipid homeostasis and lead to metabolic syndrome. However, knowledge of the effects of starvation started at different times of day is scarce. Thus, the present work examined the influence of diurnally timed starvation periods on liver metabolism and revealed immensely different transcriptomic and metabolic effects.

Male and non-transgenic C57BL/6N mice were starved for 24 h beginning in the morning and the evening, coupled with refeeding for different lengths of time, and were compared with *ad libitum*-fed control mice. The transcriptomic and lipidomic profiles of primary hepatocytes were analyzed on a global level. The transcriptomic results, obtained by microarrays, were analyzed with a rarely used but powerful approach called self-organizing map (SOM). SOMs are artificial neural networks used to reduce the complexity of high-dimensional data by clustering similarly expressed genes. For each resulting so-called metagene it can be determined whether its expression is higher or lower compared to the mean expression of this metagene in the analyzed pool. The metagenes are visualized on two-dimensional maps, and a color gradient indicates the expression levels. Thus, SOMs provide an overview of expression trends and allow an intuitive and unbiased interpretation of the data.

In contrast to the manifoldly published starvation response explained above, which was observed after starvation initiated in the morning, evening starvation led to a novel hepatic expression signature. The expression of gluconeogenic genes was decreased, and genes involved in β-oxidation and ketogenesis were unchanged after 24 h of starvation started in the evening compared to those of *ad libitum* samples. Genes related to lipid and steroid metabolism showed increased expression levels. Further, we showed an induction of steroidogenic gene expression, especially *Cyp17a1*, following starvation. One reason for this unexpected expression pattern may be the levels of the corresponding regulators. Key transcription factors of the hepatic fasting response include the peroxisome proliferator activated receptor (PPAR) family, whose expression was increased in a known manner after starvation started in the morning but decreased in the evening. Also the expression of fibroblast growth factor 21 (*Fgf21*), which activates gluconeogenesis and ketogenesis, was only highly elevated following morning starvation and much less in the evening. The differential regulation after morning and evening starvation was also reflected at the lipidomic level. The accumulation of hepatocellular storage lipids (triacylglycerides and cholesteryl esters) was significantly higher after the initiation of starvation in the morning compared to the evening. In a further approach, the mice were refed for 12 h and 21 h after the same 24 h

starvation period started in the evening. The gene expression pattern after 12 h of refeeding largely resembled that of the corresponding starvation state but approached the *ad libitum* control level after refeeding for 21 h.

The results demonstrate that the timing of food restriction altered the influence of starvation on hepatocytes and provide new knowledge about expression levels after starvation started and terminated in the evening. Due to differences in the timing and lengths of starvation periods used in different research groups, the variance in published results is considerable and suggests that a circadian influence cannot be neglected when different feeding regimes and starvation are the focus of research or medical treatment.

ZUSAMMENFASSUNG

Die Leber ist eines der größten Organe des Organismus und für vielfältige katabole und anabole Prozesse essentiell. Durch den Auf- und Abbau von Kohlenhydraten, Lipiden und Proteinen leistet die Leber einen entscheidenden Beitrag zur Aufrechterhaltung der Energiehomöostase. Zusätzlich synthetisiert und sekretiert sie viele essentielle Serumproteine wie Albumin, Koagulations- und Komplementfaktoren. Ferner ist die Leber für die Gallensäurebildung und damit den Fremdstoffmetabolismus unerlässlich, um Metabolite auszuscheiden und die Löslichkeit von lipophilen Molekülen im Darm zu erhöhen. Bedingt durch die einzigartige Architektur der Leber wird eine räumliche Trennung von Prozessen ermöglicht, wodurch die beschriebenen Stoffwechselreaktionen parallel ablaufen können.

Grundlage für einen effizienten Leberstoffwechsel ist eine komplexe, ineinandergreifende Regulation. Zusätzlich zu Hormonen und Wachstumsfaktoren wurden die morphogenen Signalwege Wnt/β-Catenin und Hedgehog identifiziert, die maßgeblich zur Regulation des zugrundeliegenden Transkriptoms beitragen. Auch Metabolite haben eine Signalfunktion und das Ausbleiben von Nährstoffen und Hunger sorgen für eine Adaptation des Lebermetabolismus, um auch dann eine ausreichende Energieversorgung des Körpers zu sichern. Seit einigen Jahren kommt außerdem der endogenen Oszillation von physiologischen Prozessen, der circadianen Rhythmik, eine erhöhte Beachtung zu und es wurde gezeigt, dass auch der gesamte Lebermetabolismus einer Synchronisierung in Abhängigkeit der Tageszeit und Aktivität unterliegt. In der vorliegenden Arbeit wurde die Adaptation des hepatischen Metabolismus nach 1) Eingriff in die Signalgebung und 2) zu verschiedenen Tageszeiten begonnenen Hungerphasen im murinen System untersucht.

Um die Bedeutung des morphogenen Hedgehog-Signalwegs in der adulten Leber zu erforschen, wurden transgene Mäuse mit einer hepatozytenspezifischen Deletion von *Smoothened* (*Smo*) gezüchtet. Da der Transmembranrezeptor SMO essentiell für die Aktivierung des intrazellulären Signalwegs und der Zielgenexpression ist, wird der Hedgehog-Signalweg in diesen Mausmodellen inhibiert. In früheren Arbeiten konnten wir dadurch zeigen, dass der hepatische Hedgehog-Signalweg die *Insulin-like growth factor* Expression reguliert und den Lipidmetabolismus so beeinflusst, dass es zur Ausbildung einer Lipidakkumulation in der Leber (Steatose) kommt. In der vorliegenden Arbeit konnte die zusätzlich auftretende Infertilität der weiblichen transgenen Mäuse charakterisiert werden.

Für die Untersuchungen wurden zwei Mausmodelle mit hepatozytenspezifischem *Smo* Knock-out (KO) verwendet. In den SAC-Mäusen wurde *Smo* während der embryonalen Ent-

wicklung ausgeschaltet und die Mäuse wurden im Alter von drei Monaten analysiert. In den SLC-Mäusen wurde der KO nach Abschluss der Wachstumsphase im Alter von zwei Monaten induziert, um einen möglichen Einfluss der *Smo* Deletion auf die pränatale Leberentwicklung auszuschließen. Die SLC-Mäuse wurden ebenfalls im Alter von drei und zusätzlich nach acht Monaten untersucht. Neben histologischen Untersuchungen wurde das Transkriptom mittels Microarray und quantitativer *real-time* PCR (qPCR) analysiert sowie die Konzentration der Steroidhormone durch Flüssigkeitschromatografie gekoppelt mit Massenspektrometrie bestimmt.

Der embryonale *Smo* KO in den weiblichen SAC-Mäusen ging mit einer Androgenisierung einher, die durch eine 3,3-fache Erhöhung der Testosteronkonzentration im Plasma gekennzeichnet war. Dieser Anstieg war die Folge einer unerwarteten Aktivierung der Expression von Genen der Steroidhormonsynthese, wie des *steroidogenic acute regulatory protein* (*Star*) und der Steroid-17α-Hydroxylase (*Cyp17a1*), die ausschließlich in den Hepatozyten der SAC-KO-Mäuse jedoch nicht in den Gonaden beobachtet wurde. Grundsätzlich ging man davon aus, dass die Steroidhormonsynthese in den Ovarien und Nebennieren stattfindet und in der Leber nur während der Embryonalentwicklung eine Rolle spielt. Die enorme Erhöhung der Testosteronwerte wurde als wesentliche Ursache von unvollständig entwickelten Reproduktionsorganen und der damit einhergehenden Infertilität in den SAC-KO-Mäusen identifiziert. Es wurde weder ein Menstruationszyklus noch eine vollständige Follikelreifung beobachtet, sodass keine Ovulation und Entstehung von Gelbkörpern festgestellt werden konnten. Analoge Untersuchungen an den SLC-Mäusen, dem zweiten *Smo* KO Mausmodell, im Alter von drei Monaten zeigten keine signifikante Beeinflussung der Fertilität, da vermutlich die Hedgehog-Inhibition in der adulten Leber einen bereits begonnenen Ovarialzyklus nicht beeinflussen kann. Dahingegen konnten nach acht Monaten die Ergebnisse der SAC-KO-Mäuse bestätigt werden. In den SLC-KO-Mäusen wurde ebenfalls eine Induktion von Genen der Steroidhormonsynthese in Hepatozyten und eine signifikant verminderte Anzahl von Gelbkörpern in den Ovarien nachgewiesen.

Infertilität ist ein bedeutsames medizinisches Thema und das humane polyzystische Ovar Syndrom (PCOS) ihre häufigste Ursache bei Frauen im gebärfähigen Alter. PCOS ist gekennzeichnet durch chronische Zyklusstörung, erhöhte Androgenspiegel und/oder polyzystische Ovarien häufig einhergehend mit Steatose. Die durch die hepatische Deletion des Hedgehog-Signalwegs ausgelöste Infertilität der SAC-KO-Mäuse ähnelt dem klinischen Bild der PCOS sehr stark. Diese Parallelen legen Untersuchungen der Regulation des Hedgehog-Signalwegs und allgemeinen Leberparametern in PCOS Patientinnen nahe. Außerdem zeigen die Ergebnisse, dass die Leber die Reproduktion entscheidend beeinflussen kann, wenn krankhafte Veränderungen im Organismus vorliegen.

Im zweiten Teil der Studie wurden Veränderungen in der Fütterung von Mäusen genutzt, um die darauffolgende regulatorische und metabolische Reaktion der Leber zu untersuchen. Der Einfluss von Hunger wird seit Jahrzehnten untersucht und es ist allgemein anerkannt, dass der Lebermetabolismus durch längere Hungerphasen von der Lipid- und Glykogensynthese auf β-Oxidation, Gluconeogenese und Ketogenese umschaltet. Dies wird durch Hormone wie Insulin und Glucagon reguliert. Außerdem ist bekannt, dass durch circadiane Regulationsmechanismen physiologische Prozesse an veränderte Umweltbedingungen angepasst werden. Zusätzlich zu dem Nucleus suprachiasmaticus (SCN) im Gehirn, dem übergeordneten Regulator der circadianen Rhythmik, generiert jedes Organ eine eigene Rhythmik. Neben der Synchronisierung mit dem SCN kann die Leberrhythmik durch Veränderungen im Schlaf- und Essverhalten beeinflusst oder gar gestört werden, was große Auswirkungen auf die Lipidhomöostase hat und zum metabolischen Syndrom führen kann. Das Wissen hinsichtlich des unterschiedlichen Einflusses von zu verschiedenen Tageszeiten gestarteten Hungerperioden ist jedoch sehr gering, sodass in der vorliegenden Arbeit die zugrundeliegende Regulation des Lebermetabolismus untersucht wurde.

Dazu wurde männlichen, nicht-transgenen C57BL/6N Mäusen, beginnend am Morgen und am Abend, das Futter für 24 h entzogen. Zusätzlich wurden Mäuse nach der Hungerphase für verschiedene Perioden wieder gefüttert. Als Kontrolle erhielt eine dritte Gruppe das Futter *ad libitum*. Das Transkriptom und das Lipidspektrum der primären Hepatozyten wurden anschließend umfassend untersucht. Die Expressionsdaten wurden mittels Microarrays erhoben und mit Selbstorganisierenden Karten (SOM), einer wenig verwendeten aber wirkungsvollen Methode, analysiert. SOMs sind künstliche neuronale Netzwerke, die es ermöglichen Gene mit ähnlichem Expressionsprofilen zu Metagenen zu gruppieren und so die Komplexität von Daten zu verringern. Für jedes resultierende Metagen kann definiert werden, ob dessen Expression höher oder niedriger ist, verglichen mit der durchschnittlichen Expression dieses Metagens in allen untersuchten Proben. Die Metagene werden auf einer zweidimensionalen Karte dargestellt, wobei ein Farbgradient das Expressionslevel widerspiegelt. Dadurch bietet die SOM einen intuitiven und unverzerrten Überblick über die Expressionssignatur und erlaubt einfachere Vergleiche zwischen einzelnen Experimenten.

Entgegen der vielfach publizierten Regulationen in Folge von Hunger, die weiter oben beschrieben und nach der am Morgen begonnenen Hungerphase beobachtet wurden, zeigte die am Abend initiierte 24-stündige Hungerphase eine andere, neue Expressionssignatur. Dabei wurde die Expression von Genen der Gluconeogenese herunterreguliert. Gene der β-Oxidation sowie Ketogenese waren dabei unverändert verglichen mit der Expression in *ad libitum* gefütterten Mäusen. Gene verantwortlich für den Lipid- und Steroidmetabolismus wurden hingegen höher exprimiert. Auch die Expression der Gene, die für die Steroid-

hormonsynthese nötig sind und insbesondere *Cyp17a1*, war erhöht durch diese Hungerphase. Ein Grund für dieses unerwartete Expressionsmuster könnten die Level der dazugehörigen Regulatoren sein. Die Mitglieder der Peroxisom-Proliferator-aktivierten Rezeptoren (PPAR) Familie sind entscheidende Transkriptionsfaktoren bei der Anpassung des Lebermetabolismus an Hunger und zeigten die bekannte erhöhte Expression nach der Hungerphase am Morgen, wohingegen am Abend eine reduzierte Expression nachgewiesen wurde. Auch der Fibroblasten-Wachstumsfaktor 21 (*Fgf21*), der für die Aktivierung von Gluconeogenese und Ketogenese unerlässlich ist, wurde nur nach der morgendlichen Hungerphase deutlich erhöht exprimiert, zeigt am Abend jedoch lediglich einen geringen Anstieg. Die unterschiedliche Regulation in Folge von Hunger beginnend am Morgen und am Abend wurde auch in den Lipidprofilen der Hepatozyten deutlich. Die Akkumulation von hepatischen Speicherlipiden, wie Triacylglyceriden und Cholesterinestern, war signifikant höher nach der Hungerphase, die am Morgen begonnen hat, als nach der am Abend. In einem weiteren Versuch wurde Mäusen nach der gleichen 24-stündigen Hungerphase beginnend am Abend entweder 12 h oder 21 h wieder Zugang zu Futter ermöglicht. Das Muster der Genexpression nach 12 h Fütterung glich größtenteils dem der dazugehörigen Hungerphase, wohingegen nach 21 h eine Annäherung an die Expression der *ad libitum* Kontrolle erfolgte.

Die Ergebnisse zeigen, dass die Uhrzeit des Nahrungsentzugs die Reaktion der Leber deutlich beeinflusst und liefern somit neue Erkenntnisse über die Effekte von einer am Abend begonnenen Hungerphase. Durch die unterschiedlichen Startzeiten und Längen von Hungerphasen, die in verschiedenen Forschungsgruppen verwendet werden, ist die Varianz in publizierten Ergebnissen sehr hoch. Dies legt nahe, dass es essentiell ist, auf den circadianen Einfluss zu achten, wenn verschiedene Fütterungsregime und Hunger in der Forschung oder Medizin untersucht werden.

INTRODUCTION

Liver architecture and metabolism

In mammals, the liver has a central role in orchestrating metabolic processes. This role is realized by hepatocytes, representing approximately 70% of the total cell quantity (Jungermann et al., 1986). On one hand, the liver is the center of regulating energy homeostasis. Nutrients absorbed by the intestine are carried to the liver by the portal vein. Dependent on the energy balance, hepatocytes store excess glucose as glycogen and synthesize fatty acids or secrete glucose originating from glycogenolysis and gluconeogenesis and metabolize lipids (Rui, 2014). On the other hand, the liver produces essential serum proteins, including albumin, coagulation and complement factors and growth factors, such as insulin-like growth factor 1 (IGF1) (Heinrich et al., 2014). In addition, the liver is essential for bile acid synthesis coupled with detoxification and xenobiotic metabolism.

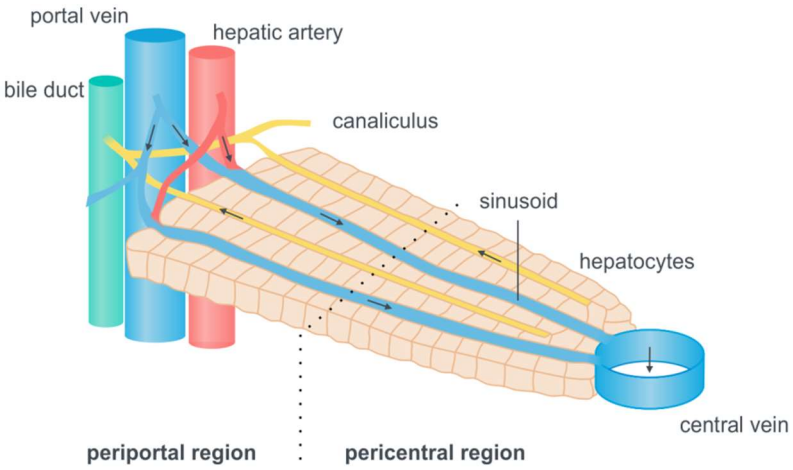

Figure 1. Architecture of the liver lobule. The liver consists of liver lobules. The blood of a branch of the portal vein and the liver artery (periportal region) flows through the sinusoids, which are wrapped up with hepatocytes and is collected in the central vein (pericentral region). Bile acids are secreted to the canaliculi, which enter a bile duct. The arrows indicate the flow direction.

The special architecture of the liver thereby allows the simultaneous performance of these diverse functions. The smallest units of the liver are the liver lobules, which have an almost hexagonal shape. Each lobule is characterized by the portal triads at the corners with a branch of the portal vein and the hepatic artery, delivering the blood, and a bile duct, collecting the produced bile acids. Each lobule is crossed by radially arranged sinusoids, the smallest capillary of the liver. In the sinusoids, nutrient-rich blood from the portal vein and oxygen-rich blood of the artery pass through towards the central vein (Ishibashi et al., 2009). Along all sinusoids formed by endothelial cells, hepatocytes are located, exchanging metabolites with the blood (Figure 1).

Diverse possibilities of liver metabolism regulation

Liver metabolism needs to be regulated to ensure i) efficient processes within the hepatocytes and ii) the adaption to the requirements of the entire organism.

The first point is guaranteed by the so-called metabolic zonation. Even if the hepatocytes along the sinusoids appear homogeneous by light microscopy, they are enormously heterogeneous on the cellular level with regard to the achieved physiological functions. The partially energetic opposing, biochemical processes are localized in different parts of the parenchyma. In the periportal region around the portal triads, gluconeogenesis, fatty acid oxidation and urea synthesis occur, while the hepatocytes around the central vein in the pericentral region carry out glucose uptake, bile acid synthesis and biotransformation (Gebhardt, 1992). In recent decades, many concepts have been postulated regarding how metabolic zonation is established and maintained in the liver parenchyma. In addition to gradients of nutrients, oxygen and hormones, the morphogenic Wnt/β-catenin signaling pathway was identified as a major regulator of zonation and the underlying genetic program (Benhamouche et al., 2006; Kietzmann, 2017).

Concerning the adjustment of liver metabolism to the organism's needs, on one hand, hormones and growth factors are responsible, as well as metabolites acting as signaling molecules, such as bile acids, which were recently shown to regulate nutrient absorption and homeostasis in addition to their long-known function as solubilizers in the intestine (Chiang, 2013). On the other hand, environmental factors, such as the diet and circadian rhythms, make a significant contribution to liver metabolism regulation.

Connection of Hedgehog signaling to hepatic metabolism

In addition to the Wnt/β-catenin signaling, the morphogenic Hedgehog pathway was recently associated to liver metabolism regulation (Gebhardt and Matz-Soja, 2014). Generally, the Hedgehog pathway, initially discovered in *Drosophila melanogaster* (Nüsslein-Volhard and Wieschaus, 1980), is involved in various developmental processes during embryogenesis (Ingham and McMahon, 2001). In the adult organism, the Hedgehog pathway retains its function to regulate proliferative processes of stem cells and regeneration, but malfunction leads to malignant degeneration of cells and tumor development (Fattahi et al., 2018). In the adult liver, non-parenchymal cells (stellate cells and cholangiocytes) are known to express Hedgehog pathway components. In particular, if regenerative processes are activated, such as after partial hepatectomy, this pathway is essential (Ochoa et al., 2010). However, the expression of Hedgehog components in hepatocytes is at a lower level and was controversial for a long time (Omenetti et al., 2011; Kietzmann, 2017). With the establishment of trans-

genic mouse models with a hepatocyte-specific knockout (KO) of Smoothened (*Smo*), it was possible to show the relevance of Hedgehog signaling in hepatocytes.

First, some mechanistic details about the pathway will help to understand the regulation in the mouse models. The impact of canonical Hedgehog signaling is mediated by activator and repressor forms of the glioma-associated oncogene family zinc finger (GLI) transcription factors, which in turn depend on ligand binding. If the signaling pathway is inactive, the twelve-pass transmembrane receptors Patched 1 and 2 (PTCH1 and PTCH2) inhibit the G protein-coupled receptor SMO (Figure 2A). Consequently, a complex of kinases consisting of protein kinase A (PKA), casein kinase 1 (CK1) and glycogen synthase kinase 3 (GSK3) phosphorylates the GLI transcription factors at six conserved serine residues, which lead to truncated GLI2 and GLI3 proteins lacking the transactivation domain and repressing target gene expression, while GLI1 is totally degraded (Wang et al., 2000; Pan et al., 2009).

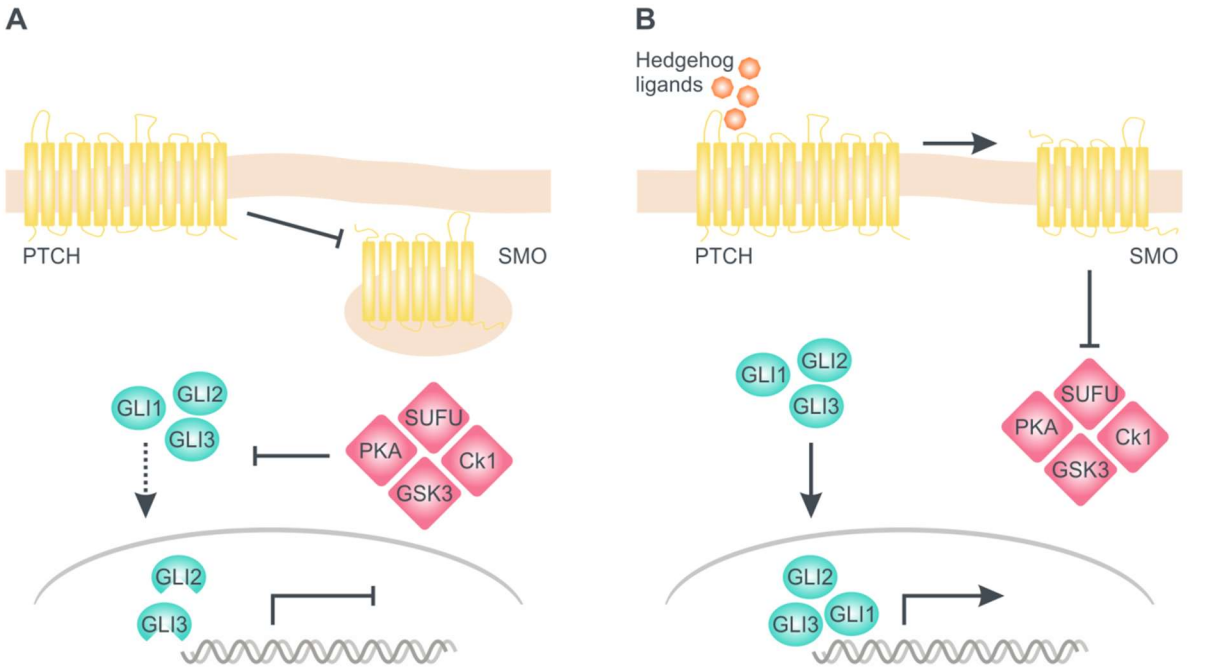

Figure 2. Hedgehog signaling pathway. (**A**) If no ligand is bound, PTCH inhibits SMO, which allows the kinase complex (PKA, CK1, GSK3) to phosphorylate the GLI transcription factors. The resulting truncated proteins GLI2 and GLI3 repress target gene expression. (**B**) By binding of Hedgehog ligands (IHH, SHH, DHH) to the PTCH receptors, the inhibition of SMO is abrogated, and SMO in turn inhibits the kinase complex and SUFU. Consequently, GLI transcription factors accumulate and activate target gene expression.

To activate the Hedgehog pathway in vertebrates, the ligands Indian (IHH), Sonic (SHH) and Desert Hedgehog (DHH) need to undergo cholesterol-dependent self-cleavage and palmitoylation (Chen et al., 2011). These modified ligands bind to their PTCH receptors, which

subsequently abrogate the repression of SMO (Figure 2B). Consequently, SMO translocates into the membrane and induces the intracellular signaling cascade. The GLI transcription factors are no longer bound by the negative regulator suppressor of fused (SUFU), and the kinases are inhibited (Humke et al., 2010). However, neither the interaction of PTCH and SMO nor the inhibition of the kinase complex by SMO are fully understood so far (Taipale et al., 2002; Teperino et al., 2014). In particular, the regulation of PKA prevents the phosphorylation of GLI transcription factors at the six repressing residues mentioned above. However, other sites need to be phosphorylated to fully activate the GLI transcription factors so that a rearrangement of the phosphorylation pattern controls the signaling (Niewiadomski et al., 2014). Furthermore, the ratio of the individual GLI transcription factors seems to be critical for activating or repressing Hedgehog target genes (Ruiz i Altaba, 1999; Schmidt-Heck et al., 2015). The identified target genes include pathway components itself such as *Ptch1* and *Gli1*, cell cycle regulators (*Myc*, *Cyclin D*, and *E*) and *Wnt* ligands (Cohen, 2003; Ingham, 2012).

The *Smo* KO mouse models showed that, independent of an embryonic (SAC mice) or conditional KO (SLC mice), Hedgehog signaling is down-regulated specifically in hepatocytes and revealed its immense impact on the balance of liver metabolism and zonation. Associated with the KO, the IGF axis is dysregulated and results in significantly reduced *Igf1* and increased *Igfbp1* gene expression in hepatocytes with analogous changes in the serum levels (Matz-Soja et al., 2014). Further, without any nutritional impact, the KO mice develop steatosis, an accumulation of lipids in hepatocytes. Central metabolic transcription factors, such as members of the peroxisome proliferator activated receptor (PPAR) and the sterol regulatory element binding protein (SREBP) family, and enzymes, such as fatty acid synthase (FASN), exhibit significantly increased gene and protein expression in the liver, and their distinct zonation is abolished. A possible cause is a changed ratio of the GLI transcription factors in the KO mice, which is critical to balance the Hedgehog regulation (Matz-Soja et al., 2016).

Studying the *Smo* KO mice revealed that the female SAC-KO mice are infertile, which needs to be investigated in detail. Further, microarray studies have suggested that Hedgehog signaling is involved in the regulation of steroidogenesis in the liver. During the synthesis of sex steroids, different cytochrome P450 enzymes (CYPs) and hydroxysteroid dehydrogenase (HSDs) finally convert cholesterol to testosterone and estradiol. Generally, the synthesis of sex steroids is located in the gonads, and it was assumed that steroidogenesis occurs in the liver only during embryogenesis and is down-regulated afterwards (Pezzi et al., 2003).

Impact of feeding schemes on hepatic metabolism

Previous studies have shown that the expression of steroidogenic enzymes is induced in the liver due to starvation (Grasfeder et al., 2009) and demonstrated that under special conditions, the liver is involved in sex steroid synthesis. It was speculated that steroids mediate starvation-dependent signaling. When the metabolic state is altered by environmental cues and nutrient availability, all tissues need to adapt their metabolism to allow a homeostatic response. In the case of starvation, the liver is the most prominent target because of its central role in energy homeostasis. Generally, in the postprandial state, the liver stores excessive metabolites or forwards them to storage organs, such as adipose tissue. During starvation, the liver releases glucose originating from glycogenolysis or gluconeogenesis, degrades lipids and synthesizes ketone bodies (Rui, 2014). At a systemic level, hormones, such as insulin and glucagon, balance metabolism. Molecular regulation is carried out by transcription factors such as the PPAR and SREBP families.

Not only the availability of food but also the circadian clock regulates liver metabolism. Most processes have an endogenous oscillation of approximately 24 h, called circadian rhythm, which links body physiology with external conditions. Most prominent is the light-dark signal, which synchronizes the master clock in the brain, the suprachiasmatic nucleus (SCN). The SCN generates endocrine output signals coupling the central pacemaker with the peripheral tissues. Based on these signals, organs, such as the liver, synchronize their own circadian oscillation (Albrecht, 2012). The entire liver metabolism was shown to be synchronized with daytime and periods of activity based on tightly regulated transcription and translation (Reinke and Asher, 2016). In addition to the SCN synchronization, the liver clock is also entrained and can be disturbed by external factors. Short-term or chronic sleeping disturbances, as with jet lag and shift work, were shown to be associated with dramatic alterations in lipid homeostasis and an increased incidence of metabolic syndrome in mice and humans (Ferrell and Chiang, 2015a, 2015b). Furthermore, the consumed food volume and the starvation intervals between the meals can alter the liver clock (Vollmers et al., 2009; Hirao et al., 2010), and restricted feeding is even able to rapidly uncouple the liver rhythm from that of the SCN (Stokkan et al., 2001). Although starvation has been studied for decades, knowledge of how the diurnal timing of starvation periods influences the hepatic starvation response is scarce.

Aims of the thesis

Liver physiology is regulated by multiple mechanisms to ensure efficient metabolism within the cells and adequate supply to the organism. Recently, it has been shown that morphogenic signaling pathways are involved in the adaption of liver metabolism. The role of the hepatic Hedgehog pathway was already characterized concerning lipid metabolism and the control of the IGF-axis in hepatocyte-specific *Smo* KO mouse models. Thus far, primary male mice have been studied. In the first part of this thesis, female SAC mice should be characterized further. The reason for the observed infertility of the female SAC-KO mice and the role of the liver in steroidogenesis should be elucidated. Additionally, the phenotype of the embryonic *Smo* KO in SAC mice should be compared with that of a conditional KO induced after adolescence in the SLC mice.

Various research initiatives have shown the relevance of circadian rhythms for almost all physiological processes. Even though starvation has been the focus of research for decades, the knowledge of how circadian regulation influences the hepatic starvation response is scarce. In the second part of the thesis, the effects of starvation started at different daytimes and the role of liver in steroidogenesis under fasting conditions should be studied in detail. Non-transgenic mice should be challenged with 24 h starvation starting either in the morning or in the evening. In a second approach, mice should be refed to estimate the duration required to restore the metabolic *ad libitum* profile. The translational and metabolic alterations in primary hepatocytes should be studied using different omics approaches. The transcriptome should be analyzed using self-organizing maps (SOM), a powerful approach visualizing transcriptional changes by clustering similarly expressed genes.

References

Albrecht U (2012). Timing to perfection: The biology of central and peripheral circadian clocks. *Neuron* 74, 246–260. doi: 10.1016/j.neuron.2012.04.006

Benhamouche S, Decaens T, Godard C, Chambrey R, Rickman D, Moinard C, Vasseur-Cognet M, Kuo C, Kahn A, Perret C, and Colnot S (2006). Apc tumor suppressor gene is the "zonation-keeper" of mouse liver. *Dev Cell* 10, 759–770. doi: 10.1016/j.devcel.2006.03.015

Chen X, Tukachinsky H, Huang C-H, Jao C, Chu Y-R, Tang H-Y, Mueller B, Schulman S, Rapoport T, and Salic A (2011). Processing and turnover of the Hedgehog protein in the endoplasmic reticulum. *J Cell Biol* 192, 825–838. doi: 10.1083/jcb.201008090

Chiang J (2013). Bile acid metabolism and signaling. *Compr Physiol* 3, 1191–1212. doi: 10.1002/cphy.c120023

Cohen M (2003). The hedgehog signaling network. *Am J Med Genet A* 123A, 5–28. doi: 10.1002/ajmg.a.20495

Fattahi S, Pilehchian Langroudi M, and Akhavan-Niaki H (2018). Hedgehog signaling pathway: Epigenetic regulation and role in disease and cancer development. *J Cell Physiol*. doi: 10.1002/jcp.26506

Ferrell J, and Chiang J (2015a). Circadian rhythms in liver metabolism and disease. *Acta Pharm Sin B* 5, 113–122. doi: 10.1016/j.apsb.2015.01.003

Ferrell J, and Chiang J (2015b). Short-term circadian disruption impairs bile acid and lipid homeostasis in mice. *Cell Mol Gastroenterol Hepatol* 1, 664–677. doi: 10.1016/j.jcmgh.2015.08.003

Gebhardt R (1992). Metabolic zonation of the liver: regulation and implications for liver function. *Pharmacol Ther* 53, 275–354. doi: 10.1016/0163-7258(92)90055-5

Gebhardt R, and Matz-Soja M (2014). Liver zonation: Novel aspects of its regulation and its impact on homeostasis. *World J Gastroenterol* 20, 8491–8504. doi: 10.3748/wjg.v20.i26.8491

Grasfeder L, Gaillard S, Hammes S, Ilkayeva O, Newgard C, Hochberg R, Dwyer M, Chang C-Y, and McDonnell D (2009). Fasting-induced hepatic production of DHEA is regulated by PGC-1alpha, ERRalpha, and HNF4alpha. *Mol Endocrinol* 23, 1171–1182. doi: 10.1210/me.2009-0024

Heinrich P, Müller M, Graeve L, and Löffler G (2014). Löffler/Petrides Biochemie und Pathobiochemie. *Berlin*: *Springer*.

Hirao A, Nagahama H, Tsuboi T, Hirao M, Tahara Y, and Shibata S (2010). Combination of starvation interval and food volume determines the phase of liver circadian rhythm in Per2:Luc knock-in mice under two meals per day feeding. *Am J Physiol Gastrointest Liver Physiol* 299, G1045-53. doi: 10.1152/ajpgi.00330.2010

Humke E, Dorn K, Milenkovic L, Scott M, and Rohatgi R (2010). The output of Hedgehog signaling is controlled by the dynamic association between Suppressor of Fused and the Gli proteins. *Genes Dev* 24, 670–682. doi: 10.1101/gad.1902910

Ingham P (2012). Hedgehog signaling. *Cold Spring Harb Perspect Biol* 4. doi: 10.1101/cshperspect.a011221

Ingham P, and McMahon A (2001). Hedgehog signaling in animal development: Paradigms and principles. *Genes Dev* 15, 3059–3087. doi: 10.1101/gad.938601

Ishibashi H, Nakamura M, Komori A, Migita K, and Shimoda S (2009). Liver architecture, cell function, and disease. *Semin Immunopathol* 31, 399–409. doi: 10.1007/s00281-009-0155-6

Jungermann K, Kauffman F, and Thurman R (1986). Regulation of Hepatic Metabolism: Intra- and Intercellular Compartmentation. *Boston, MA*: *Springer US*.

Kietzmann T (2017). Metabolic zonation of the liver: The oxygen gradient revisited. *Redox Biol* 11, 622–630. doi: 10.1016/j.redox.2017.01.012

Matz-Soja M, Aleithe S, Marbach E, Böttger J, Arnold K, Schmidt-Heck W, Kratzsch J, and Gebhardt R (2014). Hepatic Hedgehog signaling contributes to the regulation of IGF1 and IGFBP1 serum levels. *Cell Commun Signal* 12, 11. doi: 10.1186/1478-811X-12-11

Matz-Soja M, Rennert C, Schönefeld K, Aleithe S, Boettger J, Schmidt-Heck W, Weiss T, Hovhannisyan A, Zellmer S, Klöting N, Schulz A, Kratzsch J, Guthke R, and Gebhardt R (2016). Hedgehog signaling is a potent regulator of liver lipid metabolism and reveals a GLI-code associated with steatosis. *Elife* 5. doi: 10.7554/eLife.13308

Niewiadomski P, Kong J, Ahrends R, Ma Y, Humke E, Khan S, Teruel M, Novitch B, and Rohatgi R (2014). Gli protein activity is controlled by multisite phosphorylation in vertebrate Hedgehog signaling. *Cell Rep* 6, 168–181. doi: 10.1016/j.celrep.2013.12.003

Nüsslein-Volhard C, and Wieschaus E (1980). Mutations affecting segment number and polarity in Drosophila. *Nature* 287, 795–801. doi: 10.1038/287795a0

Ochoa B, Syn W-K, Delgado I, Karaca G, Jung Y, Wang J, Zubiaga A, Fresnedo O, Omenetti A, Zdanowicz M, Choi S, and Diehl A (2010). Hedgehog signaling is critical for normal liver regeneration after partial hepatectomy in mice. *Hepatology* 51, 1712–1723. doi: 10.1002/hep.23525

Omenetti A, Choi S, Michelotti G, and Diehl A (2011). Hedgehog signaling in the liver. *J Hepatol* 54, 366–373. doi: 10.1016/j.jhep.2010.10.003

Pan Y, Wang C, and Wang B (2009). Phosphorylation of Gli2 by protein kinase A is required for Gli2 processing and degradation and the Sonic Hedgehog-regulated mouse development. *Dev Biol* 326, 177–189. doi: 10.1016/j.ydbio.2008.11.009

Pezzi V, Mathis JM, Rainey W, and Carr B (2003). Profiling transcript levels for steroidogenic enzymes in fetal tissues. *J Steroid Biochem Mol Biol* 87, 181–189. doi: 10.1016/j.jsbmb.2003.07.006

Reinke H, and Asher G (2016). Circadian Clock Control of Liver Metabolic Functions. *Gastroenterology* 150, 574–580. doi: 10.1053/j.gastro.2015.11.043

Rui L (2014). Energy metabolism in the liver. *Compr Physiol* 4, 177–197. doi: 10.1002/cphy.c130024

Ruiz i Altaba A (1999). Gli proteins and Hedgehog signaling: Development and cancer. *Trends Genet* 15, 418–425. doi: 10.1016/S0168-9525(99)01840-5

Schmidt-Heck W, Matz-Soja M, Aleithe S, Marbach E, Guthke R, and Gebhardt R (2015). Fuzzy modeling reveals a dynamic self-sustaining network of the GLI transcription factors controlling important metabolic regulators in adult mouse hepatocytes. *Mol Biosyst* 11, 2190–2197. doi: 10.1039/c5mb00129c

Stokkan K, Yamazaki S, Tei H, Sakaki Y, and Menaker M (2001). Entrainment of the circadian clock in the liver by feeding. *Science* 291, 490–493. doi: 10.1126/science.291.5503.490

Taipale J, Cooper M, Maiti T, and Beachy P (2002). Patched acts catalytically to suppress the activity of Smoothened. *Nature* 418, 892–897. doi: 10.1038/nature00989

Teperino R, Aberger F, Esterbauer H, Riobo N, and Pospisilik J (2014). Canonical and non-canonical Hedgehog signalling and the control of metabolism. *Semin Cell Dev Biol* 33, 81–92. doi: 10.1016/j.semcdb.2014.05.007

Vollmers C, Gill S, DiTacchio L, Pulivarthy S, Le H, and Panda S (2009). Time of feeding and the intrinsic circadian clock drive rhythms in hepatic gene expression. *Proc Natl Acad Sci U S A* 106, 21453–21458. doi: 10.1073/pnas.0909591106

Wang B, Fallon J, and Beachy P (2000). Hedgehog-Regulated Processing of Gli3 Produces an Anterior/Posterior Repressor Gradient in the Developing Vertebrate Limb. *Cell* 100, 423–434. doi: 10.1016/S0092-8674(00)80678-9

CHAPTER 1

Conditional loss of hepatocellular Hedgehog signaling in female mice leads to the persistence of hepatic steroidogenesis, androgenization and infertility

Rennert C and Eplinius F, Hofmann U, Johänning J, Rolfs F, Schmidt-Heck W, Guthke R, Gebhardt R, Ricken AM, Matz-Soja M (2017) *Conditional loss of hepatocellular Hedgehog signaling in female mice leads to the persistence of hepatic steroidogenesis, androgenization and infertility.* Archives of Toxicology 91(11):3677-3687. doi: 10.1007/s00204-017-1999-5

Arch Toxicol
DOI 10.1007/s00204-017-1999-5

ORGAN TOXICITY AND MECHANISMS

Conditional loss of hepatocellular Hedgehog signaling in female mice leads to the persistence of hepatic steroidogenesis, androgenization and infertility

Christiane Rennert[1] · Franziska Eplinius[2] · Ute Hofmann[3] · Janina Johänning[3] · Franziska Rolfs[4] · Wolfgang Schmidt-Heck[5] · Reinhardt Guthke[5] · Rolf Gebhardt[1] · Albert M. Ricken[2] · Madlen Matz-Soja[1]

Received: 6 April 2017 / Accepted: 22 May 2017

Abstract The Hedgehog signaling pathway is known to be involved in embryogenesis, tissue remodeling, and carcinogenesis. Because of its involvement in carcinogenesis, it seems an interesting target for cancer therapy. Indeed, Sonidegib, an approved inhibitor of the Hedgehog receptor Smoothened (*Smo*), is highly active against diverse carcinomas, but its use is also reported to be associated with several systemic side effects. Our former work in adult mice demonstrated hepatic Hedgehog signaling to play a key role in the insulin-like growth factor axis and lipid metabolism. The current work using mice with an embryonic and hepatocyte-specific *Smo* deletion describes an adverse impact of the hepatic Hedgehog pathway on female fertility. In female SAC-KO mice, we detected androgenization characterized by a 3.3-fold increase in testosterone at 12 weeks of age based on an impressive induction of steroidogenic gene expression in hepatocytes, but not in the classic steroidogenic organs (ovary and adrenal gland). Along with the elevated level of testosterone, the female SAC-KO mice showed infertility characterized by juvenile reproductive organs and acyclicity. The endocrine and reproductive alterations resembled polycystic ovarian syndrome and could be confirmed in a second mouse model with conditional deletion of *Smo* at 8 weeks of age after an extended period of 8 months. We conclude that the down-regulation of hepatic Hedgehog signaling leads to an impaired hormonal balance by the induction of steroidogenesis in the liver. These effects of Hedgehog signaling inhibition should be considered when using Hedgehog inhibitors as anti-cancer drugs.

Keywords Liver · Hedgehog pathway · Hepatic steroidogenesis · Androgenization · Estrus cycle · Infertility

Christiane Rennert and Franziska Eplinius contributed equally as first authors.

Rolf Gebhardt, Albert M. Ricken and Madlen Matz-Soja contributed equally as senior authors.

Electronic supplementary material The online version of this article (doi:10.1007/s00204-017-1999-5) contains supplementary material, which is available to authorized users.

✉ Madlen Matz-Soja
madlen.matz@medizin.uni-leipzig.de

[1] Rudolf-Schönheimer-Institute of Biochemistry, Faculty of Medicine, Leipzig University, Johannisallee 30, 04103 Leipzig, Germany

[2] Institute of Anatomy, Faculty of Medicine, Leipzig University, Liebigstrasse 13, 04103 Leipzig, Germany

[3] Dr. Margarete Fischer-Bosch Institute of Clinical Pharmacology, University of Tübingen, Auerbachstrasse 112, 70376 Stuttgart, Germany

[4] Department of Visceral, Transplantation, Thoracic and Vascular Surgery, University Hospital Leipzig, Liebigstrasse 19, 04103 Leipzig, Germany

[5] Leibniz Institute for Natural Product Research and Infection Biology, Hans Knöll Institute, Beutenbergstrasse 11a, 07745 Jena, Germany

Introduction

The liver is an organ with a huge variety of metabolic functions, i.e., the control of glucose homeostasis by regulating glycogenolysis and gluconeogenesis (Han et al. 2016) as well as lipid metabolism, including de novo lipogenesis and β-oxidation (Ameer et al. 2014). Furthermore, hepatocytes are a major player in the metabolization of xenobiotics (Almazroo et al. 2017) and have the ability for autophagy (Ueno and Komatsu 2017; Gebhardt and Coffer

Published online: 30 May 2017

2013). Morphogenic pathways were recently demonstrated to be key players in the fine tuning of most of these metabolic processes. For example, Wnt/β-catenin signaling contributes to the homeostasis of hepatic glucose and ammonia metabolism (Monga 2011; Sethi and Vidal-Puig 2010). Additionally, we could show the involvement of Hedgehog (Hh) signaling in the regulation of central metabolic processes in the adult liver (Matz-Soja et al. 2013, 2014, 2016).

In mammals, the Hh pathway can act in a canonical and in two non-canonical ways that are reviewed in detail by Teperino et al. (Teperino et al. 2014). Because the canonical pathway seems to be the preferred one in hepatocytes, the following work was focused on the transcriptional effects of the canonical Hh pathway, but it cannot be ruled out that non-canonical influences occur as well. In healthy hepatocytes, mostly the ligand Indian Hedgehog (IHH) binds to the receptor proteins Patched 1 (PTCH1) and Patched 2 (PTCH2) and activates the signaling cascade by influencing the co-receptor Smoothened (SMO). Finally, these changes lead to a shift in the signature of the three transcription factors, the glioma-associated oncogene homologs 1, 2 and 3 (GLI1/2/3) (Matz-Soja et al. 2016). The GLI factors form a stable expression network with a specific code, resulting in the activation or repression of Hh target genes (Stecca and Ruiz I Altaba 2010; Aberger and Ruiz I Altaba 2014; Schmidt-Heck et al. 2015). Because Hh signaling is activated in approximately 25% of all cancer deaths (Hovhannisyan et al. 2009), the pathway, and especially SMO, is a highly interesting target for treatment, so that SMO inhibitors such as cyclopamine, vismodegib and sonidegib are tested in clinical trials (Robinson et al. 2015; Migden et al. 2015).

Although the anti-cancer effects in these trials are very promising, increased awareness for potential toxicological side effects on the body is necessary during and after the treatments. Our previous study discovered interesting aspects of the role of the Hh pathway in the adult liver. Therefore, we established two hepatocyte-specific *Smo* knockout mouse models and observed, independently of embryonic (SAC mice) (Matz-Soja et al. 2014) or conditional (SLC mice) (Matz-Soja et al. 2016) deletion of *Smo* in hepatocytes, similar phenotypic effects.

For example, we showed that hepatocyte-specific downregulation of the Hh pathway has dramatic influences on the hepatic insulin-like growth factor (IGF) axis (Matz-Soja et al. 2014) and lipid metabolism (Matz-Soja et al. 2016). We observed excessive lipid accumulation in the liver with typical features of non-alcoholic fatty liver disease (NAFLD). In the current work, we present results that a hepatic knockout of *Smo* is also associated with androgenization and infertility in female SAC mice. The mice exhibit increased testosterone levels and signs of ovulatory dysfunction. Our study shows that the Hh signaling pathway in hepatocytes has a major impact on the reproduction and regulation of adult hepatic steroid hormone synthesis.

Materials and methods

Maintenance of the mice and feeding

We established two knockout mouse models with a hepatocyte-specific deletion of *Smo*. In the SAC mice, the expression of the Cre recombinase is under the control of the mouse albumin promoter and the α-fetoprotein enhancer so that the *Smo* ablation occurs embryonically (day 9.5 post coitum) (Matz-Soja et al. 2014). In the SLC mice, the expression of the Cre recombinase is under the control of the liver activator protein (LAP) promotor and doxycycline. The deletion of *Smo* was induced at 8 weeks of age by an administration of 10 mg/ml doxycycline in the drinking water (Matz-Soja et al. 2016).

The mice were maintained in a pathogen-free facility on a 12:12 h LD cycle, according to the German guidelines and the world medical association declaration of Helsinki for the care and safe use of experimental animals. The animals had free access to regular chow (ssniff® M-Z V1124-0 composed of 22.0% protein, 50.1% carbohydrate, 4.5% fat; usable energy: 13.7 kJ/g; ssniff® Spezialdiäten GmbH, Germany) and tap water throughout life. The SAC mice were studied at 3 months of age, the SLC mice at 3 and 8 months (Fig. S1). All mice were killed between 9 and 11 am after administration of an anesthetic mixture of ketamine, xylazine and atropine.

Isolation of primary mouse hepatocytes

The primary hepatocytes were isolated from female transgenic mice by a collagenase perfusion technique as described before (Gebhardt et al. 2003). By differential centrifugation, the cell suspension was cleared of non-parenchymal cells (Matz-Soja et al. 2014).

Histology of reproductive organs

A detailed method description of the histology of the reproductive organs is given in the online Supplementary Information.

Quantification of steroid hormones in mouse serum

Steroid hormones were quantified by liquid chromatography–tandem mass spectrometry (LC–MS/MS) similar to a described method (Johänning et al. 2015) using the respective deuterium labeled analogs as internal standards. A

detailed method description is given in the online Supplementary Information.

RNA isolation and quantitative real-time PCR (qPCR)

Total RNA from hepatocytes, liver tissue and other organs was extracted by peqGOLD RNAPure™ (VWR) and RNeasy® Mini Kit (Qiagen). The RNA was reverse transcribed with the Proto Script M-MuLV First Strand cDNA Synthesis Kit (New England Biolabs) with a mix of oligo-d(T) and random primers. The resulting cDNA was quantified in duplicates by qPCR using the Rotor-Gene SYBR® Green PCR Kit and a Rotor-Gene Q (Qiagen). For each target, a gene-specific and intron-spanning primer was designed with Primer 3 (Table S1). The standard curve method was applied for an absolute quantification of the specific qPCR products. As reference gene, β-Actin was used.

Affymetrix microarray

For the microarray, the RNA from primary hepatocytes was used for hybridization with GeneChip Mouse Genome 430 2.0 Arrays (Affymetrix). A detailed method description is given in the online Supplementary Information.

Study design and statistical analyses

Most experiments were repeated 2–3 times with different quantities of biological replicates ($n = 4$–16) as indicated in each figure. The number of technical replicates depended on the type of experiment and was mostly duplicates or triplicates (not shown). Outliers were identified with the ROUT test of GraphPad Prism 6 (aggressiveness 0.2%).

The *Smo* knockout was validated by qPCR. For hepatocytes and liver tissue, all samples of KO mice with up to 50% reduced *Smo* expression in comparison to mean WT expression were used for further analyses.

Values are plotted as average of biological replicates ± standard deviation. The statistical evaluation was performed with the unpaired Student's t test. The null hypothesis was rejected at the $p < 0.05$ (*); $p < 0.01$ (**) and $p < 0.001$ (***) levels.

Results

Breeding behavior of SAC-KO mice

The transgenic mouse line with hepatocyte-specific ablation of the *Smo* gene (abbreviated SAC-KO mice) has been described in detail previously (Matz-Soja et al. 2014). Because the expression of the Cre recombinase in these mice is under the control of both the mouse albumin promoter and α-fetoprotein enhancer, the deletion of *Smo* occurs at day 9.5 post-coitum shortly after the liver bud develops (Kellendonk et al. 2000); see the timeline in Fig. S1a.

Once we started breeding SAC mice, we noticed that female, but not male, SAC-KO mice were infertile, i.e., they had no offspring. Thus, for breeding, male $Smo^{flox/flox}$ Cre recombinase-positive and female $Smo^{flox/flox}$ Cre recombinase-negative mice have to be mated.

Macroscopic and microscopic features of reproductive organs in female SAC-KO mice

The reproductive system of SAC-KO mice appeared immature; both ovaries and uteri were small compared with the organs in SAC-WT (wild-type) mice. The ovaries were of striking pearly-white-yellow appearance and only showed protruding antral follicles on their surface. Corpora lutea were not visible. By contrast, SAC-WT littermates exhibited an ovary appearance expected for their age with both follicles and corpora lutea present (Fig. 1a).

Acyclicity was further substantiated in SAC-KO mice by the uniform appearance of the vaginal mucosa (Fig. 1c). The mucosa of the SAC-KO vaginas was characterized by a non-keratinizing stratified squamous epithelium infiltrated by leucocytes (predominantly eosinophils and neutrophils). The leucocytes migrated from the lamina propria into the epithelium and accumulated in large clusters close to the epithelial surface. By contrast, the vaginal mucosa of SAC-WT mice revealed normal variation in the epithelial morphology of cycling mice, e.g., transition from a non-keratinized, mucous secreting epithelium at di-/proestrus to a keratinized epithelium with invading leucocyte at estrus/metestrus (Fig. 1c).

The tissue area of SAC-KO mice ovaries was smaller than that of SAC-WT ovaries. An area difference of 25% remained when the smaller body size of SAC-KO mice compared with that of SAC-WT mice was considered (Fig. 1b, d). The ovaries of SAC-KO mice showed no indications of ovulation and corpora lutea formation, whereas SAC-WT mouse ovaries showed 4–7 corpora lutea per ovary (Fig. 1b, e). A quadratic regression analysis of the hepatic *Smo* expression and corpora lutea quantity of SAC-WT, SAC heterozygous and SAC-KO mice showed a strong correlation with a coefficient of 0.91, confirming that the anovulatory phenotype was caused by the hepatic deletion of *Smo* (Fig. 1f).

The ovaries of the SAC-KO mice presented follicles in all stages of development and regression (Fig. S2a), except healthy preovulatory follicles (>350 µm). The amount of healthy follicles was significantly lower in SAC-KO ovaries than in SAC-WT ovaries for all three follicle size groups,

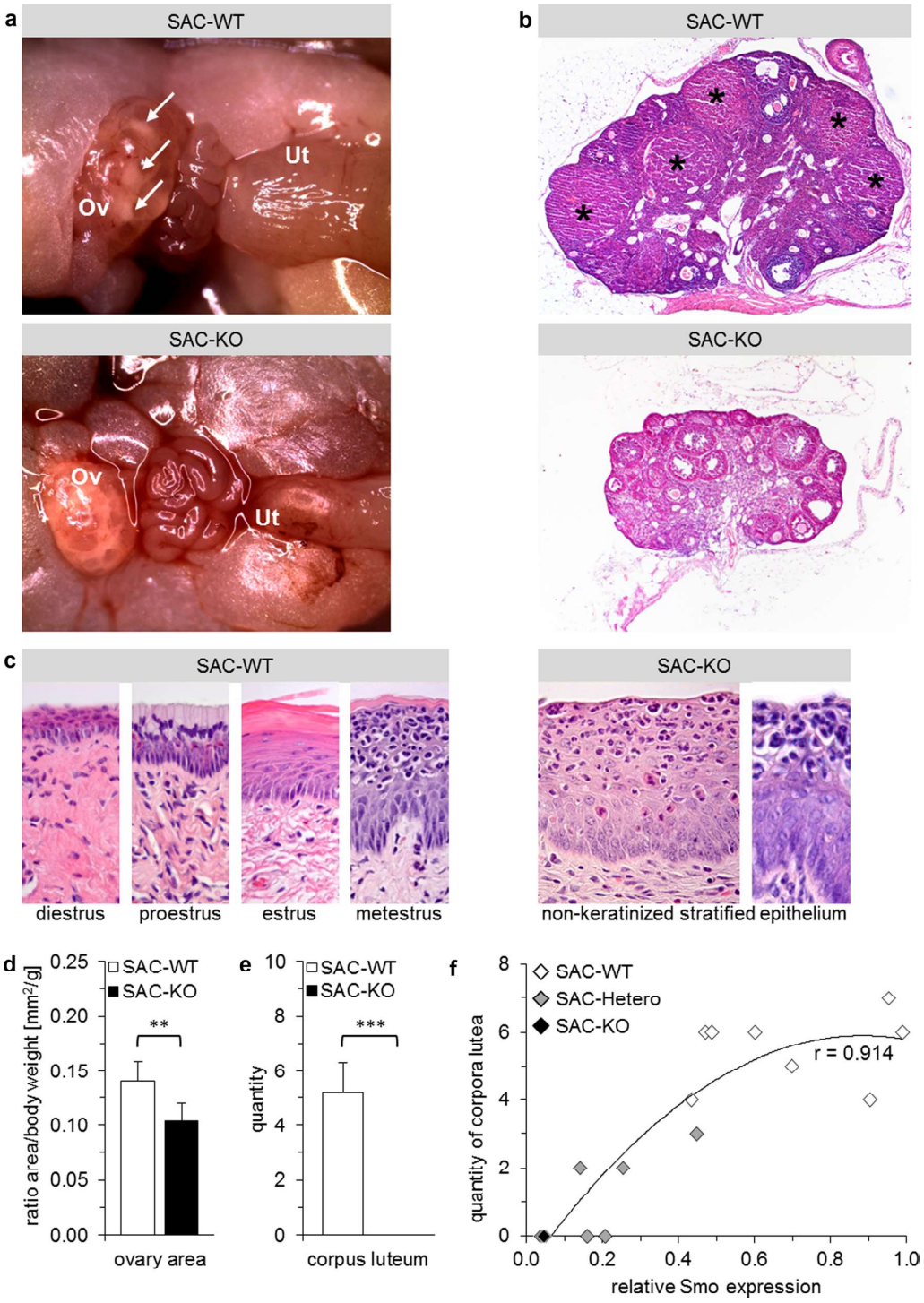

while the number of atretic follicles was comparable (Fig. S2b). In line with this finding, the rate of atresia among growing follicles was significantly higher in SAC-KO mice than in SAC-WT mice in all three follicle size groups (Fig. S2c). The higher number of atretic antral follicles in SAC-KO ovaries suggested an increase in collapsed zonae

◂**Fig. 1** Reproductive system of female SAC-WT and SAC-KO mice. **a** Picture of reproductive organs with marked ovaries (Ov), uteri (Ut) and corpora lutea (*arrow*) of SAC-WT and SAC-KO mice. **b** Representative H&E sections of SAC-WT and SAC-KO ovaries with and without corpora lutea (*stars*), respectively (magnification ×40). **c** H&E stained sections of SAC-WT and SAC-KO vaginas demonstrating variation and uniformity of the vaginal mucosa, respectively (magnification ×40). **d** Ratio of ovary area/body weight of SAC-WT ($n = 8$) and SAC-KO mice ($n = 4$). **e** Quantity of corpora lutea in SAC-WT and SAC-KO mice ($n = 5$). **f** Quadratic regression analysis of hepatic *Smo* expression and corpora lutea quantity with a correlation coefficient of $r = 0.91$. Data are plotted as mean ± standard deviation, $p < 0.01$ (**) and $p < 0.001$ (***)

pellucidae in the interstitial ovarian tissue. Interestingly, the number of collapsed zonae pellucidae was, however, not significantly different in the ovaries of SAC-KO mice compared with that in SAC-WT counterparts (Fig. S2d).

The striking pearly-white yellow color and severe disturbance of follicle maturation in the ovaries of SAC-KO mice suggested that the observed anovulation is partly a result of an abnormal morphological and functional transformation of fibroblastic elements in the interstitial tissue and in the developing thecas. The interstitial gland cells of SAC-KO mice were noticeably large, showed a lightly stained pale cytoplasm and appeared metabolically hyperactive (Fig. S2e). The absolute number of nuclei per interstitial gland cell area in the medulla was significantly lower in SAC-KO mice than in SAC-WT mice, reflecting the hypertrophic phenotype of the interstitial gland cells in SAC-KO ovaries (Fig. S2f).

Altered hepatic gene expression and regulation of steroidogenic parameters in female SAC-KO mice

Because the knockout of *Smo* is hepatocyte specific, we focused our further investigations on the liver to reveal changes in hepatocytes that might be responsible for the phenotype. An Affymetrix microarray analysis with primary hepatocytes provided a wide range of genes regulated in their expression in female SAC-KO mice compared with that in SAC-WT mice. In total, 122 and 148 genes were more than twofold up- and down-regulated, respectively (Fig. 2a). Analyses using the Cytoscape plug-ins BiNGO and CluGO identified significantly regulated GO terms (Table S3). Many of the GO terms for the up-regulated genes are associated with lipid metabolism. For instance, in the GO terms 'lipid metabolic process' (adjusted p value 3.10E−08) and 'fatty acid metabolic process' (adjusted p value 1.23E−04) are 33 and 13 genes, respectively, increased in SAC-KO mice. Interestingly, also genes of the GO terms related to steroid metabolism were significantly elevated, such as 'steroid metabolic process' (adjusted p value 7.21E−03), 'steroid biosynthetic process' (adjusted p value 2.95E−02) and 'androgen biosynthetic process' (adjusted p value 9.29E−03). The analysis with the down-regulated genes disclosed some interesting GO terms as well. In the GO term 'reproduction' (adjusted p value 9.86E−04), 20 genes were decreased, and the terms 'insulin-like growth factor receptor signaling pathway' (adjusted p value 2.24E−02), 'female mating behavior' (adjusted p value 2.24E−02) and 'fertilization' (adjusted p value 4.54E−02) showed significant alterations. Figure 2b shows a network of the possible interactions of the most interesting GO terms and associated genes.

Following the hint of the Affymetrix microarray indicating several GO terms related to increased steroid metabolism, we quantified the expression of steroidogenic enzymes in primary hepatocytes by qPCR measurements. Indeed, we found hepatic induction in the expression of genes involved in the initial steps of steroid hormone biosynthesis. For *Star* (steroidogenic acute regulatory protein), we obtained a trend of up-regulation (1.4-fold) and, for *Cyp17a1* (steroid 17α-hydroxylase), a highly significant increase (2.1-fold) in SAC-KO mice compared with that in SAC-WT mice (Fig. 2c). Interestingly, the transcripts of the enzymes further downstream, namely the hydroxysteroid dehydrogenases (Hsd), were significantly reduced in SAC-KO mice compared with those in SAC-WT mice (Fig. 2c). *Hsd3b1* and *Hsd3b2* are involved in the conversion of pregnenolone to progesterone or DHEA to androstenedione, and *Hsd17b2* inactivates testosterone by its conversion back to androstenedione.

Furthermore, we measured the concentrations of several sex steroids in the plasma of female SAC mice. The testosterone (TESTO) levels showed a more than 3.3-fold significant increase in SAC-KO compared with that in SAC-WT mice (Fig. 2e). Its precursor, androstenedione (ANDRO), was also elevated, while progesterone (PROG) was not altered. Dehydroepiandrosterone sulfate (DHEAS) and estrone sulfate (E1S) were not detectable (Fig. 2e).

Because sex steroids are mainly produced in the gonads and adrenal glands, we also quantified steroidogenic genes in the adrenal gland and ovary tissue of female SAC-KO mice but found no relevant changes in the expression (Fig. S3a and b). These results corresponded well with the deletion of *Smo* that was highly significant only in hepatocytes but not in the adrenal glands and ovaries in SAC-KO females (Fig. 2d).

Hepatocellular deletion of *Smo* during adolescence largely mirrors the phenotype induced in the embryonic state

As the Hh signaling pathway plays an important role in developmental processes during embryogenesis, a deletion of *Smo* in this stage could alter the fetal and neonatal liver functions. To exclude that the observed phenotype in female

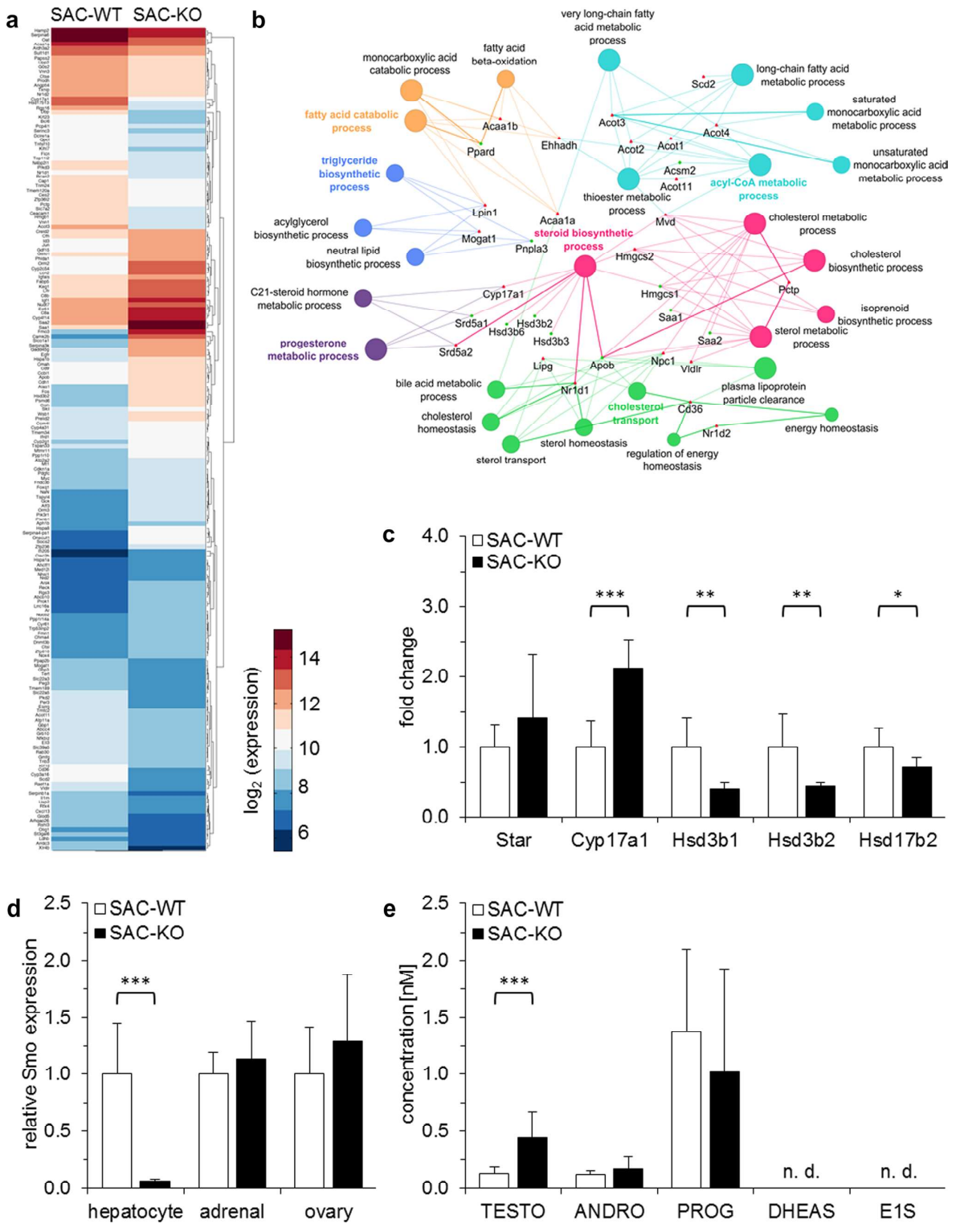
a
SAC-WT SAC-KO
log2 (expression)
14
12
10
8
6
b
very long-chain fatty acid metabolic process
monocarboxylic acid catabolic process
fatty acid beta-oxidation
long-chain fatty acid metabolic process
Scd2
fatty acid catabolic process
Acaa1b
Acot3
saturated monocarboxylic acid metabolic process
Acot4
Ppard
Ehhadh
Acot2
Acot1
unsaturated monocarboxylic acid metabolic process
triglyceride biosynthetic process
Acsm2
Acot11
acyl-CoA metabolic process
thioester metabolic process
Lpin1
Acaa1a
Mvd
cholesterol metabolic process
acylglycerol biosynthetic process
Mogat1
steroid biosynthetic process
Pnpla3
Hmgcs2
cholesterol biosynthetic process
neutral lipid biosynthetic process
C21-steroid hormone metabolic process
Cyp17a1
Hmgcs1
Pctp
Saa1
isoprenoid biosynthetic process
Srd5a1
Hsd3b2
Hsd3b6
sterol metabolic process
progesterone metabolic process
Hsd3b3
Saa2
Srd5a2
Lipg
Apob
Npc1
Vldlr
plasma lipoprotein particle clearance
bile acid metabolic process
Nr1d1
cholesterol transport
Cd36
cholesterol homeostasis
energy homeostasis
Nr1d2
sterol homeostasis
regulation of energy homeostasis
sterol transport
c
SAC-WT
SAC-KO
fold change
4.0
3.0
2.0
1.0
0.0
***
**
**
*
Star
Cyp17a1
Hsd3b1
Hsd3b2
Hsd17b2
d
SAC-WT
SAC-KO
relative Smo expression
2.5
2.0
1.5
1.0
0.5
0.0
***
hepatocyte
adrenal
ovary
e
SAC-WT
SAC-KO
concentration [nM]
2.5
2.0
1.5
1.0
0.5
0.0
***
n. d.
n. d.
TESTO
ANDRO
PROG
DHEAS
E1S

◂**Fig. 2** Altered gene expression and sex steroid content in female SAC-KO mice. **a** Heatmap of Affymetrix microarray displaying the genes with a fold change equal or higher than 2.0 in SAC-WT ($n = 1$) and SAC-KO ($n = 1$) mice. **b** ClueGO analysis of regulated genes (≥1.5-fold in Affymetrix microarray) related to lipid and steroid metabolism; node size indicates the significance of the GO term. **c** Steroidogenic gene expression in primary hepatocytes of SAC-KO ($n = 8$) compared to SAC-WT ($n = 9$) mice. Expression of *Star*, *Cyp17a1*, *Hsd3b1*, *Hsd3b2* and *Hsd17b2* was quantified by qPCR. **d** Gene expression of *Smo* in hepatocytes, adrenal glands and ovaries of SAC-WT ($n = 8$–9) and SAC-KO ($n = 8$–10) mice. **e** Concentration of sex steroid hormones in plasma of SAC-WT ($n = 10$) and SAC-KO ($n = 16$) mice. Measurement by LC–MS/MS of testosterone (TESTO), androstenedione (ANDRO) and progesterone (PROG); dehydroepiandrosterone sulfate (DHEAS) and estrone sulfate (E1S) were not detectable (n. d.). Data are plotted as mean ± standard deviation, $p < 0.05$ (*), $p < 0.01$ (**) and $p < 0.001$ (***)

SAC-KO mice might be attributed to the specific embryonal knockout of the *Smo* gene, we used a second mouse model, termed SLC mice (Matz-Soja et al. 2016), with a conditional hepatocyte-specific knockout of the *Smo* gene after adolescence at 8 weeks of age (see timeline Fig. S1b).

When the SLC mice were studied at 3 months of age (similar to that for SAC mice), no significant changes concerning the fertility were obvious, indicating that the interruption of Hh signaling in the adult liver could not immediately reverse the already initiated ovarian cyclicity (Fig. 3a). However, at 8 months of age, a significant reduction of the number of corpora lutea (0.6-fold) was obvious (Fig. 3a, b). Correspondingly, the changes in the expression of steroidogenic genes were similar to those seen in SAC-KO mice except for *Hsd3b1*, which was up-regulated in SLC-KO mice (Fig. 3c). The plasma levels of testosterone at 8 months of age were only slightly increased (Fig. S4), fitting with the reduction, but not complete loss of corpora lutea.

Collectively, the findings in SLC-KO mice suggested that the blockade of Hh signaling in the adult stage has a similar but delayed impact on the reproductive capacity of female mice.

Discussion

Our study provides strong evidence that inhibition of the Hh signaling pathway specifically in hepatocytes affects the body's steroid metabolism and reproductive system. The hepatic knockout of *Smo* is associated with androgenization and infertility in female mice.

The reproductive organs of female SAC-KO mice remain immature, and the vaginal and ovarian histologies are dramatically altered. The vaginal mucosa shows a uniform acyclic appearance. Follicle maturation is interrupted before preovulatory follicles, and corpora lutea are formed. Large clusters of hypertrophied interstitial gland cells occupy the ovarian stroma. Collectively, these findings demonstrate that the initiation of estrus cyclicity is inhibited in SAC-KO mice (Spanel-Borowski et al. 2001; Sandrock et al. 2009).

The impact of local Hh signaling on steroidogenic organs is well established and has been recently reviewed by Finco et al. (Finco et al. 2015). A wide range of publications has shown that local Hh signaling may be essentially involved in these organs' development and growth, and may also play a role in their mature function. In the adult ovary, for instance, several Hh components such as the ligands, *Ptch* receptors, *Smo* and *Gli1* are expressed, and the inhibition of Hh by cyclopamine leads to altered steroid synthesis in vitro (Russell et al. 2007). However, in our hepatocyte-specific *Smo* knockout mouse models, the steroidogenic organs showed no alterations in Hh expression. The quadratic regression of the *Smo* expression in the hepatocytes and the corpora lutea quantity demonstrates a strong correlation ($r = 0.91$), providing evidence that hepatic *Smo* deletion is the cause of the alterations in the reproductive system.

Female fertility can be negatively influenced by elevated testosterone levels as exemplified in patients with the polycystic ovarian syndrome (PCOS) where hyperandrogenism is a hallmark (Graham and Selgrade 2017). We measured the concentration of sex steroids in the plasma and found a more than 3.3-fold higher level of testosterone and an increase in androstenedione (1.4-fold) in SAC-KO mice compared with that in SAC-WT mice. The concentration of the hormones DHEAS and E1S was under the lower limit of detection (LLOD). This is consistent with the findings of Nilsson et al. who found that the DHEA concentration was always below the LLOD in mice and that E1 and E2 concentrations were very low in the metestrus (Nilsson et al. 2015). In general, it is assumed that the production of the steroids primarily occurs in the adrenal glands and gonads where cholesterol is converted by cytochrome P450 hydroxylases and hydroxysteroid dehydrogenases, finally leading to the formation of steroid hormones (Luu-The 2013). We checked the expression of steroidogenic enzymes in these tissues to determine where the additional testosterone was produced. In accordance with the normal *Smo* expression in these organs, we could not find any relevant changes in the expression of *Star*, *Cyp11a1*, *Cyp17a1*, *Cyp19a1* and *Hsd3b1* in the ovaries or adrenal glands. The embryonic liver expresses many of the steroidogenic genes at similar or slightly lower levels than the primary steroidogenic organs during postnatal life (Pezzi et al. 2003; O'Shaughnessy et al. 2013). Hepatic steroidogenic gene expression is normally downregulated during postnatal liver maturation. We suggest that the knockout of *Smo* leads to continuing steroidogenic gene expression in the hepatocytes of SAC-KO mice, and additional testosterone is produced. Our view is supported

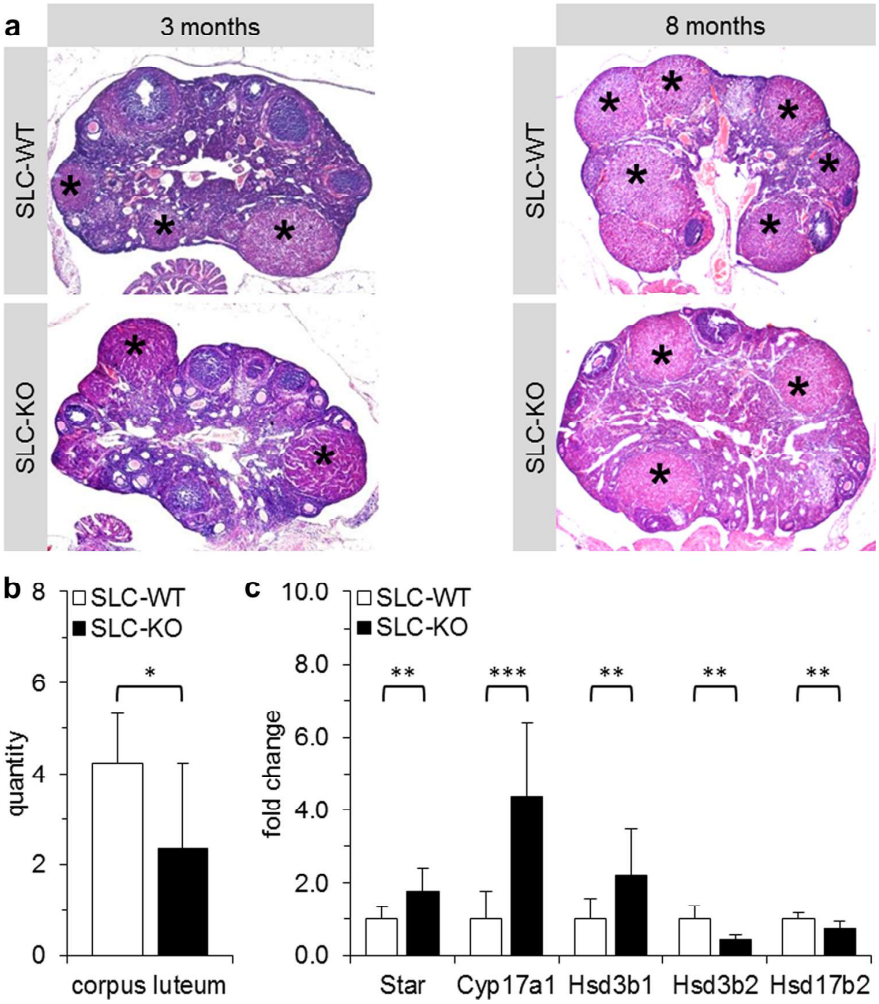

Fig. 3 Features of 8 months old female SLC-KO mice. **a** H&E section of ovaries of 3 and 8 months old SLC-WT and SLC-KO mice show corpora lutea (*stars*) (magnification ×40). **b** Quantity of corpora lutea in 8 months old SLC-WT ($n = 8$) and SLC-KO mice ($n = 6$). **c** Steroidogenic gene expression in liver tissue of 8 months old SLC-KO ($n = 8$) compared to SLC-WT ($n = 8$) mice. Expression of *Star*, *Cyp17a1*, *Hsd3b1*, *Hsd3b2* and *Hsd17b2* was quantified by qPCR. Data are plotted as mean ± standard deviation, $p < 0.05$ (*), $p < 0.01$ (**) and $p < 0.001$ (***)

by microarray analysis, revealing significant alterations of GO terms belonging to the steroid metabolism ('steroid metabolic process', 'steroid biosynthetic process' and 'androgen biosynthetic process'), and by qPCR measurements, which confirmed the up-regulation of *Star* and *Cyp17a1* in the hepatocytes of SAC-KO mice (Fig. 4). In line with these findings is the down-regulated gene expression of the enzyme responsible for the inactivation of testosterone, *Hsd17b2*. Moreover, an inhibition of the Hh pathway at a later time point such as that in SLC mice can re-induce *Cyp17a1* expression in hepatocytes. Grasfeder et al. published that fasting conditions can also induce *Cyp11a1* and *Cyp17a1* expression and DHEA synthesis in the liver mediated by peroxisome proliferator-activated receptor-γ coactivator (PGC)-1α (Grasfeder et al. 2009). Our results indicated that SAC and SLC mice, even if they have hypoinsulinaemia and steatosis, have no fasting phenotype (Matz-Soja et al. 2014, 2016). However, our results and those of Grasfeder showed that the liver indeed can play a role in steroidogenesis.

In general, the results obtained for SAC-KO mice were confirmed by the second mouse model with a hepatocyte-specific *Smo* deletion, SLC mice. In the SLC mice, the knockout was induced by doxycycline after puberty at 8 weeks of age to avoid the negative effects of Hedgehog down-regulation on fetal and neonatal liver development. At 8 months of age, the quantity of corpora lutea was significantly reduced, the steroidogenic gene expression was altered with a significant increase of *Star* and *Cyp17a1*, and the testosterone concentration was slightly increased in SLC-KO mice compared with that in SLC-WT mice. Because the deletion of *Smo* is induced 8 weeks after birth, we assumed that more time is needed for the systemic manifestation and adaption of the Hh down-regulation so that we can find the above results only in older SLC animals. Because we obtained that similar results in both the

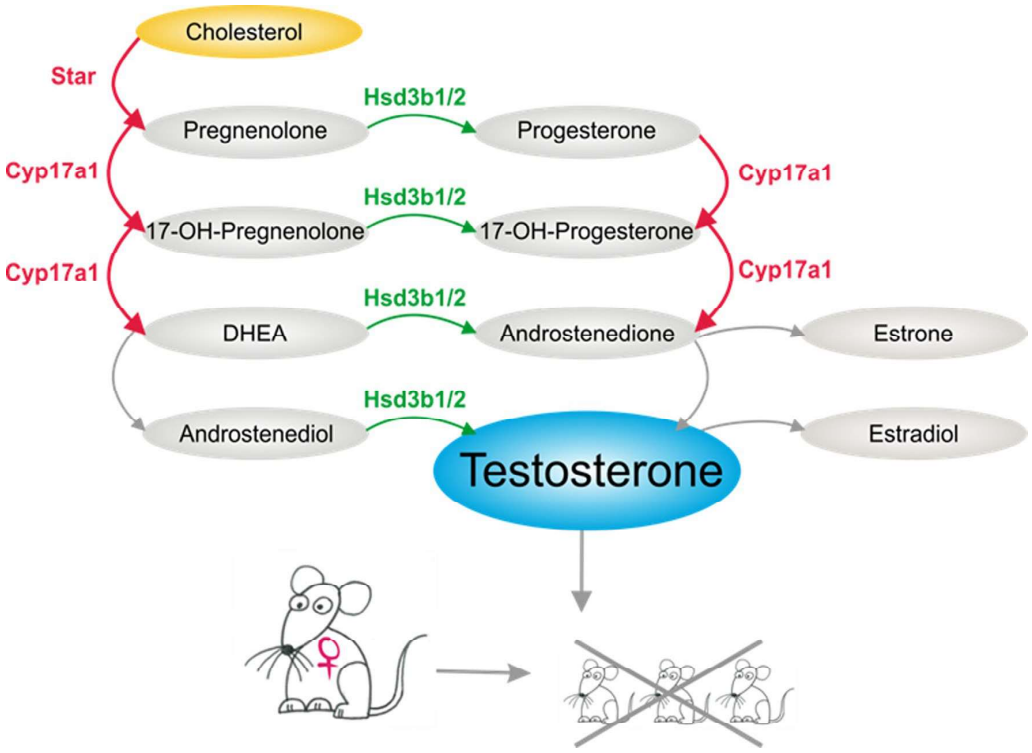

Fig. 4 Scheme of steroidogenesis with up-regulation (*red*) and down-regulation (*green*) of important genes in hepatocytes of SAC-KO compared to SAC-WT mice which lead to a raised plasma level of testosterone and results in infertility in female mice (color figure online)

SAC-KO and SLC-KO mice, independent of the strategy of *Smo* deletion, show that the observed effects have general significance and are not artefacts from the mouse model.

Matz-Soja et al. published recently that the *Smo* deletion in male and female SAC-KO mice has an impact on the IGF-axis and that the hepatic gene expression (2.7-fold in females) and serum concentration of IGF-1 (fourfold in females) are significantly decreased (Matz-Soja et al. 2014). IGF-1 is known to influence growth and fertility. By comparing the phenotype of the SAC mouse model with different Igf1 knockouts, some similarities were observed. The hepatocyte-specific Igf1 knockout mouse model shows an equal reduction of the IGF-1 concentration (Yakar et al. 1999), but the mice are fertile, although the length of their estrous cycle is doubled (Villa et al. 2012). Only whole-body knockout of Igf1 and total ablation of IGF-1 lead to infertility, a reduced ovary size by 75% and a limited follicle maturation followed by no ovulation (Baker et al. 1993, 1996). Even if some features are comparable, the reduced IGF-1 levels in the SAC-KO mice seem to be not the only explanation for the infertility. Female SAC mice show only reduced levels of IGF-1 and are still infertile such as Igf1-null mice. Furthermore, the most likely explanation of the infertility in the Igf1-null mutation is an impairment of the steroidogenesis in the gonads (Baker et al. 1996), but this is not transferable to SAC-KO mice because the expression analysis of the ovaries and adrenal glands revealed no changes. Unfortunately, no data on the impact of the liver on infertility in Igf1-mutant animals have been published. It would be interesting to study the possible changes of steroidogenesis in hepatocytes of the hepatic Igf1-knockout or Igf1-null mice.

Infertility is a huge issue because 8–12% of reproductive-aged couples worldwide are affected (Ombelet et al. 2008). There are many different causes of infertility such as age (Somigliana et al. 2016), genetic defects (Maiburg et al. 2012; Grynberg et al. 2016), medical interventions or hormonal disorders accompanied by ovulatory dysfunctions (Luciano et al. 2013). Polycystic ovarian syndrome (PCOS) is one of these diseases and is characterized by chronic anovulation, hyperandrogenism and/or polycystic ovaries (Carmina 2004). Furthermore, a strong correlation between disturbances in female fertility and liver steatosis is observed (Targher et al. 2016). SAC-KO mice share major symptoms of the PCOS disorder, i.e., androgenization and disturbed follicle maturation. As published previously, *Smo* deletion is associated with strong lipid accumulation in the liver and shows typical features of non-alcoholic fatty

liver disease (NAFLD) (Matz-Soja et al. 2016). Even if the SAC mice do not show the entire clinical manifestations of adult PCOS patients, the similarities are striking and suggest to further investigate the regulation of Hh signaling in PCOS patients. Interestingly, fertility in some cirrhotic female liver recipients is resumed after liver transplantation (Christopher et al. 2006). Overall, it seems that the liver has a crucial impact on reproduction under disease conditions.

In conclusion, hepatocyte-specific deletion of the Hh receptor *Smo* in female SAC mice results in androgenization and infertility, the latter as a consequence of partial ovarian failure (defective follicle maturation, anovulation and the absence of a luteal phase). Because it has been suggested that targeting the Hh pathway may hold the key for anti-cancer therapy, our results seem to be of considerable interest. For instance, the application of the approved SMO inhibitor Sonidegib shows promising results in reducing cancer growth but also reveals manifold and severe side effects (Migden et al. 2015). Our study raises a new concern in that it suggests that female fertility could be considerably diminished by targeting the Hh pathway, particularly during long-term treatments.

Acknowledgements We thank PD Dr. Knut Krohn for Affymetrix microarray analysis. We cordially thank Kerstin Heise, Doris Mahn, Claudia Merkwitz and Markus König for excellent technical assistance. Further, we would like to thank Petra Hirrlinger, Petra Fink-Sterba, Sigrid Weisheit and Manuela Liebig from the Experimental Centre of the Faculty of Medicine (Leipzig University) for taking excellent care of the mice.

Compliance with ethical standards

Funding This work was supported by the Federal Ministry of Education and Research (Germany) within the research network Systems Medicine of the Liver (LiSyM) [grant number 031L0054 and 031L0037] and the Virtual Liver Network (VLN) [grant number 0315735, 0315736, 0315755, and 0315775], the Deutsche Forschungsgemeinschaft (Bonn, Germany) [grant MU 1727/2-1, SCHR 1323/2-1], and the Robert Bosch Foundation (Stuttgart, Germany).

Conflict of interest The authors declare that they have no conflict of interest.

Ethical approval All procedures performed in studies involving animals were in accordance with the ethical standards of the institution or practice at which the studies were conducted. This article does not contain any studies with human participants performed by any of the authors.

References

Aberger F, Ruiz I Altaba I (2014) Context-dependent signal integration by the GLI code: the oncogenic load, pathways, modifiers and implications for cancer therapy. Semin Cell Dev Biol 33:93–104. doi:10.1016/j.semcdb.2014.05.003

Almazroo OA, Miah MK, Venkataramanan R (2017) Drug metabolism in the liver. Clin Liver Dis 21(1):1–20. doi:10.1016/j.cld.2016.08.001

Ameer F, Scandiuzzi L, Hasnain S et al (2014) De novo lipogenesis in health and disease. Metab Clin Exp 63(7):895–902. doi:10.1016/j.metabol.2014.04.003

Baker J, Liu JP, Robertson EJ et al (1993) Role of insulin-like growth factors in embryonic and postnatal growth. Cell 75(1):73–82

Baker J, Hardy MP, Zhou J et al (1996) Effects of an Igf1 gene null mutation on mouse reproduction. Mol Endocrinol (Baltimore, Md.) 10(7):903–918. doi:10.1210/mend.10.7.8813730

Carmina E (2004) Diagnosis of polycystic ovary syndrome: from NIH criteria to ESHRE-ASRM guidelines. Minerva Ginecol 56(1):1–6

Christopher V, Al-Chalabi T, Richardson PD et al (2006) Pregnancy outcome after liver transplantation: a single-center experience of 71 pregnancies in 45 recipients. Liver Transpl 12(7):1138–1143. doi:10.1002/lt.20810

Finco I, LaPensee CR, Krill KT et al (2015) Hedgehog signaling and steroidogenesis. Annu Rev Physiol 77:105–129. doi:10.1146/annurev-physiol-061214-111754

Gebhardt R, Coffer PJ (2013) Hepatic autophagy is differentially regulated in periportal and pericentral zones—a general mechanism relevant for other tissues? CCS 11(1):21. doi:10.1186/1478-811X-11-21

Gebhardt R, Hengstler JG, Muller D et al (2003) New hepatocyte in vitro systems for drug metabolism: metabolic capacity and recommendations for application in basic research and drug development, standard operation procedures. Drug Metab Rev 35(2–3):145–213. doi:10.1081/DMR-120023684

Graham EJ, Selgrade JF (2017) A model of ovulatory regulation examining the effects of insulin-mediated testosterone production on ovulatory function. J Theor Biol 416:149–160. doi:10.1016/j.jtbi.2017.01.007

Grasfeder LL, Gaillard S, Hammes SR et al (2009) Fasting-induced hepatic production of DHEA is regulated by PGC-1alpha, ERRalpha, and HNF4alpha. Mol Endocrinol (Baltimore, Md.) 23(8):1171–1182. doi:10.1210/me.2009-0024

Grynberg M, Bidet M, Benard J et al (2016) Fertility preservation in Turner syndrome. Fertil Steril 105(1):13–19. doi:10.1016/j.fertnstert.2015.11.042

Han H-S, Kang G, Kim JS et al (2016) Regulation of glucose metabolism from a liver-centric perspective. Exp Mol Med 48:e218. doi:10.1038/emm.2015.122

Hovhannisyan A, Matz M, Gebhardt R (2009) From teratogens to potential therapeutics: natural inhibitors of the Hedgehog signaling network come of age. Planta Med 75(13):1371–1380. doi:10.1055/s-0029-1185979

Johänning J, Heinkele G, Precht JC et al (2015) Highly sensitive simultaneous quantification of estrogenic tamoxifen metabolites and steroid hormones by LC-MS/MS. Anal Bioanal Chem 407(24):7497–7502. doi:10.1007/s00216-015-8907-8

Kellendonk C, Opherk C, Anlag K et al (2000) Hepatocyte-specific expression of Cre recombinase. Genesis (New York, N.Y.: 2000) 26(2):151–153

Luciano AA, Lanzone A, Goverde AJ (2013) Management of female infertility from hormonal causes. Int J Gynaecol Obstetr 123(Suppl 2):S9–17. doi:10.1016/j.ijgo.2013.09.007

Luu-The V (2013) Assessment of steroidogenesis and steroidogenic enzyme functions. J Steroid Biochem Mol Biol 137:176–182. doi:10.1016/j.jsbmb.2013.05.017

Maiburg M, Repping S, Giltay J (2012) The genetic origin of Klinefelter syndrome and its effect on spermatogenesis. Fertil Steril 98(2):253–260. doi:10.1016/j.fertnstert.2012.06.019

Matz-Soja M, Hovhannisyan A, Gebhardt R (2013) Hedgehog signalling pathway in adult liver: a major new player in hepatocyte metabolism and zonation? Med Hypotheses 80(5):589–594. doi:10.1016/j.mehy.2013.01.032

Matz-Soja M, Aleithe S, Marbach E et al (2014) Hepatic Hedgehog signaling contributes to the regulation of IGF1 and IGFBP1 serum levels. CCS 12:11. doi:10.1186/1478-811X-12-11

Matz-Soja M, Rennert C, Schonefeld K et al (2016) Hedgehog signaling is a potent regulator of liver lipid metabolism and reveals a GLI-code associated with steatosis. eLife. doi:10.7554/eLife.13308

Migden MR, Guminski A, Gutzmer R et al (2015) Treatment with two different doses of sonidegib in patients with locally advanced or metastatic basal cell carcinoma (BOLT): a multicentre, randomised, double-blind phase 2 trial. Lancet Oncol 16(6):716–728. doi:10.1016/S1470-2045(15)70100-2

Monga SPS (2011) Role of Wnt/beta-catenin signaling in liver metabolism and cancer. Int J Biochem Cell Biol 43(7):1021–1029. doi:10.1016/j.biocel.2009.09.001

Nilsson ME, Vandenput L, Tivesten A et al (2015) Measurement of a comprehensive sex steroid profile in rodent serum by high-sensitive gas chromatography-tandem mass spectrometry. Endocrinology 156(7):2492–2502. doi:10.1210/en.2014-1890

Ombelet W, Cooke I, Dyer S et al (2008) Infertility and the provision of infertility medical services in developing countries. Human Reprod Update 14(6):605–621. doi:10.1093/humupd/dmn042

O'Shaughnessy PJ, Monteiro A, Bhattacharya S et al (2013) Steroidogenic enzyme expression in the human fetal liver and potential role in the endocrinology of pregnancy. Mol Hum Reprod 19(3):177–187. doi:10.1093/molehr/gas059

Pezzi V, Mathis JM, Rainey WE et al (2003) Profiling transcript levels for steroidogenic enzymes in fetal tissues. J Steroid Biochem Mol Biol 87(2–3):181–189

Robinson GW, Orr BA, Wu G et al (2015) Vismodegib exerts targeted efficacy against recurrent sonic Hedgehog-subgroup medulloblastoma: results from phase II pediatric brain tumor consortium studies PBTC-025B and PBTC-032. J Clin Oncol 33(24):2646–2654. doi:10.1200/JCO.2014.60.1591

Russell MC, Cowan RG, Harman RM et al (2007) The hedgehog signaling pathway in the mouse ovary. Biol Reprod 77(2):226–236. doi:10.1095/biolreprod.106.053629

Sandrock M, Schulz A, Merkwitz C et al (2009) Reduction in corpora lutea number in obese melanocortin-4-receptor-deficient mice. RB&E 7:24. doi:10.1186/1477-7827-7-24

Schmidt-Heck W, Matz-Soja M, Aleithe S et al (2015) Fuzzy modeling reveals a dynamic self-sustaining network of the GLI transcription factors controlling important metabolic regulators in adult mouse hepatocytes. Mol BioSyst 11(8):2190–2197. doi:10.1039/c5mb00129c

Sethi JK, Vidal-Puig A (2010) Wnt signalling and the control of cellular metabolism. Biochem J 427(1):1–17. doi:10.1042/BJ20091866

Somigliana E, Paffoni A, Busnelli A et al (2016) Age-related infertility and unexplained infertility: an intricate clinical dilemma. Hum Reprod (Oxford, England) 31(7):1390–1396. doi:10.1093/humrep/dew066

Spanel-Borowski K, Schafer I, Zimmermann S et al (2001) Increase in final stages of follicular atresia and premature decay of corpora lutea in Insl3-deficient mice. Mol Reprod Dev 58(3):281–286. doi:10.1002/1098-2795(200103)58:3<281:AID-MRD6>3.0.CO;2-0

Stecca B, Ruiz I Altaba I (2010) Context-dependent regulation of the GLI code in cancer by HEDGEHOG and non-HEDGEHOG signals. J Mol Cell Biol 2(2):84–95. doi:10.1093/jmcb/mjp052

Targher G, Rossini M, Lonardo A (2016) Evidence that non-alcoholic fatty liver disease and polycystic ovary syndrome are associated by necessity rather than chance: a novel hepato-ovarian axis? Endocrine 51(2):211–221. doi:10.1007/s12020-015-0640-8

Teperino R, Aberger F, Esterbauer H et al (2014) Canonical and non-canonical Hedgehog signalling and the control of metabolism. Semin Cell Dev Biol 33:81–92. doi:10.1016/j.semcdb.2014.05.007

Ueno T, Komatsu M (2017) Autophagy in the liver: functions in health and disease. Nature reviews. Gastroenterol Hepatol 14(3):170–184. doi:10.1038/nrgastro.2016.185

Villa A, Della Torre S, Stell A et al (2012) Tetradian oscillation of estrogen receptor alpha is necessary to prevent liver lipid deposition. Proc Natl Acad Sci USA 109(29):11806–11811. doi:10.1073/pnas.1205797109

Yakar S, Liu JL, Stannard B et al (1999) Normal growth and development in the absence of hepatic insulin-like growth factor I. Proc Natl Acad Sci USA 96(13):7324–7329

SUPPLEMENTARY MATERIAL

Archives of Toxicology

Conditional loss of hepatocellular Hedgehog signaling in female mice leads to persistence of hepatic steroidogenesis, androgenization and infertility

Christiane Rennert*[1] and Franziska Eplinius*[2], Ute Hofmann[3], Janina Johänning[3], Franziska Rolfs[4], Wolfgang Schmidt-Heck[5], Reinhardt Guthke[5], Rolf Gebhardt[#1], Albert M Ricken[#2], Madlen Matz-Soja[#1]

Corresponding author: Madlen Matz-Soja, Rudolf-Schönheimer-Institute of Biochemistry, Faculty of Medicine, Leipzig University, Johannisallee 30, 04103 Leipzig, Germany

phone: +49 341 9722120, fax: +49 341 9722109, E-mail: madlen.matz@medizin.uni-leipzig

Table of contents

Supplementary Material and Methods

Histology of reproductive organs

Organs were immediately fixed in phosphate buffered 4 % formalin, embedded in paraffin wax and cut into 8 µm thick sections.

Vaginal sections were stained with H&E and vaginal epithelium characteristics were used to assign the mice diestrus, proestrus, estrus or metestrus as previously described in detail (Merkwitz et al. 2016).

The left ovary of each mouse was serially sectioned along the longitudinal plane and analyzed as previously outlined (Sandrock et al. 2009). The sections were grouped into three alternate series of sections through the ovary at an interval of 28 µm. The first series was stained with H&E to assess ovary size, follicle maturation, corpora lutea formation, and interstitial gland cells. The second series was subjected to the periodic-acid-Schiff (PAS) reaction to assess the occurrence of collapsed zonae pelucidae as representatives of follicular atresia. The third series was kept in reserve. To calculate the ovary area the shape of the ovary was estimated as ellipse and measured in the five largest consecutive sections defined by their horizontal and vertical axes.

Corpora lutea and follicles were counted in the H&E stained sections. Follicles were considered when the nuclei of their oocytes were in focus (Szollosi et al. 1990; Spanel-Borowski et al. 1983). Each follicle was measured with an ocular scale and assigned to small (100 - 249 µm), intermediate (250 - 349 µm) and large (> 350 µm) follicles according its diameter (Kagabu and Umezu 2004). Simultaneously the follicles were classified as healthy or atretic, following established morphological criteria where follicular atresia is defined by deformation of the follicle and/ or oocyte, more than 5 % pycnotic granulosa cells and intercellular loosening of the granulosa cell layer (Oakberg 1979). For estimating interstitial gland cell activity, the nuclei of interstitial gland cells were counted in a representative area using ImageJ 1.48v, NIH, USA. The area had to be intact and free of prominent blood vessels. In PAS stained sections, about 150 µm apart from each other, remnants of zonae pelucidae were counted, summed up and used as marker for follicular atresia (Myers et al. 2004).

Quantification of steroid hormones in mouse serum

Steroid hormones were quantified by liquid chromatography–tandem mass spectrometry (LC-MS/MS) similar to a described method (Johänning et al. 2015) using the respective deuterium labelled analogues as internal standards. Protein precipitation was performed by the addition of 200 µl of the internal standard solution in 1 % (v/v) acetic acid in acetonitrile to mouse serum (50 – 100 µl) followed by centrifugation. For determination of DHEAS and E1S, 30 µl of the supernatant were diluted with 45 µl of 0.1 % formic acid in water. After a second centrifugation step, 20 µl of the supernatant were used for LC-MS/MS analysis with electrospray (ESI) as ionization mode and negative polarity. The mass spectrometer was operated in the multiple reaction monitoring (MRM) mode. MRM transitions and MS parameters are summarized in Table S2. The remaining supernatant from the protein precipitation step was subjected to solid phase extraction (SPE) as described (Johänning et al. 2015). The dried SPE eluate was reconstituted in 50 µl of 0.1 % formic acid in water:acetonitrile 20:80 (v/v) and 20 µl were injected for LC-MS/MS analysis of testosterone, androstenedione and progesterone. Calibration samples were prepared in charcoal stripped human serum in the concentration range 0.04 nM to 10 nM for testosterone and androstenedione, 0.1 nM to 25 nM for progesterone, 0.4 nM to 100 nM for E1S, and 100 nM to 25000 nM for DHEAS.

Calibration samples were worked up as the samples, and analyzed together with the unknown samples. Calibration curves based on internal standard calibration were obtained by weighted (1/x) linear regression for the peak area ratio of the analyte to the respective internal standard against the amount of the analyte. The concentration of the unknown samples was obtained from the regression line.

Affymetrix microarray

For the microarray the RNA from primary hepatocytes were used for hybridization with GeneChip Mouse Genome 430 2.0 Arrays (Affymetrix). The analysis was done in the Interdisciplinary Centre for Clinical Research Leipzig (Faculty of Medicine, Leipzig University) as described by Zellmer et al. (Zellmer et al. 2009).

The results were processed with the 'affyPLM' package from Bioconductor. Further studies were done with the Cytoscape plugin BiNGO (Maere et al. 2005) to identify the overrepresented GO categories and ClueGO (Bindea et al. 2009) to analyze the interactions between these ones.

The following link provides the raw data of the microarray: https://seek.lisym.org/data_files/6

Supplementary Tables

Table S1 Primer sequences for qPCR analyses

Gene	forward primer	reverse primer
β-Actin	atccgtaaagacctctatgccaac	atggagccaccgatccaca
Cyp11a1	caataaagctgatgagtacaccc	gtgccatctcataaaggttcca
Cyp17a1	catcccacacaaggctaaca	cagtgcccagagattgatga
Cyp19a1	gagagttcatgagagtctggatca	catggaacatgcttgaggact
Hsd3b1	tggacaaagtattccgaccag	aggcctccaataggttctg
Hsd3b2	tgtcattcccaggcagacc	tgacactcttcctcatggcc
Hsd17b2	ccacaaaggcagctctaacc	acctctctttcaaggtcggg
Smo	gcaagctcgtgctctggt	gggcatgtagacagcacaca
Star	tgttcctcgctacgttcaag	gtcgaacttgacccatccac

Table S2 MRM transitions and MS parameters for determination of DHEAS, E1S and their internal standards with LC-MS-MS

Analyte	MRM transition [m/z]	Dwell time [ms]	Fragmentor [V]	Collision energy [V]
d_6-DHEAS	373.2 > 98	25	167	44
DHEAS	367.2 > 97	25	177	36
d_4-E1-S	353.1 > 273.2	300	157	32
E1-S	349.1 > 269.2	600	157	28

Table S3 Gene set enrichment analysis of isolated hepatocytes from SAC-KO compared to SAC-WT mice. All genes with an expression fold change equal or higher than 1.5 were considered **a** up-regulated **b** down-regulated genes

a up-regulation

GO-ID	description	adjusted p Value	regulated genes	quantity of regulated genes
GO:0008152	metabolic process	2.56E-24	D14ertd436e, Slc23a2, Dclre1a, Il1rn, Pank1, Nab2, Sat2, Txndc13, C330018d20rik, Bach1, Cyp3a16, As3mt, Lipg, Pim1, Trim24, Pim3, Foxo3a, Pdk2, Zfp39, Cpt1a, Dio1, Usp2, Acot11, Atp11a, Foxp2, Pias1, Aldh3a2, Ren1, Mtap, Rfx4, Acot2, Acot1, Txnip, Ulk2, Trib3, Il6st, Atp6v0d2, Acot4, Acot3, Slc22a5, Retsat, Anp32a, Mgst3, Cugbp2, Zfp36l2, Dedd2, Mtmr7, Pctk2, Ldhb, Tert, Amdhd1, Afmid, Grpel2, Rdh16, Zkscan3, St3gal6, Decr2, Prodh, Ppargc1a, Decr1, Brap, Fn3k, Ube2h, Srd5a2, Nr1d2, Esrrg, Nr1d1, Nr0b2, Ell3, Eif1, Ssh1, Efna1, Vnn1, Bcl6, Vnn3, Cyp1a2, Id1, Lhx6, Sae1, 2310007h09rik, Phf17, Acy1, Rnf14, Pigq, Mogat1, Ppwd1, Gtdc1, Pctp, Vldlr, Csad, Serpina6, Pkd2, Elavl1, 6430573f11rik, Gys2, Aifm3, Dbp, Aldh2, Guk1, Senp8, Nfkbiz, Scd2, Pgm2, Gnpnat1, Upp2, Hmgcs2, Cd36, Ctse, Hibch, Cap1, Klf10, Rbm16, Klf11, Hsdl2, Gsto2, Dcakd, Mterfd3, Olig1, Klf15, Car5a, Tgfbr2, Rbl2, Ptp4a2, Sult1d1, Cyp2a5, Ivd, Ppap2b, Ehhadh, C1d, Ndufs4, Adssl1, Mvd, Aspa, Mtrf1l, Sgk2, Slu7, Samd8, Gls2, Rgs16, Hsd17b13, Ppm1k, Tenc1, Acaa1a, Usp18, Papss2, Slc7a2, Cyp17a1, Pbld, Ugp2, Gna12, Mknk2, Crym, Gbp2, Xdh, Gbp3, Nqo2, Gch1, Aadat, Bbox1, Fmo2, Sod2, Cyp8b1, Sulf2, Klf1, Gstz1, Aldh4a1, Klf6, Per3, Sbk1, Nfia, Tef, Qpct, Sardh, Chpt1, Gpd1l, Lpin1, Crat, Lpin2	178
GO:0006629	lipid metabolic process	3.10E-08	Il1rn, Samd8, Retsat, Pigq, Mogat1, Rgs16, Pctp, Vldlr, Acaa1a, Serpina6, Cyp17a1, Dbp, Lipg, Rdh16, Scd2, Hmgcs2, Cd36, Cpt1a, Srd5a2, Acot11, Ppap2b, Ehhadh, Cyp1a2, Acot2, Acot1, Mvd, Chpt1, Il6st, Lpin1, Crat, Lpin2, Acot4, Acot3	33
GO:0006631	fatty acid metabolic process	1.23E-04	Cpt1a, Acot11, Acaa1a, Ehhadh, Acot2, Scd2, Acot1, Cd36, Lpin1, Crat, Lpin2, Acot4, Acot3	13
GO:0044262	cellular carbohydrate metabolic process	2.53E-03	Fn3k, Cpt1a, Mogat1, Rgs16, Car5a, Gys2, Ldhb, Ugp2, Pgm2, Gnpnat1, St3gal6, Gpd1l, Il6st, Pdk2	14
GO:0006720	isoprenoid metabolic process	6.88E-03	Retsat, Cyp1a2, Rdh16, Mvd, Hmgcs2	5
GO:0008202	steroid metabolic process	7.21E-03	Dbp, Srd5a2, Pctp, Mvd, Hmgcs2, Vldlr, Cd36, Serpina6, Cyp17a1	9
GO:0006702	androgen biosynthetic process	9.29E-03	Srd5a2, Cd36	2
GO:0008203	cholesterol metabolic process	2.84E-02	Pctp, Mvd, Hmgcs2, Vldlr, Cd36	5
GO:0006694	steroid biosynthetic process	2.95E-02	Srd5a2, Mvd, Hmgcs2, Cd36, Cyp17a1	5

b down-regulation

GO-ID	description	adjusted p value	regulated genes	quantity of regulated genes
GO:0032502	developmental process	7.42E-13	Foxa1, Errfi1, Btg2, Aw548124, Ahctf1, B4galt1, Thrb, Rif1, Onecut1, Ccnf, Tcf21, Fmn1, Arhgap5, Cldn1, Cyr61, Ctgf, Foxq1, Tgm1, Csrp3, Hhex, Alcam, Cdh1, Myc, Dnmt3b, Bbs7, Prok1, Dsp, Hsp90aa1, Cxadr, Igfbp5, Igfbp3, F2r, Rps6, Ifrd1, Wnt5a, Lifr, Fos, Prox1, Prlr, Mtss1, Aprt, Ar, Ncor1, Olfm3, Smo, 1100001g20rik, Itga6, Irf6, Ppard, Rsl1, Cnp, Tshz3, Tshz2, Pik3r1, Nid1, Egfr, Socs2, C6, Aph1b, Pdgfc, Ela1, Plxna2, Apob, Pdlim5, Skil, Arsb, Egr1, Jun, D0h4s114, Hspa5, Srd5a1, Igf1, Inhba, Gadd45g, Bmp4, Nudt7, Lrg1, Fras1, Abi2, Nox4, Id3, Cd9, Plxnb1, Mkx, Reck, Foxa2	86
GO:0000003	reproduction	9.86E-04	Foxa1, Rsl1, B4galt1, Thrb, Rif1, Srd5a1, Rps6, Wnt5a, Tcf21, Igf1, Avpr1a, Prlr, Egfr, Aprt, Socs2, Bmp4, Ar, Cd9, Apob, Ppard	20
GO:0043627	response to estrogen stimulus	1.43E-03	Ar, Prdm2, Pik3r1, Arsb, Strn3	5
GO:0048009	insulin-like growth factor receptor signaling pathway	2.24E-02	Pik3r1, Igf1	2
GO:0060180	female mating behavior	2.24E-02	Thrb, Avpr1a	2
GO:0034637	cellular carbohydrate biosynthetic process	3.27E-02	Ar, B4galt1, Atf3, Gck	4
GO:0009566	fertilization	4.54E-02	B4galt1, Rif1, Cd9, Apob	4

Supplementary Figures

Figure S1

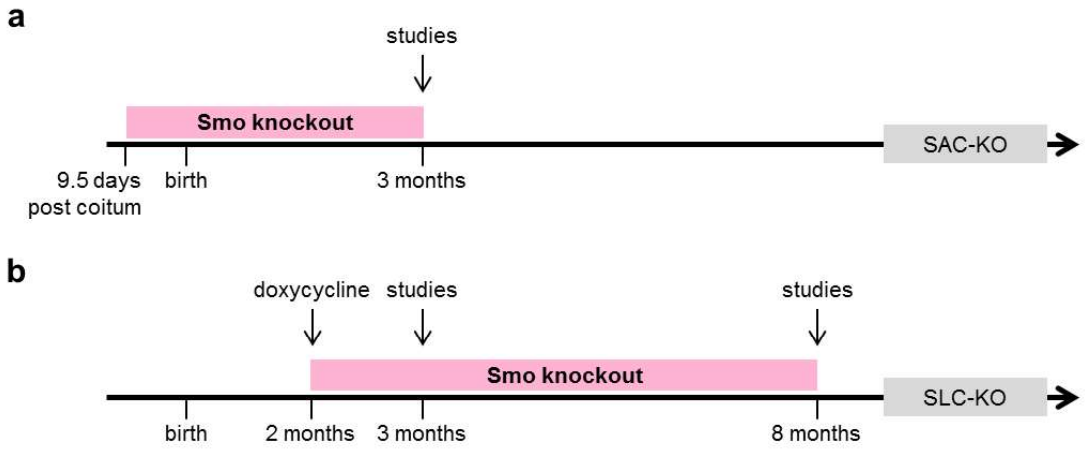

Fig. S1 Timeline of Smo deletion in SAC-KO and SLC-KO mice **a** In SAC-KO mice Smo deletion occurs at day 9.5 post coitum and mice were studied at 3 months of age **b** In SLC-KO mice the Smo deletion was induced by doxycycline at 2 months of age and the studies were performed at 3 and 8 months of age.

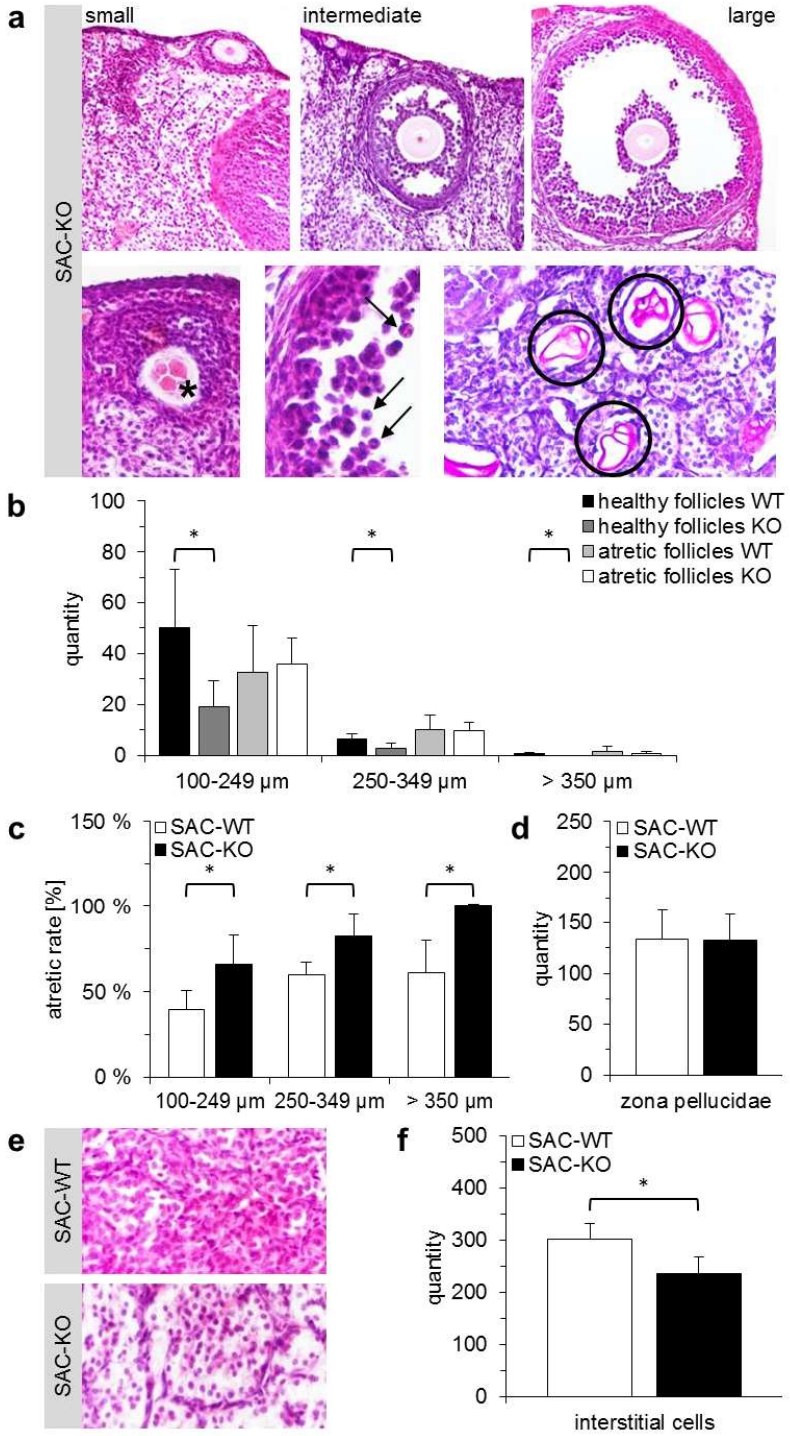

Fig. S2 Morphological features of SAC-WT and SAC-KO ovaries **a** H&E stained sections of SAC-KO ovaries. According to their diameter follicles are classified as small (100 – 249 µm), intermediate (250 – 349 µm) and large (> 350 µm) (upper row from left to right). Oocyte fragmentation (star), apoptotic bodies in a loosened granulosa cell layer (arrow) and PAS stained remnants of zona pellucidae in the interstitial tissue (circle) (lower row from left to right) (magnification: 20x) **b** Quantity of small, intermediate and large healthy and atretic follicles in SAC-WT and SAC-KO ovaries (n = 5) **c** Ratio of atretic to healthy follicles in SAC-WT and SAC-KO ovaries (n = 5) for all three groups of follicle sizes **d** Quantity of zonae pellucidae remnants in the interstitial tissue of SAC-WT and SAC-KO ovaries (n = 5) **e** H&E stained clusters of interstitial cells in a SAC-WT and SAC-KO ovary (magnification: 20x) **f** Quantity of interstitial gland cells in SAC-WT and SAC-KO mice (n = 5). Data are plotted as mean ± standard deviation, $p<0.05$ (*).

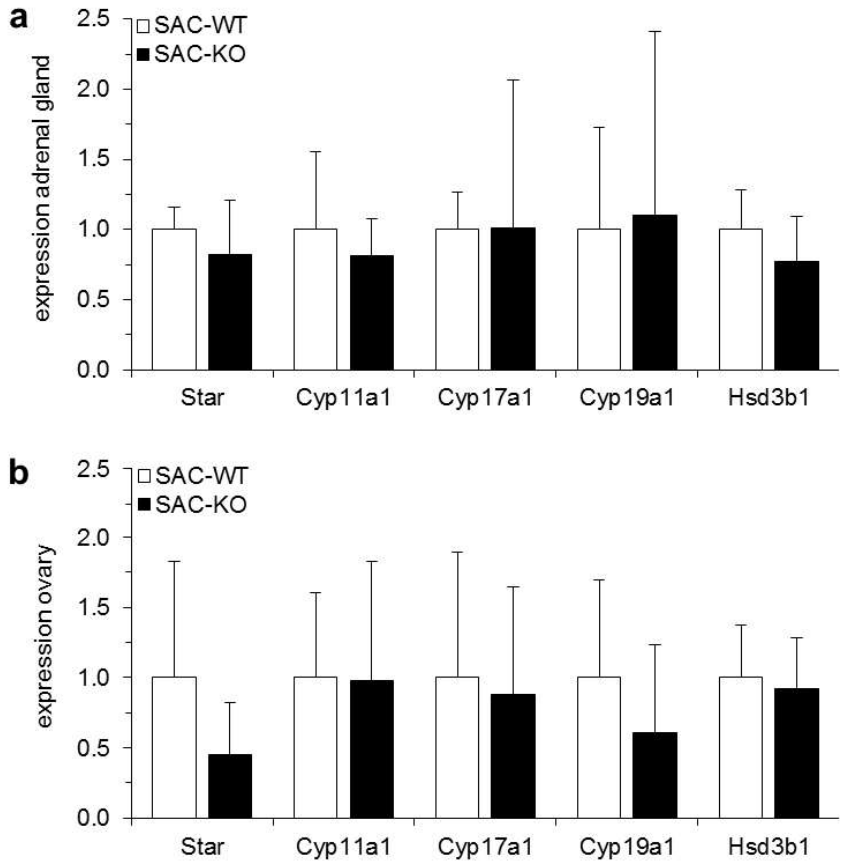

Fig. S3 Gene expression of *Star, Cyp11a1, Cyp17a1, Cyp19a1* and *Hsd3b1* in **a** adrenal glands and **b** ovaries of female SAC-KO (n = 10) compared to SAC-WT (n = 8) quantified by qPCR. Data are plotted as mean ± standard deviation.

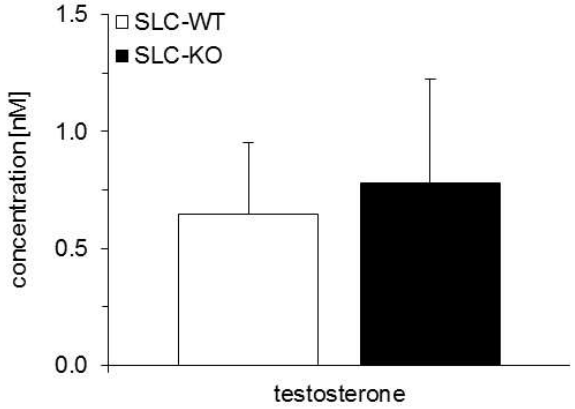

Fig. S4 Concentration of testosterone in plasma of SLC-WT (n = 7) and SLC-KO (n = 8) mice measured by LC-MS/MS. Data are plotted as mean ± standard deviation.

References

Bindea G, et al. (2009) ClueGO: a Cytoscape plug-in to decipher functionally grouped gene ontology and pathway annotation networks. Bioinformatics 25(8):1091-3. doi: 10.1093/bioinformatics/btp101

Johänning J, et al. (2015) Highly sensitive simultaneous quantification of estrogenic tamoxifen metabolites and steroid hormones by LC-MS/MS. Analytical and bioanalytical chemistry 407(24):7497–7502. doi: 10.1007/s00216-015-8907-8

Kagabu S, Umezu M (2004) Histological analysis of the 'critical point' in follicular development in mice. Reproductive Medicine and Biology 3(3):141–145. doi: 10.1111/j.1447-0578.2004.00062.x

Maere S, et al. (2005) BiNGO: a Cytoscape plugin to assess overrepresentation of gene ontology categories in biological networks. Bioinformatics 21(16):3448-9. doi: 10.1093/bioinformatics/bti551

Merkwitz C, et al. (2016) A simple method for inducing estrous cycle stage-specific morphological changes in the vaginal epithelium of immature female mice. Laboratory animals 50(5):344–353. doi: 10.1177/0023677215617387

Myers M, et al. (2004) Methods for quantifying follicular numbers within the mouse ovary. Reproduction (Cambridge, England) 127(5):569–580. doi: 10.1530/rep.1.00095

Oakberg EF (1979) Follicular growth and atresia in the mouse. In Vitro 15(1):41–49. doi: 10.1007/BF02627078

Sandrock M, et al. (2009) Reduction in corpora lutea number in obese melanocortin-4-receptor-deficient mice. Reproductive biology and endocrinology 24;7:24. doi: 10.1186/1477-7827-7-24.

Spanel-Borowski K, et al. (1983) Morphological and morphometric changes in the ovaries of white-footed mice (Peromyscus leucopus) following exposure to long or short photoperiod. The Anatomical record 205(1):13–19. doi: 10.1002/ar.1092050103

Szollosi D, et al. (1990) Sperm penetration into immature mouse oocytes and nuclear changes during maturation: an EM study. Biology of the cell 69(1):53–64

Zellmer S, et al. (2009) Heterogeneous expression of suppressor of cytokine signalling 2 (SOCS-2) in liver tissue. Journal of anatomy 215(2):176-83. doi: 10.1111/j.1469-7580.2009.01085.x

CHAPTER 2

The Diurnal Timing of Starvation Differently Impacts Murine Hepatic Gene Expression and Lipid Metabolism – A Systems Biology Analysis Using Self-Organizing Maps

Rennert C, Vlaic S, Marbach-Breitrück E, Thiel C, Sales S, Shevchenko A, Gebhardt R, Matz-Soja M (2018) *The Diurnal Timing of Starvation Differently Impacts Murine Hepatic Gene Expression and Lipid Metabolism – A Systems Biology Analysis Using Self-Organizing Maps.* Frontiers in Physiology 9:1180. doi: 10.3389/fphys.2018.01180

frontiers in Physiology

ORIGINAL RESEARCH
published: 10 September 2018
doi: 10.3389/fphys.2018.01180

The Diurnal Timing of Starvation Differently Impacts Murine Hepatic Gene Expression and Lipid Metabolism – A Systems Biology Analysis Using Self-Organizing Maps

*Christiane Rennert[1], Sebastian Vlaic[2], Eugenia Marbach-Breitrück[1,3,4], Carlo Thiel[1], Susanne Sales[5], Andrej Shevchenko[5], Rolf Gebhardt[1] and Madlen Matz-Soja[1]**

[1] Rudolf-Schönheimer-Institute of Biochemistry, Faculty of Medicine, Leipzig University, Leipzig, Germany, [2] Leibniz Institute for Natural Product Research and Infection Biology, Hans-Knöll-Institute, Jena, Germany, [3] Institute of Biochemistry, Charité – Universitätsmedizin Berlin, Berlin, Germany, [4] Berlin Institute of Health, Freie Universität Berlin, Humboldt-Universität zu Berlin, Berlin, Germany, [5] Max Planck Institute of Molecular Cell Biology and Genetics, Dresden, Germany

OPEN ACCESS

Edited by:
Andreas Teufel, Universität Heidelberg, Germany

Reviewed by:
Olga Papadodima, National Hellenic Research Foundation, Greece
Syed Aun Muhammad, Bahauddin Zakariya University, Pakistan

***Correspondence:**
Madlen Matz-Soja
madlen.matz@medizin.uni-leipzig.de

Specialty section:
This article was submitted to Systems Biology, a section of the journal Frontiers in Physiology

Received: *29 March 2018*
Accepted: *06 August 2018*
Published: *10 September 2018*

Citation:
Rennert C, Vlaic S, Marbach-Breitrück E, Thiel C, Sales S, Shevchenko A, Gebhardt R and Matz-Soja M (2018) The Diurnal Timing of Starvation Differently Impacts Murine Hepatic Gene Expression and Lipid Metabolism – A Systems Biology Analysis Using Self-Organizing Maps. Front. Physiol. 9:1180. doi: 10.3389/fphys.2018.01180

Organisms adapt their metabolism and draw on reserves as a consequence of food deprivation. The central role of the liver in starvation response is to coordinate a sufficient energy supply for the entire organism, which has frequently been investigated. However, knowledge of how circadian rhythms impact on and alter this response is scarce. Therefore, we investigated the influence of different timings of starvation on global hepatic gene expression. Mice (n = 3 each) were challenged with 24-h food deprivation started in the morning or evening, coupled with refeeding for different lengths and compared with *ad libitum* fed control groups. Alterations in hepatocyte gene expression were quantified using microarrays and confirmed or complemented with qPCR, especially for lowly detectable transcription factors. Analysis was performed using self-organizing maps (SOMs), which bases on clustering genes with similar expression profiles. This provides an intuitive overview of expression trends and allows easier global comparisons between complex conditions. Transcriptome analysis revealed a strong circadian-driven response to fasting based on the diurnal expression of transcription factors (e.g., *Ppara*, *Pparg*). Starvation initiated in the morning produced known metabolic adaptations in the liver; e.g., switching from glucose storage to consumption and gluconeogenesis. However, starvation initiated in the evening produced a different expression signature that was controlled by yet unknown regulatory mechanisms. For example, the expression of genes involved in gluconeogenesis decreased and fatty acid and cholesterol synthesis genes were induced. The differential regulation after morning and evening starvation were also reflected at the lipidome level. The accumulation of hepatocellular storage lipids (triacylglycerides, cholesteryl esters) was significantly higher after the initiation of starvation in the morning compared to the evening. Concerning refeeding, the gene expression pattern after a 12 h refeeding period largely resembled that of the corresponding starvation state but approached the *ad libitum* control state

after refeeding for 21 h. Some components of these regulatory circuits are discussed. Collectively, these data illustrate a highly time-dependent starvation response in the liver and suggest that a circadian influence cannot be neglected when starvation is the focus of research or medicine, e.g., in the case of treating victims of sudden starvation events.

Keywords: hepatocyte, circadian regulation, self-organizing map, starvation, refeeding

INTRODUCTION

Organisms handle periods of food deprivation by drawing on reserves and adapting their metabolism. Humans use fasting to lose weight and for spiritual reasons. The liver is the central hub for metabolic processes, including glucose, amino acid, and lipid metabolism. Therefore, the impact of fasting and refeeding is immense, especially on hepatic parameters (Longo and Mattson, 2014). In this study we addressed the question how the circadian regulation influences the hepatic starvation response with a rarely but powerful used approach called self-organizing map (SOM).

Livers in the post-prandial state store excessive metabolites as glycogen and produce fatty acids, which are transiently stored as triacylglycerides (TAGs) or secreted as very low density lipoprotein (VLDL) (Rui, 2014). The liver synthesizes new carbohydrates and produces ketone bodies in periods of prolonged fasting after depletion of glucose stores. Hormones, such as insulin and glucagon, regulate these processes at a systemic level, and transcription factors, such as PPARs (peroxisome proliferator activated receptor), SREBP transcripts (sterol regulatory element binding transcription protein), and ChREBP [carbohydrate-responsive element-binding protein or MLX-interacting protein-like (MLXIPL)] adjust the metabolism at the molecular level.

Besides the impact of feeding state on the liver metabolism, the timing of food supply influences the metabolic state enormously (Wehrens et al., 2017). In general, the mammalian physiology is synchronized by an inner time-keeping mechanism called the circadian clock. The molecular circadian regulation is based on central clock genes expressed in almost all tissues and cells. The translated proteins generate and regulate the circadian rhythm via transcriptional and translational feedback loops. The transcriptional activators ARNTL (aryl hydrocarbon receptor nuclear translocator-like protein 1 or BMAL1) and CLOCK (circadian locomotor output cycles kaput) stimulate the expression of the negative regulators Period (*Per1*, *Per2,* and *Per3)* and Cryprochrome (*Cry1* and *Cry2*), which in turn repress ARNTL/CLOCK activity. The overall circadian rhythm is coordinated by the suprachiasmatic nuclei (SCN) in the hypothalamus (Ralph et al., 1990; Welsh et al., 2010). Synchronized by an optic light/dark signal the SCN generates output signals coupling the central pacemaker with the peripheral tissues. On the basis of oscillating hormonal and endocrine signals (Yang et al., 2007) the peripheral organs, such as the liver, synchronize their own circadian oscillation. Approximately 15% of all genes are transcribed in a circadian manner whereby one big aspect of circadian regulation includes metabolic processes and energy homeostasis in peripheral tissues, especially in liver (Albrecht, 2012). The tight connection between circadian clock and metabolic processes is underlined by the fact that a vast majority of liver genes is expressed rhythmically, including those regulating, e.g., glucose or lipid metabolism (Stratmann and Schibler, 2006; Ferrell and Chiang, 2015). Interestingly, the liver clock was shown not only be entrained by SCN-synchronization, but also by external factors. One of the most prominent influencers of liver circadian rhythms is the feeding regime. The consumed food volume and the starvation intervals between the meals are able to alter the liver clock (Hirao et al., 2010) and restricted feeding can even rapidly uncouple the liver rhythm from that of SCN (Stokkan et al., 2001).

Disturbance of the normal eating patterns of mice using external food restriction alters the entire metabolism (Jensen et al., 2013), which were analyzed previously using different omics approaches (Bauer et al., 2004; Sokolović et al., 2008; Hakvoort et al., 2011). However, knowledge of specific modulations produced by circadian regulation is scarce. Therefore, we analyzed the impact of fasting and refeeding at two different time-points [zeitgeber time (ZT) 3 and ZT 12] on the physiological and metabolic states of primary hepatocytes at a global omics level. Evaluations of transcriptome data were performed using SOMs. SOMs are an alternative approach that allows the identification of global expression trends via clustering of similarly expressed genes. The relative expression of gene groups is color-coded and enables an intuitive and unbiased interpretation of the data (Wirth et al., 2011). The results demonstrated that the timing of food restriction altered the influence of starvation on hepatocytes. A 24-h starvation period produced different gene expression patterns and lipidome profiles in liver cells depending on the starting time. While starvation started in the morning led to the known adaptions like initiation of gluconeogenesis and suppression of fatty acid and cholesterol synthesis, starvation started in the evening decreased gluconeogenesis-associated gene expression and induced fatty acid synthesis genes. Refeeding mice for 12 h after a 24-h long starvation period was not sufficient to restore the gene expression pattern of *ad libitum* fed mice, which was revealed by persistent dysregulation of essential metabolic pathways, such as lipid metabolism and autophagy. However, an extended refeeding period of 21 h approached an expression pattern similar to that of the *ad libitum* state, but some differences persisted.

MATERIALS AND METHODS

Maintenance of the Mice and Feeding

Male C57BL/6N mice were maintained in a pathogen-free facility on a 12:12 h light–dark cycle (light on at 6 a.m = ZT 0, light off at 6 p.m. = ZT 12), according to German guidelines and those of

the world medical association declaration of Helsinki for the care and safe use of experimental animals. The animal experiments were approved by the Landesdirektion Sachsen. The mice had free access to regular chow (ssniff® R/M-H V1534; 58%, 33%, 9% calories from carbohydrates, proteins and fat, respectively; metabolisable energy: 12.8 kJ/g; ssniff® Spezialdiaeten GmbH, Germany) and tap water.

Prior to the experimental procedures, animals were randomly segregated into six groups (n = 3 each). In a first experiment, starvation was started either at ZT 3 (9 a.m.) or at ZT 12 (6 p.m.) and mice were sacrificed after 24 h at the same times on the next day together with *ad libitum* fed groups (**Figure 1A**). In the refeeding experiment two groups of mice were starved for 24 h started at ZT 15 followed by refeeding for 12 or 21 h until ZT 3 and ZT 12 on the next day, respectively (**Figure 1B**).

Isolation of Primary Mouse Hepatocytes, RNA Isolation, and Quantitative Real-Time PCR (qPCR)

The primary hepatocytes were isolated from male C57BL/6N mice, treated like explained above. Isolation was performed by a collagenase perfusion technique as described before (Gebhardt et al., 2003). The cell suspension was cleared of non-parenchymal cells by differential centrifugation steps (Matz-Soja et al., 2014). Pure hepatocyte fraction was used for further procedures.

Total RNA from hepatocytes was extracted using RNeasy® Mini Kit (Qiagen, Hilden) and the quality was controlled by agarose gel electrophoresis. The reverse transcription was performed with the Proto Script M-MuLV First Strand cDNA Synthesis Kit (New England Biolabs). Gene expression quantification by qPCR was performed in duplicates using the Rotor-Gene SYBR® Green PCR Kit and a Rotor-Gene Q (Qiagen). Gene specific intron-spanning primers were designed with Primer 3 software and are listed in **Supplementary Table 1**. The specific qPCR products were quantified using internal amplification standards; 18S was used as reference gene. Values are plotted as average of biological replicates (n = 3) ± standard deviation. The statistical evaluation was performed with the unpaired Student's t-test (GraphPad Prism 7). The null hypothesis was rejected at $^{*}p < 0.05$, $^{**}p < 0.01$, and $^{***}p < 0.001$ levels.

Illumina Microarray Processing and Data Analysis Using SOM

For each condition, the RNA from three mice was pooled and used as one sample in the microarrays (BeadChip Array MouseRef-8 v2, Illumina). The analysis was performed by the Interdisciplinary Centre for Clinical Research, Leipzig (Faculty of Medicine, Leipzig University). The following link provides the raw data of the microarray[1].

All computational analyses were performed using R software (Ihaka and Gentleman, 1996). Microarrays were annotated using the annotation provided by Illumina and raw expression data were pre-processed using the lumi package (Du et al., 2008). Pre-processing included background correction using the bgAdjust method, variance stabilization transformation, and quantile normalization. Detection calls were performed with default parameters to remove absent beads. Furthermore, the expression values for single beads were mapped to a gene symbol identifier. For each array, multiple bead IDs mapping to the same gene symbol were averaged.

General expression trends in each sample were identified using SOMs as implemented in the oposSOM package (Löffler-Wirth et al., 2015). SOMs are artificial neural networks trained by unsupervised learning (Kohonen, 1982). This machine learning approach allows dimension reduction of high-dimensional data by clustering similarly regulated genes to so-called "metagenes". For each treatment, it can be defined if the expression of a certain metagene is over or under the mean expression of this metagene in the analyzed pool (termed as over- and underexpression), and all groups are compared equivalently. The metagenes, here 20 × 20, can be visualized in a map where adjacent metagenes have similar expression profiles and more distant ones are expressed differently, with the invariant genes located in the center of the map. Furthermore, a color gradient codes the expression level of the metagenes, maroon indicating the highest expression, blue the lowest expression, and yellow and green intermediate levels (Wirth et al., 2011). This image-based analysis allows an intuitive interpretation and provides an overview of the overall regulation patterns. Apart from the creation of SOMs, the oposSOM package also provided additional analytical methods including the identification of over- or underexpressed spots in the SOMs, clustering of metagenes using k-means (Hartigan and Wong, 1979), and enrichment testing for metagene-cluster and over- or underexpressed spots using Gene Ontology (GO) terms (Ashburner et al., 2000) as provided by the Ensembl database (Aken et al., 2016).

Based on the k-means clustering as performed automatically by the oposSOM package, we performed a gene enrichment analysis (GEA) for all genes with an absolute expression change ≥ 1.5-fold and the genes from each cluster using the web-based tool DAVID (Database for Annotation, Visualization and Integrated Discovery Bioinformatics Resources 6.8[2], **RRID**:SCR_001881). We selected *Mus musculus* as the background and filtered the GO terms with a Benjamini–Hochberg corrected p-value < 0.05.

Visualization of single genes for the identified significant GO terms was performed using heatmaps. The expression levels of single genes were displayed as relative expression values compared to the mean expression in all six samples analogous to the metagenes (termed as over- and underexpression). All genes with an absolute expression change ≥ 1.5-fold [$\log_2(1.5)$] between at least two of the six groups were considered for further analysis.

The STRING database version 10.5[3] was used to explore the interactions between the studied genes/proteins related to hepatic starvation response (Szklarczyk et al., 2015). The networks were

[1]https://seek.lisym.org/data_files/98?code=YGHGwNPpYhqpiEBnnv4qb%2BchjgjUoYGhH6bc3OQp

[2]https://david.ncifcrf.gov/

[3]http://string-db.org

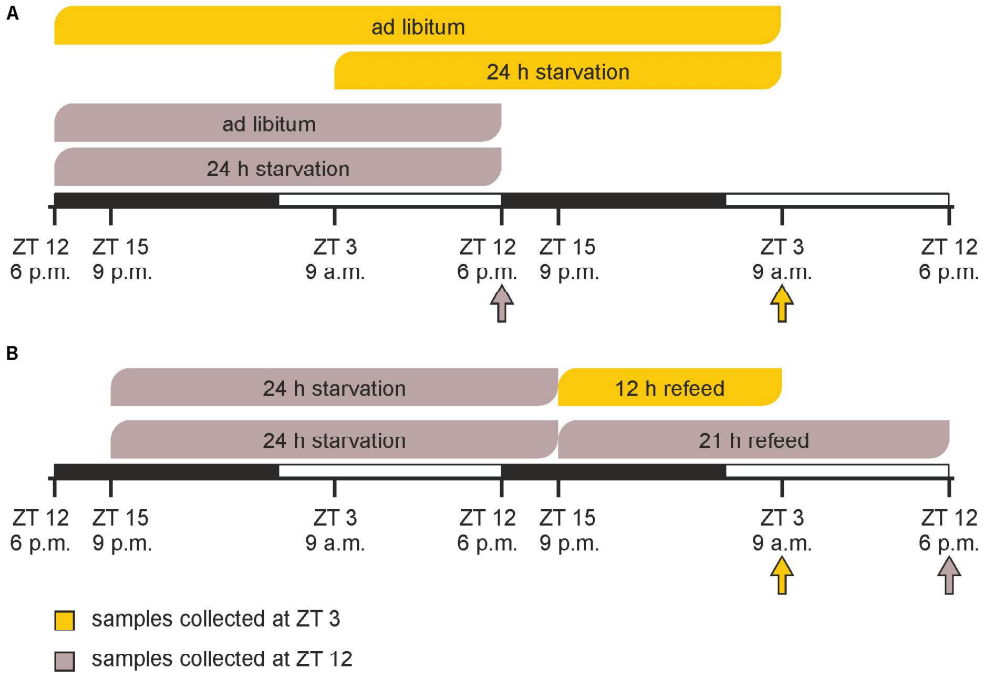

FIGURE 1 | Timeline of feeding/starving cycles and sacrifice. **(A)** Mice were fed *ad libitum* or starved for 24 h prior to sacrifice at ZT 3 (9 a.m.) or ZT 12 (6 p.m.). **(B)** Mice were starved for 24 h from ZT 15 (9 p.m.) to ZT 15 and refed for 12 or 21 h prior sacrifice. The arrows indicate the times of sacrifice.

constructed in the "confidence" mode with a high confidence score (0.7).

Shotgun Lipidomics

Lipids from primary hepatocytes were extracted by a modified protocol of Folch (Folch et al., 1957) and analyzed by shotgun mass spectrometry as described previously (Schuhmann et al., 2012). Briefly, hepatocytes (an amount equivalent to 10 µg of total protein) were dissolved in 200 µl ammonium bicarbonate solution (150 mM). For the subsequent quantification 10 µl internal standard mixture were added (20 pmol TAG 12:0-12:0-12:0, 20 pmol DAG 17:0- 17:0, 40 pmol diethyl PC 18:0-18:0, 50 pmol diethyl PE 20:0-20-0, 10 pmol PG 17:0-17-0, 40 pmol PS 12:0-12:0, 50 pmol PI 16:0-16-0, 40 pmol LPC 12:0, 40 pmol LPE 14:0, 30 pmol SM d18:1-12:0, 90 pmol CE 12:0, 20 pmol Cer d18:1-12:0, 50 pmol cholesterol d7; Avanti Polar Lipids, Inc., Alabaster, AL, United States). Then, 265 µl of methanol and 730 µl of chloroform were added and the mixture was vortexed for 1 h at 4°C. The lower organic phase was collected, dried in a vacuum centrifuge and the lipid extracts were re-dissolved in 120 µl chloroform:methanol [1:2 (v/v)] mixture. The analysis was performed in both, negative, and positive ion mode. For negative mode analyses, 10 µl extract were mixed with either 12 µl of 13 mM ammonium acetate in isopropanol or 0.1% (v/v) triethylamine in methanol. For positive mode analyses, 10 µl extract were mixed with 90 µl of 6.5 mM ammonium acetate in isopropanol before infusion. The analyses were performed on a Q Exactive mass spectrometer (Thermo Fisher Scientific, Germany) equipped with a robotic nanoflow ion source TriVersa NanoMate (Advion BioSciences, Ithaca, NY, United States). High resolution (140,000 at m/z 200) FT-MS spectra were acquired for 1 min within the range of m/z 420–1000 in negative and 450–1000 in positive mode. Cholesterol was quantified as previously described (Liebisch et al., 2006). Briefly, 30 µl of extract were dried under vacuum, then 75 µl acetyl chloride:chloroform [1:2 (v/v)] were added, incubated for 1 h at room temperature, dried under vacuum and re-dissolved in 60 µl chloroform:methanol [1:2 (v/v)]. 10 µl extract were mixed with 90 µl of 6.5 mM ammonium acetate in propanol before infusion and analyzed in positive ion mode. The following lipid classes were identified and quantified using the LipidXplorer software (Herzog et al., 2011): tri- and diacylglycerides (TAG/DAG), cholesteryl esters (CE), sphingomyelins (SM), phosphatidylethanolamines (PEs), phosphatidylcholines (PCs), and cholesterol. The concentrations are plotted in pmol lipid per µg total protein as average of the biological replicates ($n = 3$) ± standard deviation.

RESULTS

Feeding procedures immensely affect an organism's metabolism. The present study examined alterations in the physiology and the metabolism of murine hepatocytes following a 24-h starvation

period initiated at ZT 3 (morning) or ZT 12 (evening) compared to hepatocytes from mice fed *ad libitum* (**Figure 1A**). Our data indicated that the effects strongly depended on the timing of starvation. We also compared hepatocytes in refed state to the corresponding starvation group and *ad libitum* fed mice to evaluate whether 12 or 21 h of refeeding were sufficient to restore the *ad libitum* expression profile (**Figure 1B**).

Global Hepatic Gene Expression Is Influenced by Feeding and Timing

Illumina microarrays, analyzed, and visualized using SOMs, delivered an overview of the hepatic alterations induced by different feeding regimes. A GEA of all regulated genes (**Supplementary Table 2A**) produced an impression of the involved GO terms. Further we performed a separate analysis for each cluster to distinguish between them. Based on the SOMs of the *ad libitum* samples from ZT 3 and ZT 12 it strikes that a large amount of the genes in the liver were expressed in a circadian manner (**Figure 2A**), since the expression of almost all metagenes differed. ZT 3 showed two overexpression spots at the left margin, annotated as clusters A and B by a k-means clustering of the SOMs (**Figure 2D** and **Supplementary Table 2B**). Cluster A is associated with immune system processes ('complement activation,' classical pathway,' 'innate immune response') and many GO terms in regard to extracellular space and membrane ('extracellular region,' 'plasma membrane,' 'cell surface'), while cluster B contains many lipid metabolism associated GO terms ('fatty acid metabolic process,' 'acyl-CoA metabolic process') and the GO term 'autophagy.' The large underexpression spot in the upper right corner partly covered by cluster J contains many cholesterol and steroid associated GO terms ('cholesterol metabolic process,' 'steroid metabolic process,' 'fatty acid metabolic process'). In comparison to ZT 3, ZT 12 exhibited a mean expression in the area of clusters B and J (**Figures 2A,D**). But ZT 12 had a small overexpressed area in the upper left corner (cluster H) related to the GO term 'metabolic process' and an underexpression spot in the lower right corner (cluster F) containing GO terms associated with protein binding and degradation ('chaperone binding,' 'endoplasmic reticulum,' 'proteasome accessory complex').

Starvation started at both ZT 3 and ZT 12 immensely changed the expression profiles of the metagenes in the SOMs compared to the related *ad libitum* state (**Figure 2B**). Additionally, comparing ZT 3 and ZT 12 starvation no congruence is visible, which implies a diurnal-driven response to fasting. The 24-h starvation period at ZT 3 began during the day followed by a whole night of fasting (**Figure 1A**), which changed the size and shape of the overexpression spot in the lower left corner and the underexpression spot in the upper right corner (clusters B and J), regions associated with lipid and steroid metabolism (**Figures 2B,D**). In contrast, the ZT 12 starvation period started in the night followed by a whole day of fasting (**Figure 1A**) and resulted in a totally changed metagene expression, where the whole left margin is underexpressed, while the right margin shows an overexpression (**Figure 2B**). The regions (clusters B and J) where GO terms related to autophagy, lipid and steroid metabolism are localized have an opposed expression comparing ZT 3 and ZT 12 starvation.

The refeeding experiment (**Figure 1B**) revealed disparate SOMs after refeeding mice for 12 h and the ZT 3 *ad libitum* group (**Figure 2C**). However, the SOM of 12 h refeed (**Figure 2C**, upper panel) showed high similarity with the corresponding ZT 12 starvation group (**Figure 2B**, lower panel). The mice sampled at ZT 12 were starved for the same 24-h period, but were refed for 21 h prior sacrifice. This prolonged refeed period produced a somehow mixture of expression profiles from ZT 12 *ad libitum* and starvation state (**Figure 2C**). While clusters F and H resemble that of ZT 12 *ad libitum* (**Figure 2A**, lower panel), the regions where lipid and steroid metabolism are localized (clusters B and J) still showed the starvation pattern (**Figure 2B**, lower panel).

Alterations in Relevant Metabolic Features Following Starvation and Refeeding

SOM analysis identified differently regulated metabolic alterations produced by the various feeding regimes. A list of all regulated genes detected by the microarrays is compiled in **Supplementary Table 3**. The present study focused on the expression of genes related to intermediary metabolism (glucose and lipid metabolism), steroid metabolism, insulin signaling, and autophagy. We also analyzed central clock gene expression because the circadian aspect of the feeding regimes was particularly interesting. The interactions of the involved genes/proteins were visualized within a protein interaction network, illustrating the mutual connections (**Supplementary Figure 1**).

Circadian Regulation

Diurnal influence

Being the first order clock genes, *Arntl* and *Clock* gene products activate the expression of different target genes, including *Per1/2/3* homolog and *Cry*. PER and CRY, in turn, repress their own expression by interacting with ARNTL and CLOCK (Partch et al., 2014). Consequently to these regulations the expression of *Arntl*/*Clock* and *Per* occurs in antiphase, which is seen in **Figure 3** (*ad libitum*). In the *ad libitum* state *Arntl* and *Clock* were overexpressed at ZT 3 and underexpressed at ZT 12, *Per1* and *Per2* were regulated vice versa. *Nr1d2* (Rev-erb beta), another gene of the negative feedback loop, exhibited a typical rhythmic regulation with a higher expression at ZT 12 than at ZT 3. These results were verified by qPCR and used to validate the microarray (data not shown).

Starvation

Expression of central clock genes were primarily regulated in a diurnal manner (**Figure 3**). However, fasting also influenced central circadian genes. A 24-h starvation period initiated at ZT 3 or ZT 12 increased *Arntl* and *Clock* expression levels, but the typical diurnal regulation of these genes remained. The opponent *Per2* was down-regulated after starvation initiated at ZT 3 and up-regulated in the ZT 12 starvation mice compared to the corresponding *ad libitum* samples. The *Per1* expression was only

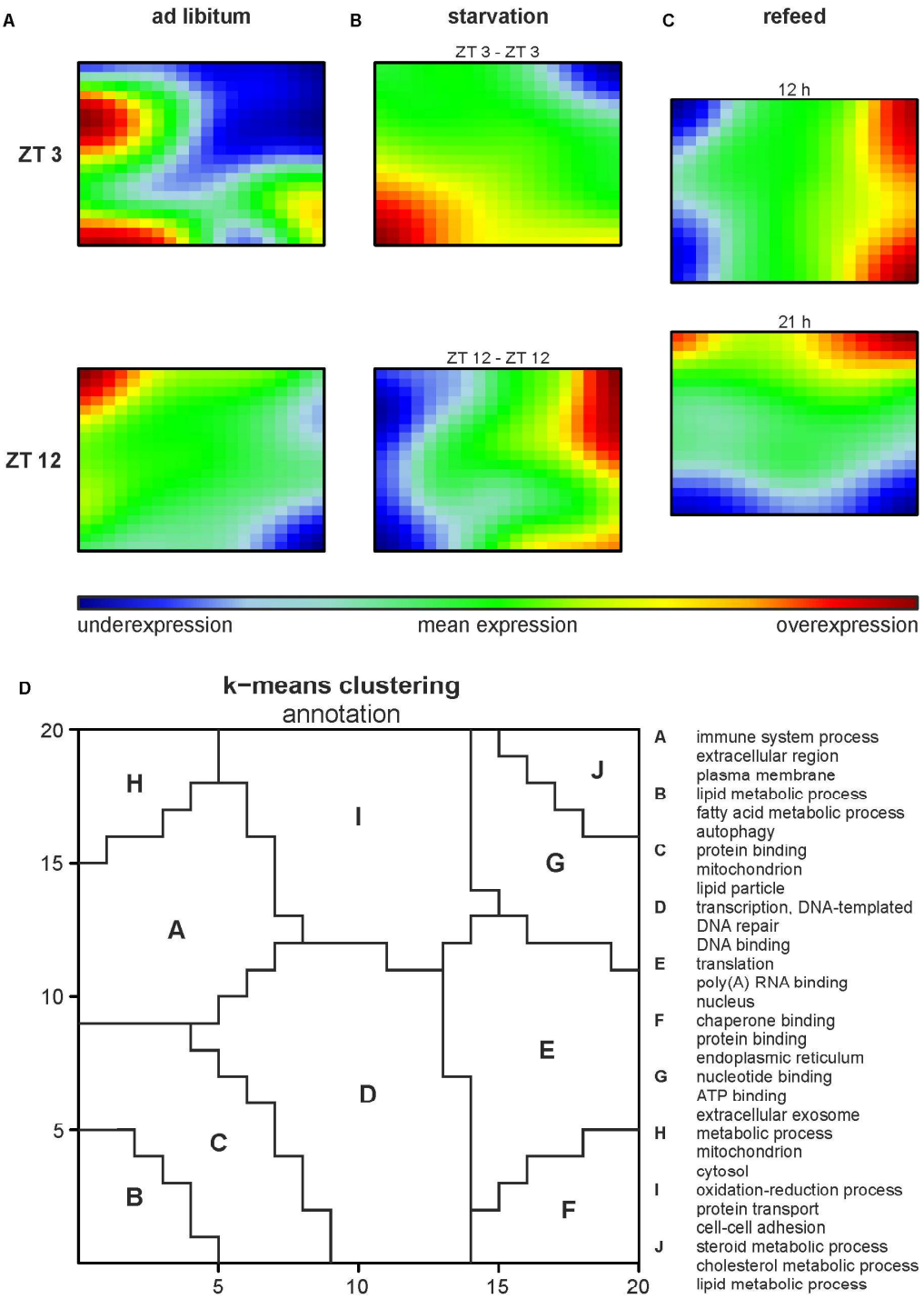

FIGURE 2 | Global hepatic gene expression dependent on feeding patterns and timing. **(A–C)** Self organizing maps (SOMs) illustrating the expression of metagenes (20 × 20); maroon indicates an overexpression, blue an underexpression. Mice were sacrificed at ZT 3 and ZT 12 after **(A)** fed *ad libitum*, **(B)** starved for 24 h or **(C)** starved for 24 h and refed for 12 h until ZT 3 or 21 h until ZT 12. **(D)** Annotation of the SOMs using k-means clustering and following gene-enrichment analysis. Selected GO terms are shown. A full list is available in **Supplementary Table 2B**.

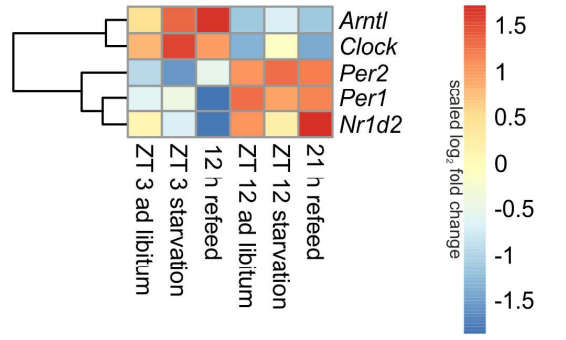

FIGURE 3 | Heatmap of differentially expressed central circadian genes. Red indicates an overexpression, and blue indicates an underexpression.

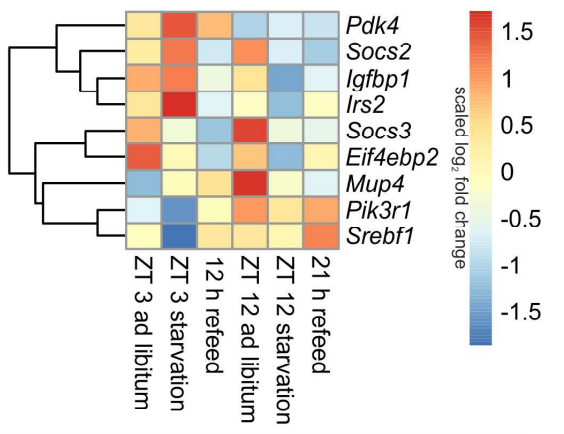

FIGURE 4 | Heatmap of differentially expressed genes related to insulin signaling. Red indicates an overexpression, and blue indicates an underexpression.

marginally changed by 24-h starvation in the morning and the evening, while *Nr1d2* was decreased after both starvation periods.

Refeed

When mice were fasted for 24 h and refed for 12 h until ZT 3, the *Arntl* expression was highly increased, while a prolonged refeed period of 21 h abolished the effect of starvation (**Figure 3**). The *Clock* expression was no longer altered after both refeed periods. *Per1* expression was decreased after a 12 h refeed, but the 21 h refeed already restored the *ad libitum* expression. *Per2* expression was higher after both refeed periods in comparison to *ad libitum*. The expression of *Nr1d2* showed big changes after both refeed periods, the expression was further decreased after 12 h and increased after 21 h refeed.

All in all, a 21 h refeeding seemed to be sufficient to abolish the alterations in the expression of the genes of the primary negative-feedback loop (*Arntl*, *Clock*, *Per1,* and *Per2*) caused by starving the mice. But after 12 h refeed the expression of *Arntl*, *Per1,* and *Per2* still showed major changes compared to the *ad libitum* sample.

Insulin Signaling

Diurnal influence

Insulin is one of the master regulators of the metabolism and its effects are partially mediated by insulin receptor signaling (Boucher et al., 2014). The microarray analyses revealed diurnal regulation of several genes of this pathway (**Figure 4**). For example, *Pik3r1* (phosphatidylinositol 3-kinase, regulatory subunit, polypeptide 1), part of the inositol phosphorylation complex, showed a lower expression in the morning (ZT 3) compared to the evening (ZT 12). The same regulation occurs for *Mup4* (major urinary protein 4) whose influence on energy metabolism is not well understood yet. However, *Pdk4* (pyruvate dehydrogenase kinase, isoenzyme 4), regulator of glucose metabolism, was higher expressed in the morning than in the evening.

Starvation

The 24-h starvation period initiated in the morning produced strong overexpression of central hepatic insulin signaling genes [e.g., *Pdk4*, *Mup4*, *Irs2* (insulin receptor substrate 2) and *Igfbp1* (insulin like growth factor binding protein 1)]. Notably, all of these genes, except *Pdk4*, were strongly down-regulated after starvation initiated at ZT 12. The expression of *Pik3r1* and *Eif4ebp2* (eukaryotic translation initiation factor 4E binding protein 2), which is a regulator of translation, was lowered in both starvation periods (**Figure 4**). The transcription factor *Srebf1c* was down-regulated only due to starvation started at ZT 3, and it was unaffected by evening starvation (**Figure 6**).

Socs2 and *Socs3* (suppressor of cytokine signaling), which were not regulated diurnally in *ad libitum* fed mice, are associated to the negative regulation of insulin signaling. The data for *Socs2* and *Socs3* revealed a change from an overexpression in ZT 12 *ad libitum* sample to a strong underexpression due to starvation started at ZT 12. *Socs3* expression also slightly decreased when starvation was initiated at ZT 3, but *Socs2* expression slightly increased (**Figure 4**).

Refeed

The expression of nearly all detected genes of insulin receptor signaling did not recover during the 12 h refeeding and resembled the expression of the ZT 12 starvation mice (**Figure 4**). Exceptions included *Pdk4*, which almost reached *ad libitum* levels, and *Srebf1c*, which was highly induced during refeeding. The gene expression levels of *Pdk4*, *Eif4ebp2*, *Pik3r1,* and *Irs2* after a refeeding period of 21 h were similar to the corresponding *ad libitum* levels. The *Socs2* and *Socs3* genes were considerably underexpressed after both refeeding periods.

Autophagy

Diurnal influence

In *ad libitum* fed mice, central genes of the mammalian autophagy pathway, such as *Ulk2* (unc-51 like kinase 2) and *Uvrag* (UV radiation resistance associated gene), were lower expressed in the morning compared to evening. However, *Sqstm1*

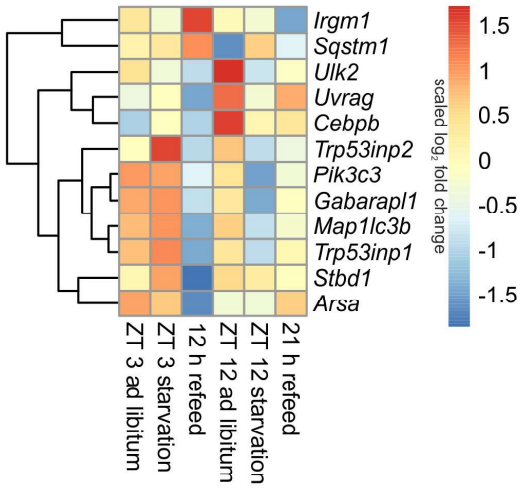

FIGURE 5 | Heatmap of differentially expressed genes related to autophagy. Red indicates an overexpression, and blue indicates an underexpression.

(sequestosome 1), which is required for the recognition of protein aggregates by the autophagy machinery (Bjorkoy et al., 2005), was significantly down-regulated at ZT 12 compared to ZT 3 *ad libitum*. A regulator of autophagy, *Cebpb* (CCAAT/enhancer binding protein beta) was higher expressed in the evening than in the morning (**Figure 5**).

Starvation

When starvation was started at ZT 3 expression of many of the autophagy-associated genes [e.g., *Ulk2*, *Uvrag*, *Sqstm1*, *Pik3c3* (phosphatidylinositol 3-kinase catalytic subunit type 3), *Trp53inp1* (transformation related protein 53 inducible nuclear protein 1), *Gabarapl1* (gamma-aminobutyric acid A receptor-associated protein-like 1), *Map1lc3b* (microtubule-associated protein 1 light chain 3 beta)] was not altered (**Figure 5**). Only *Trp53inp2*, which is essential for autophagosome formation, was markedly up-regulated during the ZT 3 starvation period.

This observation dramatically changed when the starvation period of 24-h was started at ZT 12. The above-mentioned central autophagy genes, with the exception of *Sqstm1*, were dramatically down-regulated during this fasting period, which was especially prominent for *Ulk2* expression. The transcription factor *Cebpb* was up-regulated after food deprivation started at ZT 3 and down-regulated in the evening (**Figure 5**).

Refeed

Our study revealed that the dramatic down-regulation of central autophagy genes due to the initiation of starvation in the evening remained during a refeeding period of 12 h (**Figure 5**). The expression of *Uvrag*, *Trp53inp1*, *Stbd1* (starch binding domain 1) and *Arsa* (arylsulfatase A) was further reduced. However, *Sqstm1* and *Irgm1* (immunity-related GTPase family M member 1), which are involved in autophagic protein degradation (Traver et al., 2011), were up-regulated during the 12 h refeeding period. After a prolonged refeeding of 21 h, most autophagy-related genes approached the ZT 12 *ad libitum* expression levels, but did not reach it. *Cebpb* was expressed at the *ad libitum* level after the 12 h refeed, but its expression was lowered after the 21 h refeed (**Figure 5**).

Intermediary Metabolism

Diurnal influence

Many genes associated with intermediary metabolism (lipid and glucose metabolism) showed a time-dependent expression. The transcription factors that mainly regulate intermediary metabolism, such as *Ppara*, *Pparg*, and *Hnf4a* (hepatocyte nuclear factor 4 alpha), were higher expressed at ZT 12 than at ZT 3, *Mlxipl* (ChREBP) exhibits a vice versa regulation (**Figures 6**, **7**). *Srebf1* transcripts showed no diurnal changes (**Figure 6**). The members of the Elovl (elongation of very long chain fatty acids protein) family (*Elovl2*, *Elovl3*, and *Elovl5*), which are involved in lipid metabolism, were higher expressed at ZT 3 compared to ZT 12, but *Elovl6* exhibited an inverse regulation (**Figure 7**).

Starvation

The regulation of hepatic lipid and glucose metabolisms is based on different transcription factors. The expression of *Ppara*, *Pparg*, and *Hnf4a* was elevated after starvation initiation at ZT 3 compared to the *ad libitum* group (**Figures 6**, **7**).

Notably, starvation initiated at ZT 12 decreased the expression of *Pparg* by significantly by more than 40% and *Ppara* and *Hnf4a* were only marginally regulated. *Hes6*, which is an interaction partner of HNF4a, exhibited diminished expression during starvation started at ZT 3 and increased expression under ZT 12 starvation. *Fgf21* (fibroblast growth factor 21), which is another regulatory element that is closely connected to the PPAR family and the starvation response, exhibited an expression increase by approximately 20-fold after starvation initiated at ZT 3, but this increase was much lower in the ZT 12 group (**Figure 6**). *Mlxipl* was strongly down-regulated after starvation in the morning and was not altered in the evening group. The *Srebf1c* mRNA levels decreased by more than threefold after food deprivation started ZT 3 but were not affected in the ZT 12 group.

The liver ensures the synthesis of sufficient amounts of acetyl coenzyme A (CoA), especially during starvation. Therefore, beta-oxidation is increased due to starvation by the up-regulated expression of many of the involved enzymes, including *Cpt2* (carnitine palmitoyltransferase 2), *Hadhb* (hydroxyacyl-CoA dehydrogenase/3-ketoacyl-CoA thiolase/enoyl-CoA hydratase), *Ehhadh*, *Acaa1b* (acetyl-CoA acyltransferase 1B), *Acsl1* (acyl-CoA synthetase long-chain family member 1) and *Decr1* (2,4-dienoyl CoA reductase 1) (**Figure 7**). However, this increase was much greater when starvation was initiated at ZT 3 rather than at ZT 12. Members of the *Acsl* family are responsible for the activation of long fatty acids and exhibited different regulation. While *Acsl1* strongly increased by starvation started at ZT 3, *Acsl3* and *Acsl5* strongly decreased. In contrast, starting starvation of mice at ZT 12, *Acsl1* and *Acsl5* expression was not altered and *Acsl3* increased.

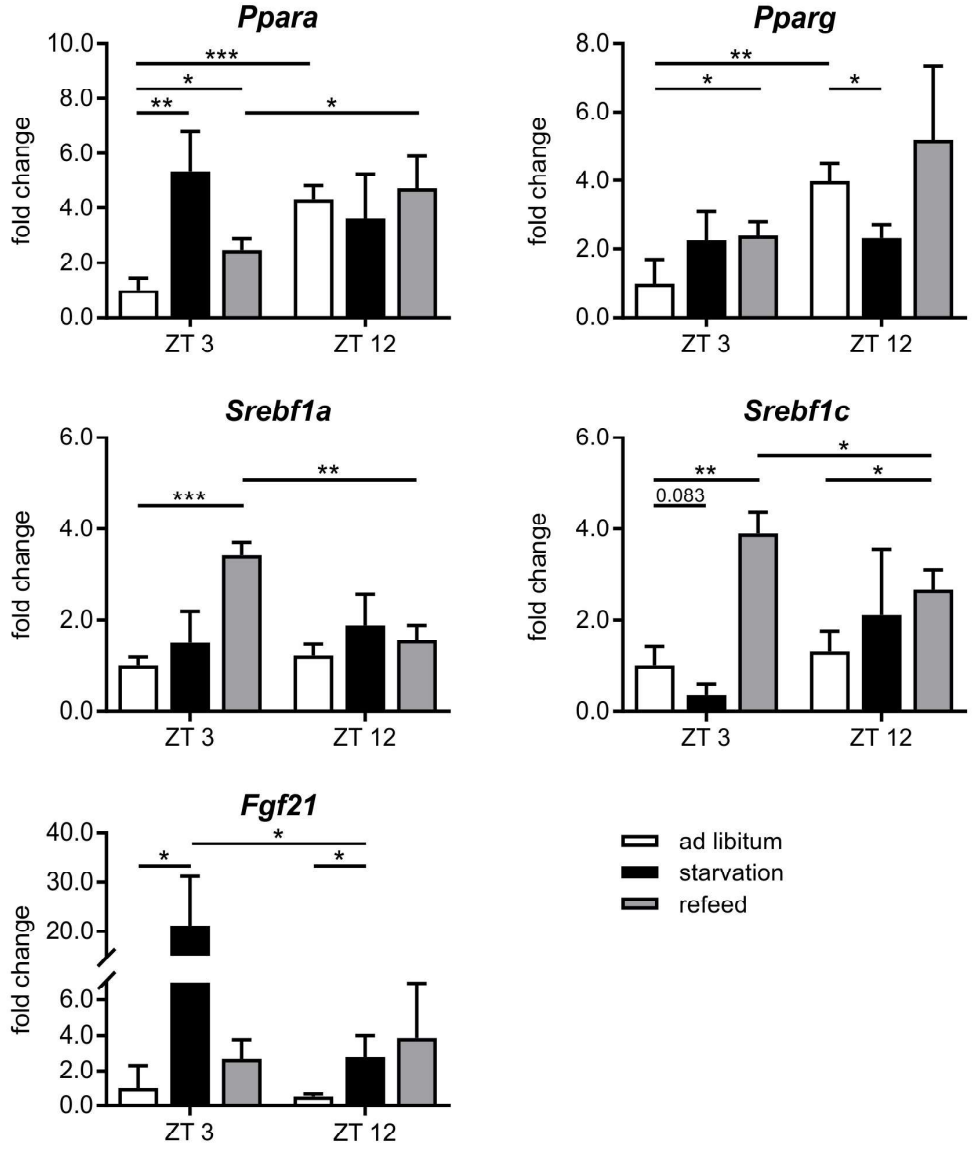

FIGURE 6 | Response of regulatory factors to starvation and refeeding in a diurnal manner. Expression of *Ppara*, *Pparg*, *Srebf1a*, *Srebf1c,* and *Fgf21* in primary hepatocytes of mice fed *ad libitum* (white bars), starved 24 h (black bars) or starved 24 h and refed 12 h (until ZT 3) and 21 h (until ZT 12) (gray bars) quantified using qPCR ($n = 3$). Data are plotted as mean ± standard deviation relative to ZT 3 *ad libitum*, $^{*}p < 0.05$, $^{**}p < 0.01$, and $^{***}p < 0.001$.

Ketogenesis is an essential metabolic pathway to generate ketone bodies during starvation. Genes for the two essential enzymes of ketone body formation, *Hmgcs2* (3-hydroxy-3-methylglutaryl-CoA synthase 2) and *Hmgcl* (3-hydroxymethyl-3-methylglutaryl-CoA lyase), were highly increased after 24-h starvation started at ZT 3, but regulation was only marginal at ZT 12. *Hmgcs2*, *Hmgcl*, *Ehhadh*, *Hadhb,* and *Acaa1b* are also involved in the degradation of the amino acids valine, isoleucine, and leucine. The up-regulation of all enzymes after starvation initiated at ZT 3 ensured an efficient supply of acetyl-CoA (**Figure 7**).

The key enzyme of fatty acid synthesis, *Fasn* (fatty acid synthase), was decreased by 24-h starvation started at ZT 3 and, surprisingly, increased in the ZT 12 group. The gene expression of enzymes involved in elongation and formation of unsaturated fatty acids [e.g., *Scd1* (stearoyl-CoA desaturase 1), *Fads1* (fatty acid desaturase 1), *Hsd17b12* (hydroxysteroid-17-beta dehydrogenase 12), *Thrsp* (thyroid hormone responsive), and

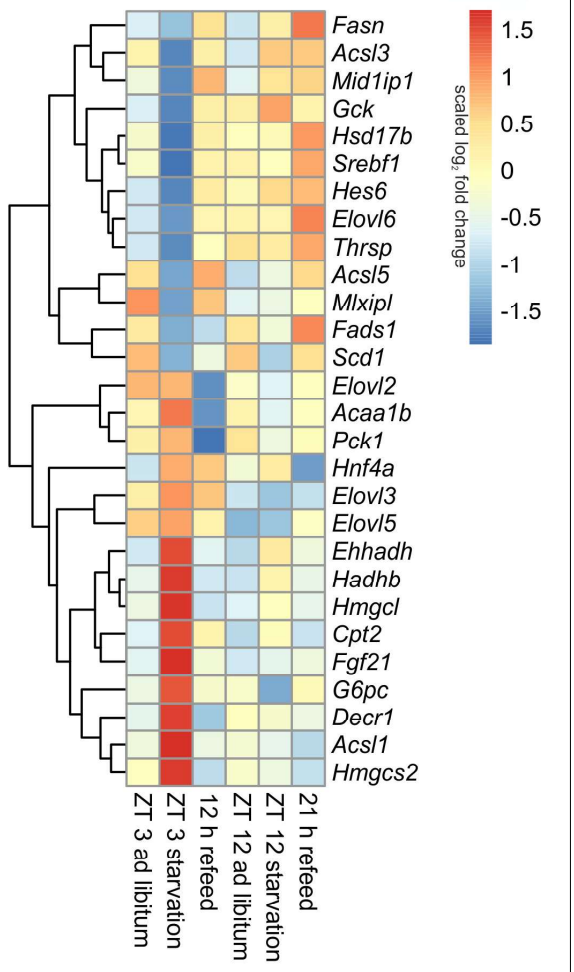

FIGURE 7 | Heatmap of differentially expressed genes related to intermediary metabolism. Red indicates an overexpression, and blue indicates an underexpression.

Mid1ip1 (Mid1 interacting protein 1)] were predominantly down-regulated after starvation initiated at ZT 3 (**Figure 7**). In contrast, starvation initiated at ZT 12 elevated *Scd1* and *Mid1ip1* expression and did not change *Fads1*, *Hsd17b12,* and *Thrsp*. The members of the Elovl family showed only a regulation when starvation was started at ZT 3, but were not influenced at ZT 12. The *Elovl6* level strongly decreased at ZT 3 starvation, whereas *Elovl3* increased (**Figure 7**).

By gluconeogenesis the liver can synthesize glucose, which is an essential pathway during starvation. As expected, *Pck1* (phosphoenolpyruvate carboxykinase 1), the enzyme for the rate-limiting step of gluconeogenesis, and *G6pc* (glucose-6-phosphatase catalytic subunit), essential to release glucose in the last step of gluconeogenesis, were both increased due to starvation started at ZT 3, but decreased at ZT 12. *Gck* (glucokinase), catalyzing the opposite reaction, shows an inverse regulation (**Figure 7**).

Taken together, the expression patterns at ZT 3 predominantly corresponded to the known starvation responses of the liver. However, the initiation of fasting at ZT 12 revealed unknown regulatory events that produced more subtle and inversely regulated expression levels.

Refeeding

Refeeding mice after a 24 h starvation challenges the liver. The depleted stores must be refilled, and the metabolism should return to a normal feeding state. The transcription factors *Ppara* and *Pparg* remained elevated after the 12 h refeeding compared to the *ad libitum* group, but *ad libitum* expression was nearly restored after refeeding for 21 h. *Fgf21* expression remained increased after both refeeding periods (**Figure 6**). By contrast, *Hnf4a* expression after the 12 h refeeding was comparable to that after starvation started at ZT 12 and decreased after the 21 h refeeding compared to *ad libitum*. *Mlxipl* expression was restored after the 12 h refeeding (**Figure 7**). The expression of *Srebf1c* increased significantly after both refeeding periods (**Figure 6**).

Hepatocytes exhibited a strong up-regulation of *Fasn* expression, especially after the 21 h refeed; while after 12 h refeed the increase was comparable with starvation started at ZT 12. The genes *Scd1*, *Acsl5*, *Elovl6*, *Hsd17b12*, *Fads1,* and *Thrsp* showed a similar regulation pattern as *Fasn*. However, the expression of other enzymes, such *Acsl1*, *Acsl3*, *Elovl2,* and *Elovl3* resembled the corresponding *ad libitum* sample after 12 and 21 h refeed (**Figure 7**). Expression of the enzymes of beta-oxidation and mitochondrial fatty acid synthesis were restored (*Cpt2*, *Ehhadh*, *Hadhb*, *Decr1*) or remained decreased (*Acaa1b*) after both refeeding periods (**Figure 7**).

The synthesis of ketone bodies and degradation of amino acids are no longer a necessary energy source when sufficient amounts of nutrients are available. Accordingly, the expression of *Hmgcs2* was slightly decreased after 12 and 21 h of refeeding compared to the corresponding *ad libitum* samples, and *Hmgcl* exhibited the same expression as the *ad libitum* state. The level of *Pck1* strongly decreased after the 12 h refeeding compared to *ad libitum* and was slightly reduced after refeeding for 21 h. Both refeeding times restored *G6pc* expression to *ad libitum* levels (**Figure 7**).

Steroid Metabolism

Diurnal influence

Steroid metabolism, especially cholesterol synthesis, is another important function of the liver, and it is partially regulated diurnally (**Figure 8A**). Comparing ZT 3 and ZT 12 *ad libitum Pmvk* (phosphomevalonate kinase), *Mvd* (mevalonate decarboxylase), *Ebp* (phenylalkylamine Ca^{2+} antagonist binding protein), *Sc5d* (sterol-C5-desaturase), and *Cyp17a1* (cytochrome P450, family 17, subfamily a, polypeptide 1) exhibited a higher expression in the morning than in the evening. The regulators of SREBP1, *Scap* (SREBP cleavage-activating protein) and *Insig1/2* (insulin induced gene), were also expressed higher at ZT 3 than at ZT 12. In accordance with enhanced synthesis over the day, the amount of hepatic cholesterol is 1.3-fold higher in the evening

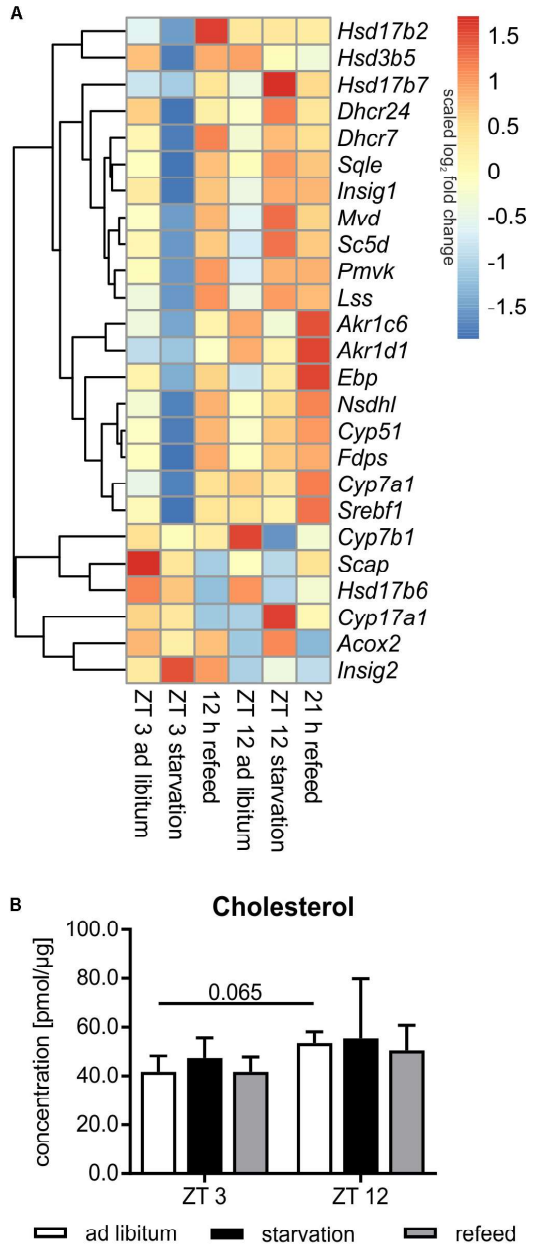

FIGURE 8 | Regulation of steroid metabolism. **(A)** Heatmap of differentially expressed genes related to steroid metabolism. Red indicates an overexpression, and blue indicates an underexpression. **(B)** Concentration of cholesterol in primary hepatocytes of mice fed *ad libitum* (white bars), starved 24 h (black bars) or starved 24 h and refed 12 h (until ZT 3) and 21 h (until ZT 12) (gray bars) (n = 3). Data are plotted as mean ± standard deviation.

than in the morning (**Figure 8B**). Concerning steroidogenesis and cholesterol conversion, the hydroxysteroid dehydrogenases *Hsd3b5* and *Hsd17b2* showed a higher expression in the evening.

The expression of many enzymes [*Cyp7a1*, *Cyp7b1*, *Akr1d1*, *Akr1c6* (aldo-keto reductase family 1, member D1/C6)] involved in steroid degradation by formation of bile acids were also higher expressed in the evening than in the morning.

Starvation

Already in the early fifties it was shown that the synthesis rate of cholesterol is markedly decreased by starvation. This metabolic profile was true in mice starved from ZT 3, in which most genes encoding cholesterol synthesizing enzymes [*Pmvk*, *Mvd*, *Fdps* (farnesyl diphosphate synthetase), *Sqle* (squalene epoxidase), *Lss* (lanosterol synthase), *Dhcr24* (24-dehydrocholesterol reductase), *Cyp51*, *Nsdhl* (NAD(P) dependent steroid dehydrogenase-like), *Hsd17b7*, *Ebp*, *Sc5d,* and *Dhcr7*] exhibited reduced expression compared to *ad libitum* mice (**Figure 8A**). By contrast, the shift of starvation time to the evening produced a reverse regulation and a primarily elevated expression of these genes. Notably, 24 h starvation did not significantly alter the cholesterol content (**Figure 8B**). The regulatory transcription factor of cholesterol synthesis, *Srebf1a*, was not significantly altered following starvation (**Figure 6**). Due to starvation initiated at ZT 3, *Insig1* and *Insig2* exhibited a reciprocal expression, reflecting published data (Ye and DeBose-Boyd, 2011), while the evening starvation period resulted in an equal increase in *Insig1* and *Insig2* expression. *Scap* expression was slightly lower after starvation in both periods (**Figure 8A**).

Cytochrome P450 enzymes (CYPs) and hydroxysteroid dehydrogenases (HSDs) synthesize steroid hormones with cholesterol as starting compound. The expression of *Cyp17a1* (steroid 17α-monooxygenase), which is a key enzyme of steroidogenesis, was highly induced after starvation started at ZT 12 and not altered in ZT 3 mice. By contrast, Hsd expression (*Hsd3b5*, *Hsd17b2,* and *Hsd17b6*) was more or less down-regulated after both starvation periods (**Figure 8A**).

The breakdown of cholesterol is performed by the synthesis of bile acids in the liver. *Cyp7a1*, which is the rate-limiting enzyme, was dramatically down-regulated following starvation initiated at ZT 3 and unchanged in ZT 12 mice compared to *ad libitum*. *Cyp7b1* was almost unaffected after starvation started at ZT 3 and highly decreased in ZT 12 mice. *Akr1c6* is another enzyme of bile acid synthesis and was down-regulated after both starvation periods. *Akr1d1* was marginally altered. *Acox2* was unchanged after starvation initiated at ZT 3, but it was increased in ZT 12 mice (**Figure 8A**).

Cholesterol metabolism exhibits a similar regulation in response to fasting like the lipid metabolism: cholesterol synthesis was regulated in the known manner in ZT 3 mice, but its synthesis exhibited unknown regulation in ZT 12 mice.

Refeeding

The genes of cholesterol synthesis (*Pmvk*, *Mvd*, *Sqle*, *Lss*, *Dhcr24*, *Hsd17b7,* and *Scd5*) remained elevated after the 21 h refeeding period compared to ZT 12 *ad libitum* (**Figure 8A**). *Fdps*, *Cyp51*, *Nsdhl,* and *Ebp* were even higher expressed after 21 h refeeding compared to the corresponding starvation period at ZT 12. The expression of almost all above-mentioned genes was elevated after the 12 h refeed compared to ZT 3 *ad libitum* and was

very similar to that under ZT 12 starvation. Only *Ebp* and *Scd5* exhibited restored expression after 12 h refeeding (**Figure 8A**). Expression of the regulator *Srebf1a* was highly induced after the 12 h refeeding compared to ZT 3 *ad libitum*, and it was restored after refeeding for 21 h (**Figure 6**). *Scap* and *Insig2* exhibited a similar expression after 21 h refeed and at ZT 12 *ad libitum*. After 12 h refeed the expression of *Insig1* was slightly increased and *Insig2* was elevated much more, whereas *Scap* was decreased (**Figure 8A**).

Cyp17a1 expression remained increased after the 21 h refeeding and decreased after 12 h compared to the corresponding *ad libitum* samples. *Hsd17b6* expression was lower after 12 and 21 h refeed than in the *ad libitum* samples. *Hsd3b5* remained down-regulated after 21 h refeeding. *Hsd17b2* expression increased after 12 h refeed (**Figure 8A**).

The key enzyme of bile acid synthesis *Cyp7a1* was up-regulated after both refeeding times. *Akr1d1* and *Akr1c6* were also up-regulated, especially after the 21 h refeed. *Acox2*

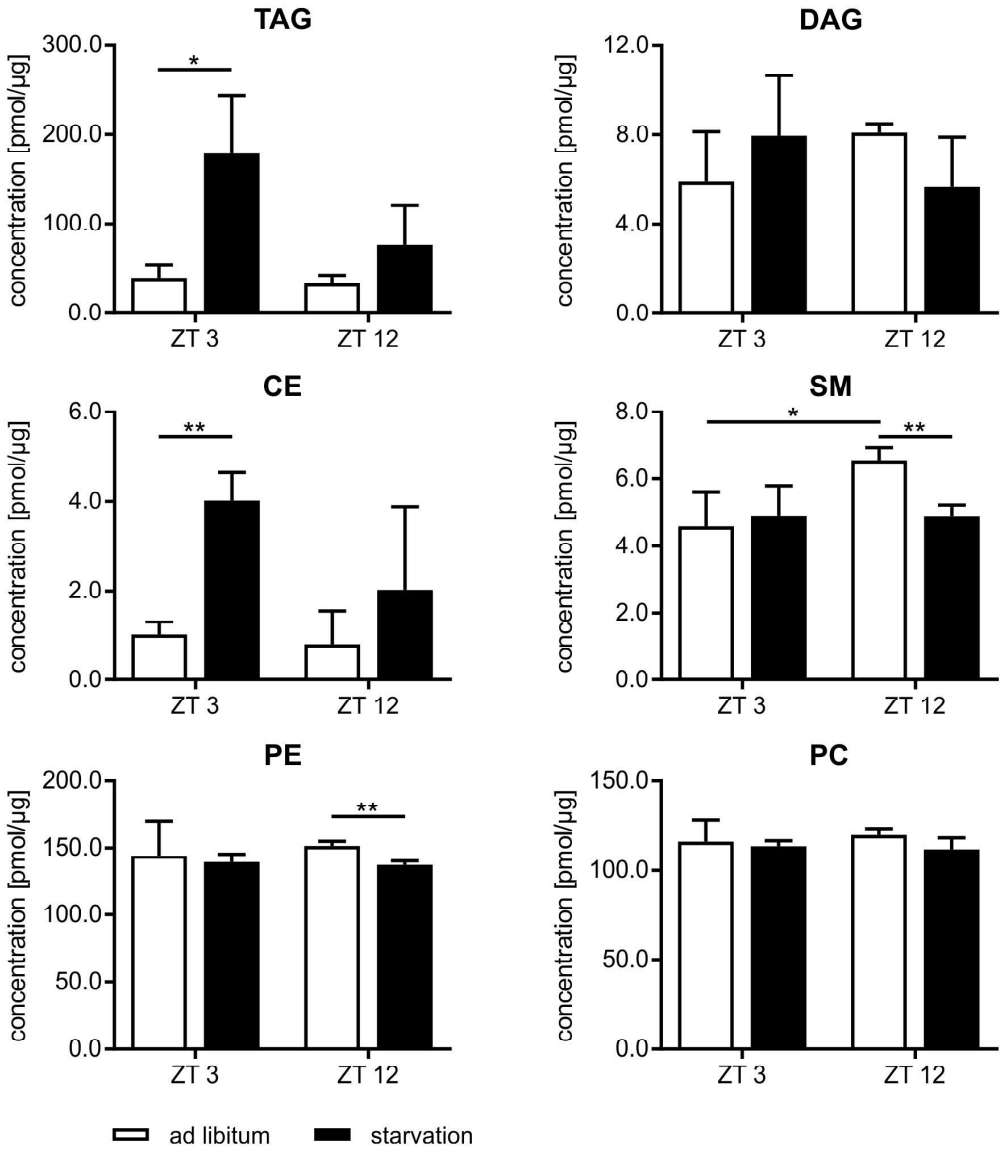

FIGURE 9 | Lipidome profile of primary hepatocytes. Mice were fed *ad libitum* (white bars) or starved 24 h (black bars). Concentration of tri- and diacylglycerides (TAG/DAG), cholesteryl esters (CE), sphingomyelins (SM), phosphatidylethanolamines (PE), and phosphatidylcholines (PC) ($n = 3$). Data are plotted as mean ± standard deviation, $^{*}p < 0.05$ and $^{**}p < 0.01$.

expression was restored after refeeding (12 and 21 h), but *Cyp7b1* remained down-regulated after 21 h of refeeding (**Figure 8A**).

Lipidome Analysis of Hepatocytes

Beside the evaluation of the gene expression, we analyzed the lipidome profile of the hepatocytes via mass spectrometry (**Figure 9**). The amount of lipids in mice fed *ad libitum* exhibited a basal level and no diurnal changes, with the exception of sphingomyelin (SM), where the content was 1.4-fold higher in ZT 12 than in ZT 3 mice. However, hepatic lipids used for storage, such as TAGs and cholesteryl esters (CEs), were strongly elevated in starving mice, and this regulation is highly time-dependent. Starvation started at ZT 3 produced a greater than fourfold increase in TAGs and CEs compared to *ad libitum* mice. By contrast, 24 h starvation initiated at ZT 12 produced only an approximately twofold increase. Polyunsaturated TAG species primarily reflected these differences in TAG levels (**Supplementary Figure 2**). However, TAGs with a high saturation level (50:1 and 52:2) were equally increased after both starvation periods because these TAGs are less reactive and remain longer in the cells. Diacylglycerides (DAGs) are transient precursor of TAG, and these molecules are produced at a much lower level. Both starvation periods slightly altered DAG levels. The membrane components SM and phosphatidylethanolamines (PE) were significantly reduced when starvation was initiated at ZT 12. The PC content did not change (**Figure 9**). Hepatic TAG exhibited still a 2.5-fold increase after the 12 h refeeding compared to *ad libitum* mice. However, the 21 h refeeding normalized the TAG concentration. Refeeding did not significantly alter the other lipid classes (**Supplementary Figure 3**).

DISCUSSION

The results of our study revealed a strong circadian-driven response to fasting in the liver (**Figure 10**). Twenty-four hour starvation initiated and terminated in the morning (ZT 3 to ZT 3) induced the expression of genes involved in metabolic pathways that produce energy-rich substrates for the organism. The gene expression of energy-consuming and temporary expendable processes diminished. However, starvation started in the evening (ZT 12 to ZT 12) produced a totally different hepatic expression signature, with partially opposing regulations, e.g., genes involved in gluconeogenesis decreased, while genes of fatty acid and cholesterol synthesis were induced. These novel findings were unraveled by the analysis of transcriptome data using SOMs. SOMs perfectly visualized the opposing expression profiles of the above-mentioned processes by comparing ZT 3 and ZT 12 starvation (clusters B and J, **Figure 2**). These differences in the expression of metabolic enzymes and their regulators are discussed below in detail.

Metabolic Adaptions Upon Starvation

So far, it was assumed that starvation adapts liver metabolism in two ways: (i) by activating processes producing energy-rich metabolites and (ii) by suppressing energy-consuming pathways. However, our study revealed new diurnal-dependent aspects of these mechanisms. Acetyl-CoA and glucose or equivalents are essential energy-rich substrates produced by the liver upon starvation. Our study confirmed the strong induction of the expression of genes responsible for beta-oxidation, especially when starvation was initiated at ZT 3. However, this induction was much lower at ZT 12. Expression levels of essential enzymes of gluconeogenesis (*Pck1* and *G6pc*) and ketone body synthesis (*Hmgcs2* and *Hmgcl*) were distinctly decreased after food deprivation started in the evening and increased in the morning in the known way (Potthoff et al., 2009). Because both processes use similar starting compounds, IRS2 and PDK4 balance the rate of gluconeogenesis and ketone body synthesis in the liver upon fasting, respectively. Our microarray demonstrated increased *Irs2* and *Pdk4* expression when food deprivation began at ZT 3, as shown previously (Wu et al., 2000; Ide et al., 2004), whereas evening starvation did not affect *Pdk4* expression and decreased *Irs2*. Another process of delivering energy is autophagy, whereby, especially during starvation, expendable or dysfunctional cellular components are degraded and recycled (Yin et al., 2008). As a consequence of starvation started at ZT 12, however, the autophagic genes exhibited a lower expression level compared to ZT 12 *ad libitum* conditions. This result was consistent with the strongly decreased expression of a potent activator of autophagy, *Cebpb*, after starvation in the evening. In contrast, upon starvation in the morning, *Cebpb* exhibited induced expression, although most autophagic genes were not relevantly altered. It was published that the activation of autophagy is based on a changed phosphorylation pattern (Shang et al., 2011), but our results indicate a transcriptional regulation as well, which needs to be further investigated. The transcriptional data suggest a so far unknown down-regulation of energy-supplying processes after starvation started in the evening, while morning starvation led to the known activation of those pathways.

For energy-consuming and temporary expendable metabolic processes, we discovered similar diurnal regulation differences by starvation. The synthesis of fatty acids, manly carried out by fatty acid synthase, seems to be increased based on the elevated expression of *Fasn* after food deprivation in the evening. This observation was contrary to the decreased *Fasn* expression detected after starvation started in the morning and the published knowledge of diminished lipogenesis upon fasting (Horton et al., 1998). The hypothesis of the opposing lipogenesis regulation after different starvation periods was strengthened by the expression of *Gck*, forming the carbon source (pyruvate) for lipogenesis, which was also induced after starvation started in the evening and decreased in the known way after morning starvation (Iynedjian et al., 1987). Cholesterol synthesis is another process known to be diminished while starving. However, enzymes of cholesterol synthesis exhibited elevated gene expression following starvation initiated at ZT 12. Food deprivation initiated at ZT 3 reduced the expression levels of most down-stream genes encoding cholesterol synthesizing enzymes, which indicates diminished cholesterol synthesis, as previously shown (Tomkins and Chaikoff, 1952), even if expression of the rate-limiting enzyme of cholesterol synthesis,

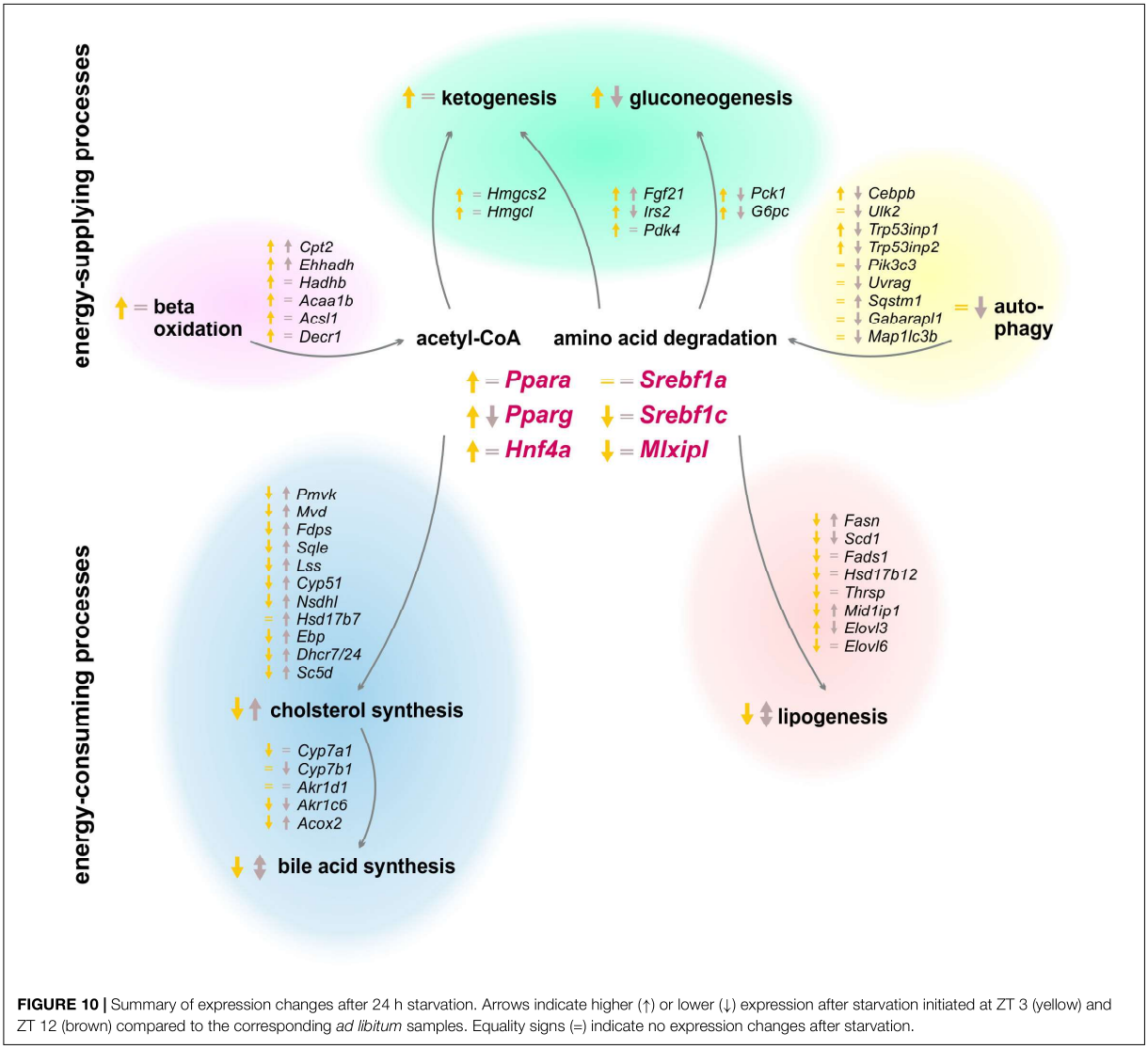

FIGURE 10 | Summary of expression changes after 24 h starvation. Arrows indicate higher (↑) or lower (↓) expression after starvation initiated at ZT 3 (yellow) and ZT 12 (brown) compared to the corresponding *ad libitum* samples. Equality signs (=) indicate no expression changes after starvation.

Hmgcr (3-hydroxy-3-methyl-glutaryl-coenzyme A reductase), was not found in our microarray. Bile acids are secreted into the intestine to increase the solubility of hydrophobic molecules and allow their absorption (Hofmann and Borgström, 1964) and have a poorly understood function as potent signaling compounds (Chiang, 2017). Our study revealed a higher expression of genes involved in bile acid synthesis in the evening than in the morning in *ad libitum* fed mice. This result was consistent with the known diurnal expression of the rate-limiting enzyme CYP7A1, which is highest when the greatest amount of food is consumed (Gooley, 2016). Mice are nocturnal and consume approximately three times more food during scotophase than during photophase (Kurokawa et al., 2000). Bile acid production is a redundant process during starvation, and our analysis revealed a lower expression of *Cyp7a1* after food deprivation at ZT 3. However, starvation in the evening did not alter *Cyp7a1* expression. Several groups reported a similar pattern of *Cyp7a1* expression after starvation (Noshiro et al., 1990; Li et al., 2012), but other studies demonstrated an induction (De Fabiani et al., 2003; Shin et al., 2003). The timing and length of the starvation period used by different groups may explain these diverse results and illustrate the importance of our study. Steroid hormone synthesis is generally localized in the gonads and adrenal glands, but the adult liver also performs steroidogenesis under specific conditions (Grasfeder et al., 2009; Rennert et al., 2017). *Cyp17a1* expression, which is a central steroidogenic enzyme, was induced following evening starvation. This result confirms previous work and strengthens the idea of steroids as mediators of starvation responses (Bauer et al., 2004; Grasfeder et al., 2009). Our data show a novel regulation

of energy-consuming processes after starvation started in the evening, contrary to the established down-regulation frequently published as the hepatic starvation response after fasting initiated in the morning.

The accumulation of lipids in the liver (steatosis) often accompanies starvation (Kok et al., 2003; van Ginneken et al., 2007). Adipose tissues secrete fatty acids, which are taken up by hepatocytes and esterified to the storage lipids TAG and CE or secreted as VLDL. Lipidomics analysis revealed significantly elevated TAG and CE contents due to starvation, but this increase was twice as great after food deprivation initiated in the morning than when it was initiated in the evening. This may be based on the diurnal regulation of adipose triglyceride lipase (ATGL) and hormone-sensitive lipase (HSL), which are the lipolysis pacemaker enzymes in adipose tissue and direct targets of CLOCK/ARNTL (Shostak et al., 2013). The lower level of TAG and CE after starvation started in the evening appears inconsistent with the increased expression of *Fasn*. Two possible explanations are (i) since *Fasn* was only detected at the mRNA level, the synthesis of enough enzyme protein and the accumulation of a measurable increase of TAG may be delayed for several hours and/or (ii) the synthesized fatty acids were not stored in the liver but secreted, and the analysis could not capture them. To unravel this uncertainty, additional studies have to be performed.

Regulation of the Hepatic Starvation Response

Additionally, for the transcription factors regulating the observed starvation-induced transcriptional alterations, our study exhibited novel diurnal expression profiles. A main activator of the energy-supplying processes is the PPAR family. Elevated expression of *Ppara* and *Pparg* in the liver upon fasting induces beta-oxidation, stimulating lipid uptake and fatty acid storage (Kersten et al., 1999; Gavrilova et al., 2003; Tanaka et al., 2005). However, we detected this up-regulated expression only when starvation was initiated at ZT 3 and not at ZT 12, which explains the weak induction of beta-oxidation, the decreased gluconeogenesis and ketogenesis and the lower amount of TAG accumulation in the liver after evening starvation. Furthermore, HNF4A contributes to this regulation due to additional activation of *Ppara* and diminishment of the repressor *Hes6* (Martinez-Jimenez et al., 2010). Our data nicely reflected this mechanism after starvation started in the morning. However, after evening starvation, *Hnf4a* was unchanged and the *Hes6* level increased.

The SREBP1 family and ChREBP (*Mlxipl*) are transcription factors more responsible for the post-prandial state and are supposed to be down-regulated during starvation to not activate energy-consuming pathways. For *Mlxipl*, we detected a transcriptional response with a strong down-regulation after starvation in the morning, but no changes were observed when starvation was initiated in the evening. This was contrary to the published regulation carried out only at the post-translational level via phosphorylation (Iizuka and Horikawa, 2008) and requires a more focused study. *Srebf1c* expression was reduced only after food deprivation initiation in the morning, and its expression was unchanged following starvation in the evening, which may explain the induced expression of the target *Fasn* when starvation was started at ZT 12. SREBP-1a is known to regulate cholesterol synthesis, but even if its expression was not relevantly altered, neither after starvation initiated in the morning nor in the evening, the genes encoding cholesterol synthesizing enzymes responded with a down- or up-regulation, respectively. Additionally, the influence of the SREBP1 inhibitors, INSIG1/2, seemed to depend on diurnality, since *Insig1/2* expression was elevated after both starvation periods, but the regulatory output differed. Therefore, the known regulatory mechanisms of *Srebf1* expression did not seem applicable when starvation was initiated in the evening, and further investigations are needed to delineate these mechanisms. All in all, the diurnally regulated expression of the transcription factors *Ppara*, *Pparg*, *Mlxipl*, *Srebf1a,* and *Srebf1c* following starvation likely underlie many of the observed metabolic alterations.

Concerning the regulation of the fed and starved state, two hormones are omnipresent: insulin and glucagon. Since the hormones were not determined in our study, we can only speculate about their levels and influence. Shi et al. (2013) demonstrated diurnal differences in mice with enhanced insulin activity during the night and a metabolism that was characterized by insulin resistance during the day. However, 24 h starvation started in the morning changed the diurnal insulin regulation, and serum insulin levels dropped by approximately two-thirds, resulting in the known starvation responses (Ahrén and Havel, 1999), but no data were available for evening starvation. Glucagon, on the other hand, regulates metabolism in the fasted state. It was shown that glucagon induces the expression of the hormone *Fgf21* (Berglund et al., 2010), which in turn activates gluconeogenesis and ketogenesis. The expression of *Fgf21* was much more induced when starvation was started in the morning than in the evening, which explains the diurnal differences in gluconeogenic and ketogenic gene expression and suggests that the glucagon response also depends on the timing of starvation.

The overall regulators of circadian rhythm are the core clock genes *Arntl*, *Clock* and *Per*, which were elevated after both starvation periods but maintained their typical diurnal expression pattern. This result was consistent with a previous study that demonstrated induced *Arntl* expression due to raised glucagon levels (Sun et al., 2015). Since the transcriptional analysis was performed in hepatocytes, a screen of other organs would help to fully understand the regulatory differences following starvation started in the morning and in the evening.

Metabolic Adaptions and Regulations Upon Refeed

Peripheral tissues first refill their glucose stores when an organism switches from a starved to a refed state, and the liver subsequently synthesizes and stores glycogen, fatty acids, and cholesterol (Berg et al., 2002). Our experimental setting investigated the effects of two refeeding durations (12 and 21 h) after the same starvation period (**Figure 11**). The already mentioned clusters B and J in the SOMs, where most genes of intermediary and steroid metabolism were localized, exhibited similar expression profiles

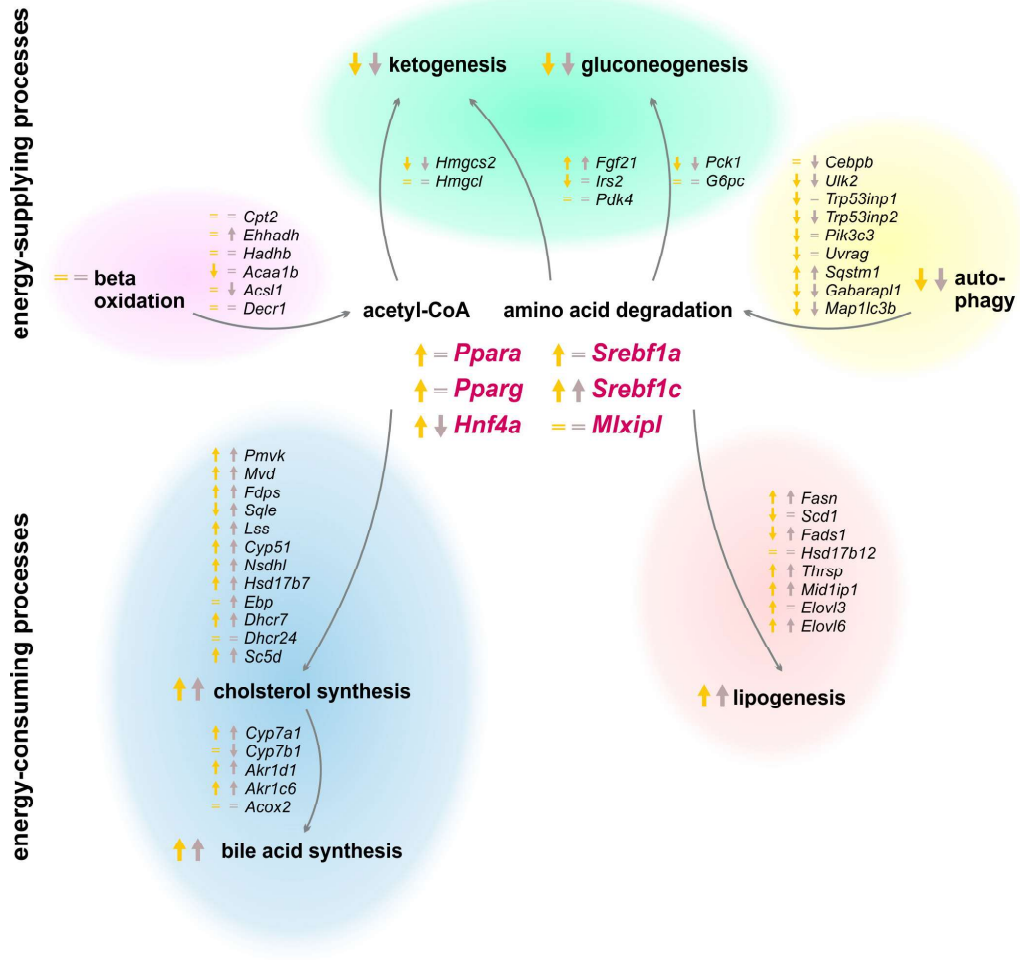

FIGURE 11 | Summary of expression changes following 12 and 21 h refeeding after 24 h starvation. Arrows indicate higher (↑) or lower (↓) expression after refeeding for 12 h until ZT 3 (yellow) and 21 h until ZT 12 (brown) compared to the corresponding *ad libitum* samples. Equality signs (=) indicate a restored *ad libitum* expression levels.

after both refeeding periods, which were totally different from the *ad libitum* groups. The expression levels in other regions of the SOM after 21 h refeeding partially resembled the *ad libitum* group, which indicated a return to the untreated state.

Since food intake delivers all essential metabolites, the liver (i) activates the energy-consuming metabolism and (ii) the production of energy-rich substrates returns to normal. The liver no longer synthesizes ketone bodies and glucose after refeeding, and the expression of the relevant genes reached *ad libitum* or decreased levels. The genes of beta-oxidation were expressed at *ad libitum* levels as well. Early findings demonstrated that refeeding suppressed autophagy (Mortimore et al., 1983), which was confirmed since most of the autophagic genes exhibited a much lower expression after 12 h refeeding compared to starvation, and these genes returned to an approximately *ad libitum* level after 21 h. In contrast, the synthesis of fatty acids and steroids is induced by refeeding. Our study demonstrated that the expression of *Fasn* was highly increased to a maximum after the 21 h refeed. The genes encoding cholesterol synthesizing enzymes were elevated after 12 and 21 h of refeeding as well. This led to an induced synthesis of fatty acids and cholesterol to refill the emptied stores. Bile acid synthesis is associated with the food consumption, and it increased due to elevated expression levels of *Cyp7a1*, as reported previously (Li et al., 2012). The lipidome profile revealed that TAG content remained increased after 12 h refeeding but reached *ad libitum* levels after 21 h. Previous studies demonstrated a normalization of liver lipid content after 48 h of refeeding (Kok et al., 2003).

Since SREBF1 stimulates lipogenesis and cholesterol synthesis, the expression of the transcription factors *Srebf1a* and *Srebf1c*

was highly induced after 12 h refeeding, which was consistent with previous results (Horton et al., 1998; Ide et al., 2004) and resulted in the observed induction of fatty acid and cholesterol synthesis. Resulting from differences in the timing of applied starvation periods, our results revealed another profile than what has been suggested thus far for the expression of the inhibitors *Insig1* and *Insig2*. We demonstrated that *Insig1* levels were almost unchanged and *Insig2* remained highly elevated after 12 h refeeding compared to the corresponding ZT 12 starvation group, contrary to the published decrease of *Insig1* and *Insig2a* expression after refeeding (Attie, 2004; Lee et al., 2017). This discrepancy illustrates the importance of further knowledge of the circadian-driven response to fasting in the liver. The transcription factors, *Ppara* and *Pparg*, remained elevated after the 12 h refeeding but reached *ad libitum* levels after 21 h. Geisler et al. (2016) demonstrated a similar decline in *Ppara* levels with advanced refeeding times.

Linkage of Starvation and Refeed

SOMs that the overall hepatic expression after 12 h refeeding highly resembled starvation initiated at ZT 12, which was confirmed according to the details of different metabolic pathways (e.g., lipogenesis, cholesterol synthesis, autophagy). This may be a consequence of the nocturnal eating behavior of mice, because the expression of many genes may be decreased as a direct consequence of starvation when mice were sacrificed after 24 h starvation in the morning directly after the scotophase when they typically consume their major meal. By contrast, when mice are sacrificed in the evening, the previous period was the photophase during which they consume less food, and the diurnal regulation of mice anticipating food may predominate. Furthermore, mice in which starvation was started in the evening consumed only small amounts of food in the prior period because it was daytime, and the fasting period was actually longer and the stores may be more depleted. These differences may also explain the differences in TAG content. We can only speculate on these points because refeeding in our experiments was only initiated in the evening and not in the morning. We also cannot distinguish between the effects of the longer refeeding period and circadian regulation because samples were taken during another circadian time.

CONCLUSION

Our experiments convincingly demonstrate that the response to starvation periods differed depending on the timing of starvation initiation and report valuable new information about expression levels based on the initiation and termination of starvation in the evening. Performing analogous experiments in humans may provide useful information of the metabolic state after differently timed starvation periods, which may lead to better understanding stressful starvation conditions and develop medical treatment strategies for affected patients. In chronic disturbances of meal timing and the circadian rhythm, e.g., upon shift work, various metabolic disorders are known (Canuto et al., 2013; James et al., 2017). The diverse timings and lengths of starvation periods used in different research groups may explain the variance in published results and support the necessity for clearly designed and recorded experimental procedures. Accordingly, the circadian influence must be considered in all *in vivo* experiments including starvation.

AUTHOR CONTRIBUTIONS

CR performed the experiments and analyzed the data. SV performed the bioinformatical analysis. EM-B and CT collected the samples. SS and AS performed the lipidomics analysis. RG designed the study. CR, SV, EM-B, RG, and MM-S wrote or edited the manuscript.

FUNDING

This work was supported by the Federal Ministry of Education and Research (BMBF, Germany) within the projects Virtual Liver Network (VLN) (Grant No. 0315735, 0315736, and 0315775) and the Systems Medicine of the Liver (LiSyM) (Grant No. 031L0054), by the Deutsche Forschungsgemeinschaft (DFG, Germany) (Grant No. MA 6610/2-1), and the Joachim Herz Foundation. We acknowledge support from the German Research Foundation (DFG) and Leipzig University within the program of Open Access Publishing.

ACKNOWLEDGMENTS

We thank PD Dr. Knut Krohn for Illumina microarray analysis from the Interdisciplinary Centre for Clinical Research Leipzig (Faculty of Medicine, Leipzig University). We cordially thank Kerstin Heise and Doris Mahn for excellent technical assistance. Further, we would like to thank Petra Hirrlinger, Petra Fink-Sterba, and Sigrid Weisheit from the Experimental Centre of the Faculty of Medicine (Leipzig University) for taking excellent care of the mice.

SUPPLEMENTARY MATERIAL

The Supplementary Material for this article can be found online at: https://www.frontiersin.org/articles/10.3389/fphys.2018.01180/full#supplementary-material

REFERENCES

Ahrén, B., and Havel, P. J. (1999). Leptin increases circulating glucose, insulin and glucagon via sympathetic neural activation in fasted mice. *Int. J. Obes. Relat. Metab. Disord.* 23, 660–665. doi: 10.1038/sj.ijo.0800899

Aken, B. L., Ayling, S., Barrell, D., Clarke, L., Curwen, V., Fairley, S., et al. (2016). The Ensembl gene annotation system. *Database* 2016:baw093. doi: 10.1093/database/baw093

Albrecht, U. (2012). Timing to perfection: the biology of central and peripheral circadian clocks. *Neuron* 74, 246–260. doi: 10.1016/j.neuron.2012.04.006

Ashburner, M., Ball, C. A., Blake, J. A., Botstein, D., Butler, H., Cherry, J. M., et al. (2000). Gene ontology: tool for the unification of biology. The gene ontology consortium. *Nat. Genet.* 25, 25–29. doi: 10.1038/75556

Attie, A. D. (2004). Insig: a significant integrator of nutrient and hormonal signals. *J. Clin. Invest.* 113, 1112–1114. doi: 10.1172/JCI200421450

Bauer, M., Hamm, A. C., Bonaus, M., Jacob, A., Jaekel, J., Schorle, H., et al. (2004). Starvation response in mouse liver shows strong correlation with life-span-prolonging processes. *Physiol. Genomics* 17, 230–244. doi: 10.1152/physiolgenomics.00203.2003

Berg, J. M., Tymoczko, J. L., Stryer, L., and Clarke, N. D. (2002). *Biochemistry*. New York, NY: W. H. Freeman.

Berglund, E. D., Kang, L., Lee-Young, R. S., Hasenour, C. M., Lustig, D. G., Lynes, S. E., et al. (2010). Glucagon and lipid interactions in the regulation of hepatic AMPK signaling and expression of PPARalpha and FGF21 transcripts in vivo. *Am. J. Physiol. Endocrinol. Metab.* 299, E607–E614. doi: 10.1152/ajpendo.00263.2010

Bjorkoy, G., Lamark, T., Brech, A., Outzen, H., Perander, M., Overvatn, A., et al. (2005). p62/SQSTM1 forms protein aggregates degraded by autophagy and has a protective effect on huntingtin-induced cell death. *J. Cell Biol.* 171, 603–614. doi: 10.1083/jcb.200507002

Boucher, J., Kleinridders, A., and Kahn, C. R. (2014). Insulin receptor signaling in normal and insulin-resistant states. *Cold Spring Harb. Perspect. Biol.* 6:a009191. doi: 10.1101/cshperspect.a009191

Canuto, R., Garcez, A. S., and Olinto, M. T. A. (2013). Metabolic syndrome and shift work: a systematic review. *Sleep Med. Rev.* 17, 425–431. doi: 10.1016/j.smrv.2012.10.004

Chiang, J. Y. L. (2017). Bile acid metabolism and signaling in liver disease and therapy. *Liver Res.* 1, 3–9. doi: 10.1016/j.livres.2017.05.001

De Fabiani, E., Mitro, N., Gilardi, F., Caruso, D., Galli, G., and Crestani, M. (2003). Coordinated control of cholesterol catabolism to bile acids and of gluconeogenesis via a novel mechanism of transcription regulation linked to the fasted-to-fed cycle. *J. Biol. Chem.* 278, 39124–39132. doi: 10.1074/jbc.M305079200

Du, P., Kibbe, W. A., and Lin, S. M. (2008). Lumi: a pipeline for processing Illumina microarray. *Bioinformatics* 24, 1547–1548. doi: 10.1093/bioinformatics/btn224

Ferrell, J. M., and Chiang, J. Y. L. (2015). Circadian rhythms in liver metabolism and disease. *Acta Pharm. Sin. B* 5, 113–122. doi: 10.1016/j.apsb.2015.01.003

Folch, J., Lees, M., and Sloane Stanley, G. H. (1957). A simple method for the isolation and purification of total lipides from animal tissues. *J. Biol. Chem.* 226, 497–509.

Gavrilova, O., Haluzik, M., Matsusue, K., Cutson, J. J., Johnson, L., Dietz, K. R., et al. (2003). Liver peroxisome proliferator-activated receptor gamma contributes to hepatic steatosis, triglyceride clearance, and regulation of body fat mass. *J. Biol. Chem.* 278, 34268–34276. doi: 10.1074/jbc.M300043200

Gebhardt, R., Hengstler, J. G., Müller, D., Glöckner, R., Buenning, P., Laube, B., et al. (2003). New hepatocyte in vitro systems for drug metabolism: metabolic capacity and recommendations for application in basic research and drug development, standard operation procedures. *Drug Metab. Rev.* 35, 145–213. doi: 10.1081/DMR-120023684

Geisler, C. E., Hepler, C., Higgins, M. R., and Renquist, B. J. (2016). Hepatic adaptations to maintain metabolic homeostasis in response to fasting and refeeding in mice. *Nutr. Metab.* 13:62. doi: 10.1186/s12986-016-0122-x

Gooley, J. J. (2016). Circadian regulation of lipid metabolism. *Proc. Nutr. Soc.* 75, 440–450. doi: 10.1017/S0029665116000288

Grasfeder, L. L., Gaillard, S., Hammes, S. R., Ilkayeva, O., Newgard, C. B., Hochberg, R. B., et al. (2009). Fasting-induced hepatic production of DHEA is regulated by PGC-1alpha, ERRalpha, and HNF4alpha. *Mol. Endocrinol.* 23, 1171–1182. doi: 10.1210/me.2009-0024

Hakvoort, T. B. M., Moerland, P. D., Frijters, R., Sokoloviæ, A., Labruyère, W. T., Vermeulen, J. L. M., et al. (2011). Interorgan coordination of the murine adaptive response to fasting. *J. Biol. Chem.* 286, 16332–16343. doi: 10.1074/jbc.M110.216986

Hartigan, J. A., and Wong, M. A. (1979). Algorithm AS 136: a K-means clustering algorithm. *Appl. Stat.* 28, 100–108. doi: 10.2307/2346830

Herzog, R., Schwudke, D., Schuhmann, K., Sampaio, J. L., Bornstein, S. R., Schroeder, M., et al. (2011). A novel informatics concept for high-throughput shotgun lipidomics based on the molecular fragmentation query language. *Genome Biol.* 12:R8. doi: 10.1186/gb-2011-12-1-r8

Hirao, A., Nagahama, H., Tsuboi, T., Hirao, M., Tahara, Y., and Shibata, S. (2010). Combination of starvation interval and food volume determines the phase of liver circadian rhythm in Per2::Luc knock-in mice under two meals per day feeding. *Am. J. Physiol. Gastrointest. Liver Physiol.* 299, G1045–G1053. doi: 10.1152/ajpgi.00330.2010

Hofmann, A. F., and Borgström, B. (1964). The intraluminal phase of fat digestion in man: the lipid content of the micellar and oil phases of intestinal content obtained during fat digestion and absorption. *J. Clin. Invest.* 43, 247–257. doi: 10.1172/JCI104909

Horton, J. D., Bashmakov, Y., Shimomura, I., and Shimano, H. (1998). Regulation of sterol regulatory element binding proteins in livers of fasted and refed mice. *Proc. Natl. Acad. Sci. U.S.A.* 95, 5987–5992. doi: 10.1073/pnas.95.11.5987

Ide, T., Shimano, H., Yahagi, N., Matsuzaka, T., Nakakuki, M., Yamamoto, T., et al. (2004). SREBPs suppress IRS-2-mediated insulin signalling in the liver. *Nat. Cell Biol.* 6, 351–357. doi: 10.1038/ncb1111

Ihaka, R., and Gentleman, R. (1996). R: a language for data analysis and graphics. *J. Comput. Graph. Stat.* 5, 299–314. doi: 10.2307/1390807

Iizuka, K., and Horikawa, Y. (2008). ChREBP: a glucose-activated transcription factor involved in the development of metabolic syndrome. *Endocr. J.* 55, 617–624. doi: 10.1507/endocrj.K07E-110

Iynedjian, P. B., Ucla, C., and Mach, B. (1987). Molecular cloning of glucokinase cDNA. Developmental and dietary regulation of glucokinase mRNA in rat liver. *J. Biol. Chem.* 262, 6032–6038.

James, S. M., Honn, K. A., Gaddameedhi, S., and van Dongen, H. P. A. (2017). Shift work: disrupted circadian rhythms and sleep-implications for health and well-being. *Curr. Sleep Med. Rep.* 3, 104–112. doi: 10.1007/s40675-017-0071-6

Jensen, T. L., Kiersgaard, M. K., Sørensen, D. B., and Mikkelsen, L. F. (2013). Fasting of mice: a review. *Lab. Anim.* 47, 225–240. doi: 10.1177/0023677213501659

Kersten, S., Seydoux, J., Peters, J. M., Gonzalez, F. J., Desvergne, B., and Wahli, W. (1999). Peroxisome proliferator-activated receptor alpha mediates the adaptive response to fasting. *J. Clin. Invest.* 103, 1489–1498. doi: 10.1172/JCI6223

Kohonen, T. (1982). Self-organized formation of topologically correct feature maps. *Biol. Cybern.* 43, 59–69. doi: 10.1007/BF00337288

Kok, T., Wolters, H., Bloks, V. W., Havinga, R., Jansen, P. L. M., Staels, B., et al. (2003). Induction of hepatic ABC transporter expression is part of the PPARalpha-mediated fasting response in the mouse. *Gastroenterology* 124, 160–171. doi: 10.1053/gast.2003.50007

Kurokawa, M., Akino, K., and Kanda, K. (2000). A new apparatus for studying feeding and drinking in the mouse. *Physiol. Behav.* 70, 105–112. doi: 10.1016/S0031-9384(00)00226-2

Lee, J.-H., Kang, H. S., Park, H. Y., Moon, Y.-A., Kang, Y. N., Oh, B.-C., et al. (2017). PPARα-dependent Insig2a overexpression inhibits SREBP-1c processing during fasting. *Sci. Rep.* 7:9958. doi: 10.1038/s41598-017-10523-7

Li, T., Francl, J. M., Boehme, S., Ochoa, A., Zhang, Y., Klaassen, C. D., et al. (2012). Glucose and insulin induction of bile acid synthesis: mechanisms and implication in diabetes and obesity. *J. Biol. Chem.* 287, 1861–1873. doi: 10.1074/jbc.M111.305789

Liebisch, G., Binder, M., Schifferer, R., Langmann, T., Schulz, B., and Schmitz, G. (2006). High throughput quantification of cholesterol and cholesteryl ester by electrospray ionization tandem mass spectrometry (ESI-MS/MS). *Biochim. Biophys. Acta* 1761, 121–128. doi: 10.1016/j.bbalip.2005.12.007

Löffler-Wirth, H., Kalcher, M., and Binder, H. (2015). oposSOM: r-package for high-dimensional portraying of genome-wide expression landscapes on bioconductor. *Bioinformatics* 31, 3225–3227. doi: 10.1093/bioinformatics/btv342

Longo, V. D., and Mattson, M. P. (2014). Fasting: molecular mechanisms and clinical applications. *Cell Metab.* 19, 181–192. doi: 10.1016/j.cmet.2013.12.008

Martinez-Jimenez, C. P., Kyrmizi, I., Cardot, P., Gonzalez, F. J., and Talianidis, I. (2010). Hepatocyte nuclear factor 4alpha coordinates a transcription factor network regulating hepatic fatty acid metabolism. *Mol. Cell. Biol.* 30, 565–577. doi: 10.1128/MCB.00927-09

Matz-Soja, M., Aleithe, S., Marbach, E., Böttger, J., Arnold, K., Schmidt-Heck, W., et al. (2014). Hepatic Hedgehog signaling contributes to the regulation of IGF1

and IGFBP1 serum levels. *Cell Commun. Signal.* 12:11. doi: 10.1186/1478-811X-12-11

Mortimore, G. E., Hutson, N. J., and Surmacz, C. A. (1983). Quantitative correlation between proteolysis and macro- and microautophagy in mouse hepatocytes during starvation and refeeding. *Proc. Natl. Acad. Sci. U.S.A.* 80, 2179–2183. doi: 10.1073/pnas.80.8.2179

Noshiro, M., Nishimoto, M., and Okuda, K. (1990). Rat liver cholesterol 7 alpha-hydroxylase. Pretranslational regulation for circadian rhythm. *J. Biol. Chem.* 265, 10036–10041.

Partch, C. L., Green, C. B., and Takahashi, J. S. (2014). Molecular architecture of the mammalian circadian clock. *Trends Cell Biol.* 24, 90–99. doi: 10.1016/j.tcb.2013.07.002

Potthoff, M. J., Inagaki, T., Satapati, S., Ding, X., He, T., Goetz, R., et al. (2009). FGF21 induces PGC-1alpha and regulates carbohydrate and fatty acid metabolism during the adaptive starvation response. *Proc. Natl. Acad. Sci. U.S.A.* 106, 10853–10858. doi: 10.1073/pnas.0904187106

Ralph, M. R., Foster, R. G., Davis, F. C., and Menaker, M. (1990). Transplanted suprachiasmatic nucleus determines circadian period. *Science* 247, 975–978. doi: 10.1126/science.2305266

Rennert, C., Eplinius, F., Hofmann, U., Johänning, J., Rolfs, F., Schmidt-Heck, W., et al. (2017). Conditional loss of hepatocellular Hedgehog signaling in female mice leads to the persistence of hepatic steroidogenesis, androgenization and infertility. *Arch. Toxicol.* 91, 3677–3687. doi: 10.1007/s00204-017-1999-5

Rui, L. (2014). Energy metabolism in the liver. *Compr. Physiol.* 4, 177–197. doi: 10.1002/cphy.c130024

Schuhmann, K., Almeida, R., Baumert, M., Herzog, R., Bornstein, S. R., and Shevchenko, A. (2012). Shotgun lipidomics on a LTQ Orbitrap mass spectrometer by successive switching between acquisition polarity modes. *J. Mass Spectrom.* 47, 96–104. doi: 10.1002/jms.2031

Shang, L., Chen, S., Du, F., Li, S., Zhao, L., and Wang, X. (2011). Nutrient starvation elicits an acute autophagic response mediated by Ulk1 dephosphorylation and its subsequent dissociation from AMPK. *Proc. Natl. Acad. Sci. U.S.A.* 108, 4788–4793. doi: 10.1073/pnas.1100844108

Shi, S.-Q., Ansari, T. S., McGuinness, O. P., Wasserman, D. H., and Johnson, C. H. (2013). Circadian disruption leads to insulin resistance and obesity. *Curr. Biol.* 23, 372–381. doi: 10.1016/j.cub.2013.01.048

Shin, D.-J., Campos, J. A., Gil, G., and Osborne, T. F. (2003). PGC-1alpha activates CYP7A1 and bile acid biosynthesis. *J. Biol. Chem.* 278, 50047–50052. doi: 10.1074/jbc.M309736200

Shostak, A., Meyer-Kovac, J., and Oster, H. (2013). Circadian regulation of lipid mobilization in white adipose tissues. *Diabetes Metab. Res. Rev.* 62, 2195–2203. doi: 10.2337/db12-1449

Sokolović, M., Sokolović, A., Wehkamp, D., van Loren Themaat, E., de Waart, D. R., Gilhuijs-Pederson, L. A., et al. (2008). The transcriptomic signature of fasting murine liver. *BMC Genomics* 9:528. doi: 10.1186/1471-2164-9-528

Stokkan, K. A., Yamazaki, S., Tei, H., Sakaki, Y., and Menaker, M. (2001). Entrainment of the circadian clock in the liver by feeding. *Science* 291, 490–493. doi: 10.1126/science.291.5503.490

Stratmann, M., and Schibler, U. (2006). Properties, entrainment, and physiological functions of mammalian peripheral oscillators. *J. Biol. Rhythms* 21, 494–506. doi: 10.1177/0748730406293889

Sun, X., Dang, F., Zhang, D., Yuan, Y., Zhang, C., Wu, Y., et al. (2015). Glucagon-CREB/CRTC2 signaling cascade regulates hepatic BMAL1 protein. *J. Biol. Chem.* 290, 2189–2197. doi: 10.1074/jbc.M114.612358

Szklarczyk, D., Franceschini, A., Wyder, S., Forslund, K., Heller, D., Huerta-Cepas, J., et al. (2015). STRING v10: protein-protein interaction networks, integrated over the tree of life. *Nucleic Acids Res.* 43, D447–D452. doi: 10.1093/nar/gku1003

Tanaka, T., Masuzaki, H., Ebihara, K., Ogawa, Y., Yasue, S., Yukioka, H., et al. (2005). Transgenic expression of mutant peroxisome proliferator-activated receptor gamma in liver precipitates fasting-induced steatosis but protects against high-fat diet-induced steatosis in mice. *Metab. Clin. Exp.* 54, 1490–1498. doi: 10.1016/j.metabol.2005.05.015

Tomkins, G. M., and Chaikoff, I. L. (1952). Cholesterol synthesis by liver. I. Influence of fasting and of diet. *J. Biol. Chem.* 196, 569–573.

Traver, M. K., Henry, S. C., Cantillana, V., Oliver, T., Hunn, J. P., Howard, J. C., et al. (2011). Immunity-related GTPase M (IRGM) proteins influence the localization of guanylate-binding protein 2 (GBP2) by modulating macroautophagy. *J. Biol. Chem.* 286, 30471–30480. doi: 10.1074/jbc.M111.251967

van Ginneken, V., Verhey, E., Poelmann, R., Ramakers, R., van Dijk, K. W., Ham, L., et al. (2007). Metabolomics (liver and blood profiling) in a mouse model in response to fasting: a study of hepatic steatosis. *Biochim. Biophys. Acta* 1771, 1263–1270. doi: 10.1016/j.bbalip.2007.07.007

Wehrens, S. M. T., Christou, S., Isherwood, C., Middleton, B., Gibbs, M. A., Archer, S. N., et al. (2017). Meal timing regulates the human circadian system. *Curr. Biol.* 27, 1768–1775.e3. doi: 10.1016/j.cub.2017.04.059

Welsh, D. K., Takahashi, J. S., and Kay, S. A. (2010). Suprachiasmatic nucleus: cell autonomy and network properties. *Annu. Rev. Physiol.* 72, 551–577. doi: 10.1146/annurev-physiol-021909-135919

Wirth, H., Löffler, M., von Bergen, M., and Binder, H. (2011). Expression cartography of human tissues using self organizing maps. *BMC Bioinformatics* 12:306. doi: 10.1186/1471-2105-12-306

Wu, P., Blair, P. V., Sato, J., Jaskiewicz, J., Popov, K. M., and Harris, R. A. (2000). Starvation increases the amount of pyruvate dehydrogenase kinase in several mammalian tissues. *Arch. Biochem. Biophys.* 381, 1–7. doi: 10.1006/abbi.2000.1946

Yang, X., Lamia, K. A., and Evans, R. M. (2007). Nuclear receptors, metabolism, and the circadian clock. *Cold Spring Harb. Symp. Quant. Biol.* 72, 387–394. doi: 10.1101/sqb.2007.72.058

Ye, J., and DeBose-Boyd, R. A. (2011). Regulation of cholesterol and fatty acid synthesis. *Cold Spring Harb. Perspect. Biol.* 3:a004754. doi: 10.1101/cshperspect.a004754

Yin, X.-M., Ding, W.-X., and Gao, W. (2008). Autophagy in the liver. *Hepatology* 47, 1773–1785. doi: 10.1002/hep.22146

Conflict of Interest Statement: The authors declare that the research was conducted in the absence of any commercial or financial relationships that could be construed as a potential conflict of interest.

Supplementary Material

The Diurnal Timing of Starvation Differently Impacts Murine Hepatic Gene Expression and Lipid Metabolism – A Systems Biology Analysis Using Self-Organizing Maps

Christiane Rennert[1], Sebastian Vlaic[2], Eugenia Marbach-Breitrück[1,3], Carlo Thiel[1], Susanne Sales[4], Andrej Shevchenko[4], Rolf Gebhardt[1], Madlen Matz-Soja[1]*

[1] Rudolf-Schönheimer-Institute of Biochemistry, Faculty of Medicine, Leipzig University, Leipzig, Germany

[2] Leibniz Institute for Natural Product Research and Infection Biology, Hans-Knöll-Institute, Jena, Germany

[3] Institute of Biochemistry, Charité – Universitätsmedizin Berlin, corporate member of Freie Universität Berlin, Humboldt-Universität zu Berlin, and Berlin Institute of Health, Berlin, Germany

[4] Max Planck Institute of Molecular Cell Biology and Genetics, Dresden, Germany

*** Correspondence:** Madlen Matz-Soja: madlen.matz@medizin.uni-leipzig.de

Supplementary Material

1 Supplementary Figures and Tables

1.1 Supplementary Figures

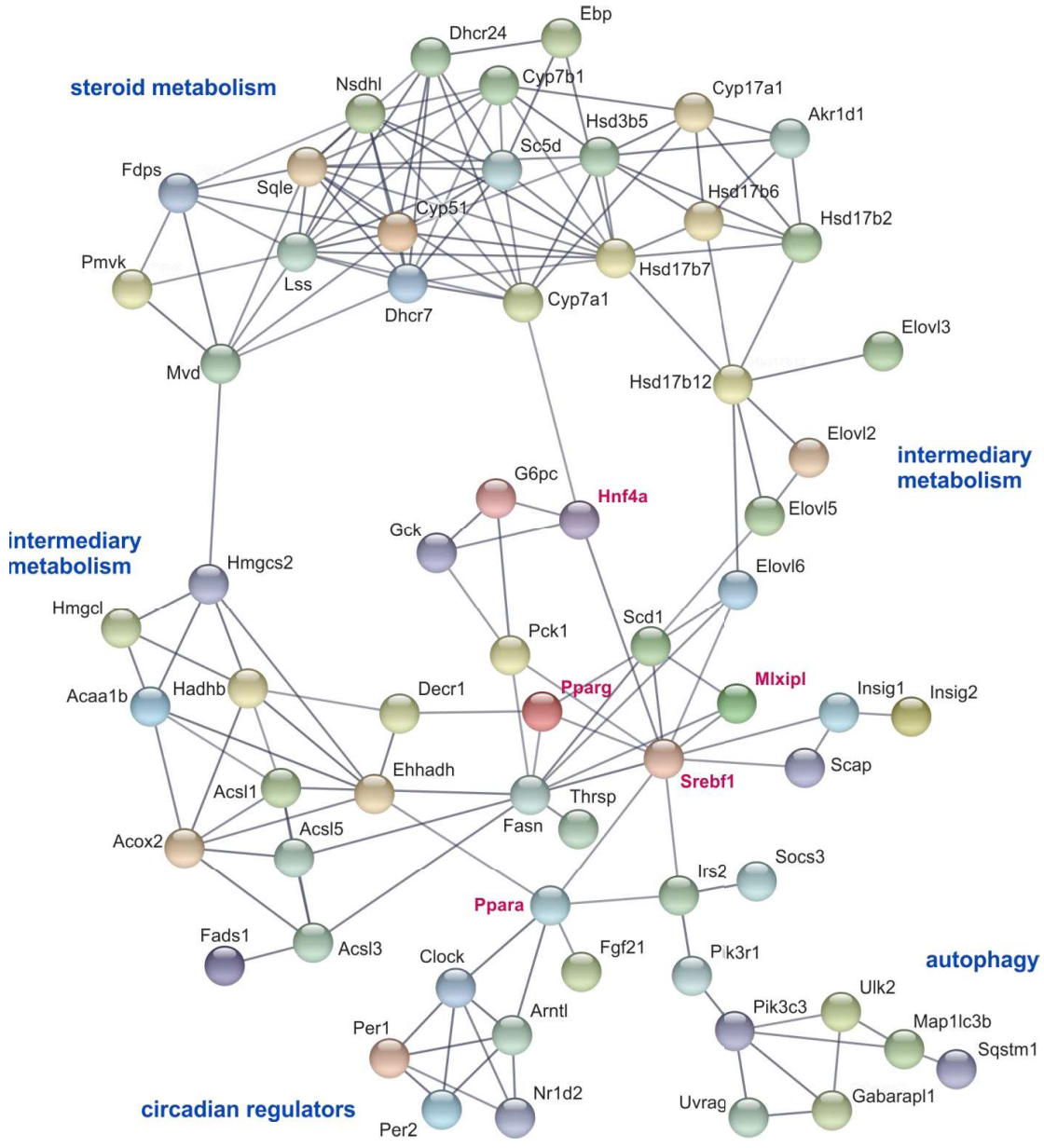

Supplementary Figure 1. The protein interaction network obtained from the STRINGv10.5 database displays the connections of the studied genes/proteins related to hepatic starvation response. The related pathways are marked in blue, transcription factors are marked in pink. The networks were constructed in the "confidence" mode with a high confidence score (0.7).

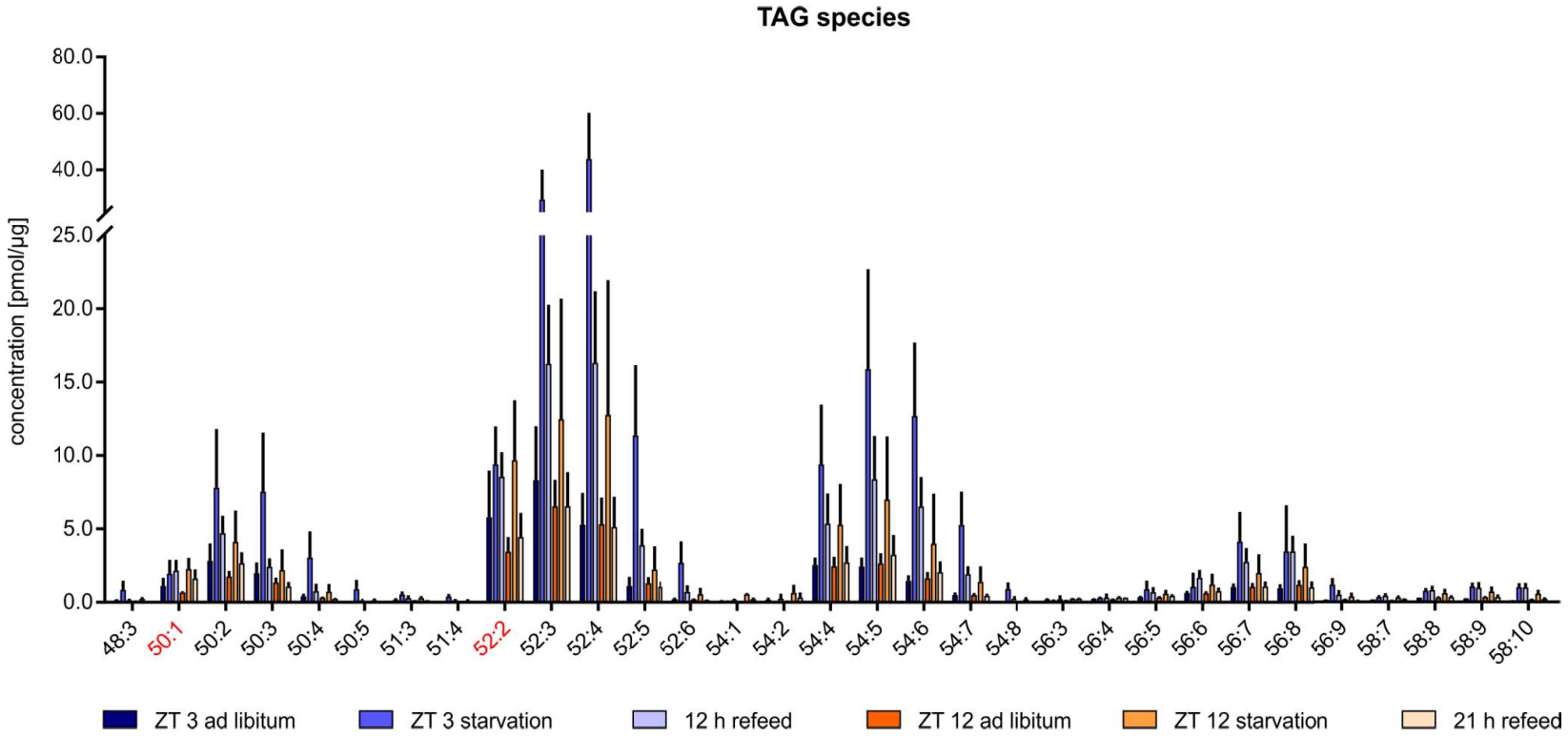

Supplementary Figure 2. TAG species in hepatocytes. Lipidomics analysis of primary hepatocytes of mice fed ad libitum, starved 24 h or starved 24 h and refed 12 and 21 h prior to sacrifice at ZT 3 or ZT 12. All detected TAG species are named with the total number of carbon atoms and double bonds in the fatty acids. Data are plotted as mean ± standard deviation.

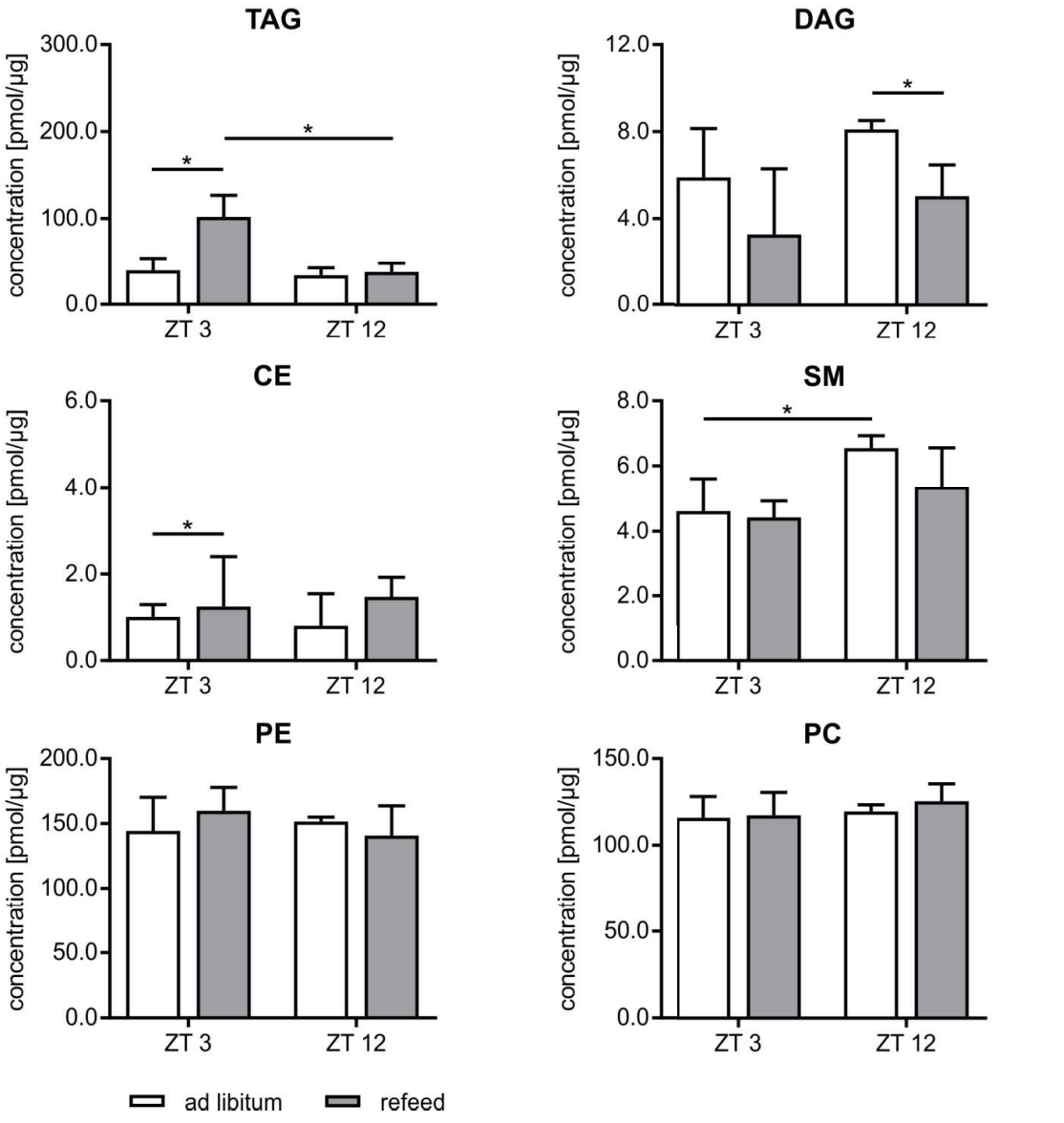

Supplementary Figure 3. Lipidome profile of primary hepatocytes. Mice were fed ad libitum (white bars) or starved 24 h and refed 12 h (until ZT 3) and 21 h (until ZT 12) (grey bars). Concentration of tri- and diacylglycerides (TAG/DAG), cholesteryl esters (CE), sphingomyelins (SM), phosphatidylethanolamines (PE) and phosphatidylcholines (PC) (n = 3). Data are plotted as mean ± standard deviation, $p < 0.05$ (*).

1.2 Supplementary Tables

Supplementary Table 1. Primer sequences for qPCR analyses.

gene	forward primer	reverse primer
18S	gcaattattccccatgaacg	gggacttaatcaacgcaagc
Fgf21	agatggagctctctatggatcg	gggcttcagactggtacacat
Ppara	cgtacggcaatggctttatc	tcatctggatggttgctctg
Pparg	atggaagaccactcgcattc	gctttatccccacagactcg
Srebf1a	cagacactggccgagatg	aaacaggcccgggaagtc
Srebf1c	gagccatggattgcacatttg	aggccagagaagcagaagag

Supplementary Table 2. (**A**) Gene-enrichment analysis (GEA) of all genes with an absolute expression change ≥ 1.5-fold. (**B**) Annotation of the SOMs by k-means clustering and following gene-enrichment analysis. List of all GO terms with Benjamini-Hochberg corrected p value < 0.05. BP = Biological Process, MF = Molecular Function, CC = Cellular Component

see separate Excel file 'Supplementary Table 2'

https://www.frontiersin.org/articles/10.3389/fphys.2018.01180/full#supplementary-material

Supplementary Table 3. Regulated genes detected by Illumina microarrays. The list contains $\log_2$ expression values of all genes with an absolute expression change ≥ 1.5-fold ($\log_2(1.5)$) between at least two of the six groups. Hepatocytes were isolated from mice fed ad libitum, starved 24 h or starved 24 h and refed 12 h (until ZT 3) and 21 h (until ZT 12).

see separate Excel file 'Supplementary Table 3'

https://www.frontiersin.org/articles/10.3389/fphys.2018.01180/full#supplementary-material

PERSPECTIVE

The present studies revealed an unexpected involvement of liver and hepatic Hedgehog signaling in steroid synthesis and reproduction. Since infertility is a major issue, the results gained with the mouse models can help to elucidate similar diseases in humans. Most of the characteristics of PCOS - anovulation, hyperandrogenism and steatosis - were generated in the SAC mice by a hepatocyte-specific KO of *Smo*, which altered signaling in the liver but not in the gonads. Analyzing liver samples of human PCOS patients could provide valuable knowledge about the underlying regulations and help to understand and treat the causes and not only the symptoms.

To date, two developmental disturbances have been associated with hepatic *Smo* KO mouse models: the persistence of steroidogenesis after embryogenesis in the liver associated with infertility and reduced levels of IGF1 gene and protein expression associated with short stature. It was shown that the short stature was not solely caused by growth hormone deficiency but was correlated with the IGF1 level. The liver seems to have a significant role in development-dependent processes, and further research should consider liver parameters in general and the regulation of hepatic Hedgehog signaling in particular.

The second part of the present thesis revealed the immense impact of the timing of starvation periods on the response of liver metabolism. To date, the transcriptome and lipidome of hepatocytes have been studied. Because both transcription and translation can be regulated differently, it would be interesting to study the corresponding proteome data and detect those genes with a diurnal translation. The quantification of hormones, such as insulin, glucagon, leptin and FGF21, after differently timed starvation and refeeding periods would be essential to understand the underlying regulation. The extension of the studied starvation and refeeding periods would allow us to distinguish between effects caused by different starvation and refeeding durations and different circadian times of sampling. The transfer of this knowledge to humans may help to develop treatment strategies for victims of sudden starvation events. Estimating their metabolic state in regard to the starvation period may allow optimized medical care.

CURRICULUM VITAE

Name	Christiane Rennert
Contact	christiane.rennert2@medizin.uni-leipzig.de
Date of birth	13.03.1989
Place of birth	Suhl
Nationality	German

Education

since 2017	**Research Associate**, Department of Hepatobiliary Surgery and Visceral Transplantation, University Hospital, Leipzig University Laboratory: Prof. Dr. D. Seehofer
2013 – 2018	**Doctoral student**, Leipzig University Topic dissertation: *Influence of Hedgehog signaling and starvation on selected aspects of liver metabolism* Laboratory: Prof. Dr. R. Gebhardt and Dr. M. Matz-Soja
2016	**CASyM Fellow**, Ljubljana University, Slovenia
2011 – 2013	**Master of Science Biochemistry**, Leipzig University Final mark: 1.4 Area of study: Biomedicine Topic Master's thesis: *Influence of liver x receptor on lipid metabolism and Hedgehog signaling in cultivated hepatocytes* Laboratory: Prof. Dr. R. Gebhardt
2012	**Erasmus semester**, Oulu University, Finland
2008 – 2011	**Bachelor of Science Biochemistry**, Leipzig University Final mark: 2.2 Topic Bachelor's thesis: *Cloning, expression and purification of Bone Morphogenetic Protein-2 in a prokaryotic system* Laboratory: Prof. Dr. A. Beck-Sickinger
1999 – 2007	**Abitur**, Staatliches Gymnasium Suhl Final mark: 1.9

Further qualifications and fellowships

2016	Advanced course on laboratory animal science, Leipzig University
2016	Seminar on radiation protection, Helmholtz Centre, Leipzig
2015	Course 'R statistics', London
2015	Course on laboratory animal science, Leipzig University
2015 – 2018	'Add-on Fellowship for Interdisciplinary Science' by Joachim Herz foundation
2016	Young Scientist Fellow IUBMB Conference, Vancouver, Canada

PUBLICATIONS AND PRESENTATIONS

Publications

Rennert C, Vlaic S, Marbach-Breitrück E, Thiel C, Sales S, Shevchenko A, Gebhardt R, Matz-Soja M. *The Diurnal Timing of Starvation Differently Impacts Murine Hepatic Gene Expression and Lipid Metabolism – A Systems Biology Analysis Using Self Organizing Maps.* Front Physiol. 2018. doi: 10.3389/fphys.2018.01180

Rennert C and Eplinius F, Hofmann U, Johänning J, Rolfs F, Schmidt-Heck W, Guthke R, Gebhardt R and Ricken AM and Matz-Soja M. *Conditional loss of hepatocellular Hedgehog signaling in female mice leads to the persistence of hepatic steroidogenesis, androgenization and infertility*. Arch Toxicol. 2017. doi: 10.1007/s00204-017-1999-5

Marbach-Breitrück E and Matz-Soja M, Abraham U, Schmidt-Heck W, Sales S, Vlaic S, Rennert C, Kern M, Aleithe S, Thiel C, Arnold K, Böttger J, Klöting N, Guthke R, Rozman D, Teperino R, Shevchenko A, Kramer A, Gebhardt R. *Tick-Tock Hedgehog – Mutual crosstalk with liver circadian clock renders hepatic hedgehog signaling a risk factor of steatosis*. J Hepatol. 2018. under revision

Matz-Soja M, Rennert C, Schönefeld K, Aleithe S, Boettger J, Schmidt-Heck W, Weiss T, Hovhannisyan A, Zellmer S, Klöting N, Schulz A, Kratzsch J, Guthke R, Gebhardt R. *Hedgehog signaling is a potent regulator of liver lipid metabolism and reveals a GLI-code associated with steatosis*. eLife. 2016. doi: 10.7554/eLife.13308

Böttger J, Arnold K, Thiel C, Rennert C, Aleithe S, Hofmann U, Vlaic S, Sales S, Shevchenko A, Matz-Soja M. *RNAi in murine hepatocytes: the agony of choice – a study of the influence of lipid-based transfection reagents on hepatocyte metabolism*. Arch Toxicol. 2015. doi: 10.1007/s00204-015-1571-0

Oral presentations

Rennert C *Unravelling the role of the Hedgehog signaling pathway in the hepato-ovarian axis*. LiSyM PhD and PostDoc Retreat 2017, Hünfeld, Germany

Rennert C *Connection of Hedgehog signaling pathway and steroidogenesis in the liver*. 16th International Conference of Biochemistry and Molecular Biology (IUBMB) Young Scientist Program 2016, Vancouver, Canada

Poster presentations

Rennert C, Matz-Soja M, Gebhardt R. *How Hedgehog signaling pathway activity controls steroidogenesis in the liver*. Conference on Systems Biology of Mammalian Cells (SBMC), 06.-08.04.2016, München

Rennert C, Matz-Soja M, Gebhardt R. *Up and Down of Hedgehog Signaling leads to Down and Up of Steroidogenesis in the Liver*. 32. Jahrestagung der Deutschen Arbeitsgemeinschaft zum Studium der Leber (GASL), 22.-23.01.2016, Düsseldorf

Rennert C, Matz-Soja M, Eplinius F, Ricken A, Gebhardt R. *Hepatic hedgehog signaling and steroidogenesis – an evil partnership?* 50th International Liver Congress (EASL), 22.-26.04.2015, Vienna, Austria

Rennert C, Böttger J, Matz-Soja M, Gebhardt R. *Morphogenic pathways and steroidogenesis in the liver*. International Meeting of the German Society for Cell Biology (DGZ), 24.-27.03.2015, Köln

Rennert C, Aleithe S, Böttger J, Matz-Soja M, Gebhardt R. *Cooperation of Hedgehog and Wnt/β-Catenin signalling in regulation of steroidogenesis in the liver*. 31. Jahrestagung der Deutschen Arbeitsgemeinschaft zum Studium der Leber (GASL) 30.-31.01.2015, München

Rennert C, Böttger J, Matz-Soja M, Gebhardt R. *Steroidogenese in der Leber- jetzt doch?!* 13th Leipzig Research Festival for Life Sciences, 18.12.2014, Leipzig

Rennert C, Böttger J, Matz-Soja M, Gebhardt R. *Steroidogenesis in the liver*.
Signal Transduction Society (STS): 18th Joint Meeting Signal Transduction – Receptors, Mediators and Genes, 05.-07.11.2014, Weimar

Rennert C, Schmidt-Heck W, Böttger J, Matz-Soja M, Gebhardt R. *Sex-specific gene regulation in liver*. Conference on Systems Biology of Mammalian Cells (SBMC), 12.-14.05.2014, Berlin

AUTHOR CONTRIBUTION STATEMENT

Nachweis über Anteile der Co-Autoren, Christiane Rennert
Influence of Hedgehog signaling and starvation on selected aspects of liver metabolism

---

Nachweis über Anteile der Co-Autoren

Titel	**Conditional loss of hepatocellular Hedgehog signaling in female mice leads to the persistence of hepatic steroidogenesis, androgenization and infertility**
Journal	Archives of Toxicology
Autoren	Christiane Rennert, Franziska Eplinius, Ute Hofmann, Janina Johänning, Franziska Rolfs, Wolfgang Schmidt-Heck, Reinhardt Guthke, Rolf Gebhardt, Albert M. Ricken, Madlen Matz-Soja

---

Christiane Rennert (geteilter Erstautor)

- Generierung von Proben (Lebergewebe, Hepatozyten, Blutplasmaproben, Reproduktionsorgane)
- Analyse von Proben (qPCR, histologische Bestimmung von Zyklusstadien)
- Analyse von Daten (bioinformatische Analyse von Microarray-Daten, Auswertung von qPCR-Analysen)
- Visualisierung der Daten
- Schreiben der Publikation
- Bearbeiten der Revision

Franziska Eplinius (geteilter Erstautor)

- Histologische Färbungen
- Histologische Charakterisierung von Reproduktionsorganen (Zyklusstadien, Ovarien, Follikulogenese)
- Quantifizierung von Follikulogenese

Ute Hofmann

- Messung von Steroidhormonkonzentrationen

Janina Johänning

- Messung von Steroidhormonkonzentrationen

Franziska Rolfs

- Histologische Untersuchungen von Reproduktionsorganen (Ovarien)

Wolfgang Schmidt-Heck

- bioinformatische Analysen

Reinhardt Guthke

- bioinformatische Analysen

Rolf Gebhardt (geteilter Seniorautor)

- Projektidee
- Konzeption der Studie
- Editieren der Publikation

Albert M. Ricken (geteilter Seniorautor)

- Projektidee
- Konzeption der Studie
- Histologische Charakterisierung von Reproduktionsorganen (Zyklusstadien, Ovarien, Follikulogenese)
- Editieren der Publikation

Madlen Matz-Soja (geteilter Seniorautor)

- Konzeption der Studie
- Züchtung der Mauslinien
- Generierung von Proben (Hepatozyten, Reproduktionsorgane)
- Analyse von Proben (qPCR)
- Schreiben und editieren der Publikation

Christiane Rennert

Albert M. Ricken

Franziska Eplinius

Madlen Matz-Soja

Rolf Gebhardt

Nachweis über Anteile der Co-Autoren, Christiane Rennert

Influence of Hedgehog signaling and starvation on selected aspects of liver metabolism

---

Nachweis über Anteile der Co-Autoren

Titel	**The Diurnal Timing of Starvation Differently Impacts Murine Hepatic Gene Expression and Lipid Metabolism – A Systems Biology Analysis Using Self-Organizing Maps**
Journal	Frontiers in Physiology
Autoren	Christiane Rennert, Sebastian Vlaic, Eugenia Marbach-Breitrück, Carlo Thiel, Susanne Sales, Andrej Shevchenko, Rolf Gebhardt, Madlen Matz-Soja

---

Christiane Rennert (Erstautor)

- Analyse von Proben (qPCR)
- Analyse von Daten (bioinformatische Analysen von Microarray-Daten, Auswertung von Lipidom- und qPCR-Analysen)
- Visualisierung der Daten
- Schreiben der Publikation
- Bearbeiten der Revision

Sebastian Vlaic

- bioinformatische Analysen von Microarray-Daten
- Editieren der Publikation

Eugenia Marbach-Breitrück

- Generierung von Proben
- Editieren der Publikation

Carlo Thiel

- Generierung von Proben

Susanne Sales

- Lipidom-Analysen

Andrej Shevchenko

- Lipidom-Analysen

Rolf Gebhardt

- Projektidee
- Konzeption der Studie
- Editieren der Publikation
- Bearbeiten der Revision

Madlen Matz-Soja (Seniorautor)

- Konzeption der Studie
- Generierung von Proben
- Schreiben und editieren der Publikation
- Bearbeiten der Revision

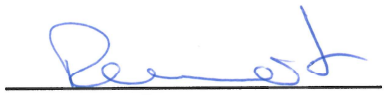

Christiane Rennert

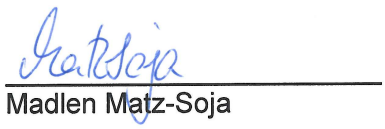

Madlen Matz-Soja

SELBSTSTÄNDIGKEITSERKLÄRUNG

Ich, Christiane Rennert, versichere, dass die vorliegende Arbeit ohne unzulässige Hilfe und ohne Benutzung anderer als der angegebenen Hilfsmittel angefertigt wurde und dass die aus fremden Quellen direkt oder indirekt übernommenen Gedanken in der Arbeit als solche kenntlich gemacht worden sind. Ich versichere außerdem, dass keine weiteren außer den genannten Personen bei der geistigen Herstellung der vorliegenden Arbeit beteiligt waren, ich nicht die Hilfe eines Promotionsberaters in Anspruch genommen habe und dass Dritte weder unmittelbar noch mittelbar geldwerte Leistungen für Arbeiten erhalten haben, die im Zusammenhang mit dem Inhalt der vorgelegten Dissertation stehen.

Die vorliegende Arbeit wurde weder in gleicher noch ähnlicher Form bei einer anderen wissenschaftlichen Einrichtung zum Zwecke einer Promotion oder eines anderen Prüfungsverfahrens vorgelegt.

Leipzig, 12. November 2018

Christiane Rennert

DANKSAGUNG

Mein herzlicher Dank gilt Prof. Rolf Gebhardt für die Möglichkeit an einem der faszinierendsten Organe forschen zu dürfen. Ich danke ihm für die Motivation, die er in mir geweckt hat und die vielfältige Unterstützung, um meine Forschung voranzubringen. Madlen Matz-Soja verdanke ich die Möglichkeit der Fertigstellung meiner Dissertation. Ich bin ihr von Herzen dankbar für die Aufnahme in ihre Juniorarbeitsgruppe, ihr immer offenes Ohr und die tolle Zeit, die wir zusammen hatten. Ich danke Prof. Torsten Schöneberg für die Übernahme der Betreuung meiner Dissertation und Prof. Claus Hellerbrand für die Anfertigung eines Zweitgutachtens.

Mein Dank gilt unseren Kooperationspartnern Ute Hofmann und Janina Johänning für die Etablierung und Messung der Steroidhormonkonzentrationen sowie Susanne Sales und Andrej Shevchenko für die Anfertigung diverser Lipidomprofile. Ich danke der ehemaligen Arbeitsgruppe Guthke am IKP Jena, die mir die Bioinformatik und Systembiologie nahegebracht haben. Ich danke Wolfgang Schmidt-Heck für das Lehren der Microarray Auswertung und die stete Bereitschaft kurzfristig Abbildungen anzufertigen und mich zu unterstützen. Außerdem danke ich Sebastian Vlaic für seine Analysen und Ideen sowie die unzähligen Stunden am Telefon mit Diskussionen über Datenauswertung.

Ich danke der Joachim Herz Stiftung, die mich drei Jahre mit einem Stipendium unterstützt hat, das mir die Freiheit gab, mich nach meinen Wünschen weiterzubilden und großartige Konferenzen zu besuchen.

Ich danke Eugenia Marbach und Jan Böttger für ihre stete Unterstützung meiner Forschung und dass sie immer Zeit für meine Anliegen hatten, auch als sie Leipzig verlassen haben. Ich danke Katrin Arnold, Katrin Günter und Carlo Thiel für eine lustige und tolle Zeit in der ehemaligen AG Gebhardt und den Mitgliedern der Nachwuchsgruppe Matz-Soja. Außerdem gilt mein Dank Doris Mahn, Vivien Teßmar und Kerstin Heise für die ausgezeichnete Unterstützung im Laboralltag und die Übernahme vieler Routinearbeiten. Ich danke Bianca Löffler für die Lösung organisatorischer und bürokratischer Probleme.

Meine Eltern haben mich gelehrt, immer an mich zu glauben. Danke für euer Vertrauen, die motivierenden Worte und all die Hilfe, wann immer ich sie brauchte. Außerdem danke ich meinen Eltern und meinem Bruder Johannes für die Zeit der Ablenkung und Zerstreuung.

Ich danke meinem Freund Stefan, der meine Erfolge und schlechten Tage am meisten gespürt hat, Verzagtheit aber nicht zulässt. Außerdem danke ich meinen Studienfreunden für ein großartiges Jahrzehnt und den gemeinsam beschrittenen Weg mit geteiltem Freud und Leid.